

UNIVERSITA' DEGLI STUDI DI PARMA

Dottorato di Ricerca in Scienze Chimiche

Ciclo XXIX (2014-2016)

**Development of innovative competitive amperometric immunosensors as promising tools in clinical diagnosis and food safety applications**

Coordinatore: Chiar.mo Prof. Roberto Cammi

Tutor: Chiar.mo Prof. Maria Careri

Co-Tutor: Chiar.mo Dott. Marco Giannetto

Dottoranda: Monica Costantini

*To my Family*

## CONTENT

1. BIOSENSORS.....	1
1.1 INTRODUCTION.....	1
1.2 ANTIGENS AND ANTIBODIES .....	2
1.3 IMMUNOSENSORS AND ELISA TESTS.....	5
1.3.1 ELISA Formats .....	5
1.3.2 Comparison of Direct and Indirect ELISA detection methods.....	7
1.3.3 ELISA detection step .....	7
1.4 AMPEROMETRIC IMMUNOSENSORS .....	8
1.5 VOLTAMMETRIC METHODS .....	10
2. ELECTRODES: CHARACTERISTICS AND FUNCTIONALIZATION.....	13
2.1 SCREEN-PRINTED ELECTRODES .....	13
2.2 BIO-RECEPTOR IMMOBILIZATION METHODS .....	14
2.3 NANOSTRUCTURED MATERIALS .....	16
2.3.1 Carbon Nanotubes (CNTs).....	16
2.3.2 Metal Nonoparticles .....	17
2.4 ANTIGEN AND ANTIBODY IMMOBILIZATION.....	19
2.4.1 Antibody immobilization: direct and protein-assisted orientation.....	19
2.4.2 Antibody immobilization through covalent immobilization- Self assembled- monolayer .....	20
2.4.3 Direct immobilization of antigen .....	21
2.4.4 Antigen immobilization through SAM system .....	22
2.4.5 Chitosan/glutaraldehyde system .....	22
3. HIV AND HCV .....	26
3.1 HIV.....	26
3.1.1 HIV virion morphology .....	26
3.2 HCV.....	28
3.2.1 HCV virion morphology .....	28
3.3 HIV-HCV ROUTE OF TRANSMISSION .....	29
3.4 HIV-HCV CO-INFECTION .....	30
3.5 METHOD OF DIAGNOSIS .....	30
3.5.1 HIV methods of diagnosis.....	31
3.5.2 HCV methods of diagnosis .....	32
3.5.3 HIV and HCV biosensors: state of the art.....	34

4.	PROJECT PURPOSE.....	37
4.1	DEVELOPEMENT OF AN INNOVATIVE IMMUNOSENSOR FOR CO- DETERMINATION OF HIV AND HCV SERUM BIOMARKERS .....	37
4.2	DEVELOPEMENT OF AN IMMUNOSENSOR FOR THE DETECTION OF HIV CAPSID PROTEIN p24.....	40
4.2.1	Reagents and solutions.....	40
4.2.2	Apparatus and electrodes .....	41
4.2.3	Methods.....	41
4.2.4	Results discussion .....	44
4.3	DEVELOPEMENT OF A COMPETITIVE IMMUNOSENSOR FOR THE DETECTION OF HCV CAPSID PROTEIN NS4 .....	58
4.3.1	Reagents and solutions.....	58
4.3.2	Apparatus and electrodes .....	59
4.3.3	Methods.....	59
4.3.4	Preliminary Results .....	60
4.4	PRELIMINARY STUDIES ON DUAL-CHIP DEVICE .....	61
4.4.1	Reagents and solutions.....	62
4.4.2	Apparatus and electrodes .....	62
4.4.3	Method and results discussion .....	62
5.	MAGNETOIMMUNOSENSOR BASED ON GOLD/SILVER BI-METALLIC NANOPARTICLES FOR SENSITIVE DETECTION OF HIV CAPSID PROTEIN p24 .....	66
5.1	INTRODUCTION.....	66
5.1.1	Metal nanoparticles for immunosensing applications.....	66
5.2	GOLD/SILVER BI-METALLIC NANOPARTICLES (BNPs): ELECTROCHEMICAL CHARACTERIZATION.....	68
5.2.1	Experimental .....	68
5.2.2	Results and discussion .....	69
5.2.3	Conclusions.....	74
5.3	STUDY FOR DEVELOPMENT OF MAGNETOIMMUNOSENSOR FOR SENSITIVE DETECTION OF HIV CAPSID PROTEIN p24 .....	75
5.3.1	Experimental .....	76
5.3.2	Results and discussion .....	77
5.3.3	Conclusions.....	78
6.	BIOSENSORS FOR FOOD SAFETY APPLICATION.....	79
6.1	CELIAC DISEASE AND GLUTEN-FREE FOODS.....	79

6.2	ANALYTICAL METHODS FOR GLUTEN DETECTION.....	80
6.3	Published Paper: Competitive immunosensor based on gliadin immobilization on disposable carbon-nanogold screen-printed electrodes for rapid determination of celiotoxic prolamins: compatibility assessment of the immunodevice with different sample treatment approaches.....	81
6.3.1	Experimental .....	82
6.3.2	Results and discussion .....	85
6.3.3	Conclusions.....	91
	REFERENCES.....	92

# 1. BIOSENSORS

## 1.1 INTRODUCTION

According to the IUPAC definition, a chemical sensor is a device that transforms chemical information, ranging from concentration of a specific sample component to total composition analysis, into an analytically useful signal [1].

These sensors usually contain three basic components connected in series: a chemical recognition system (receptor), a physicochemical transducer and an electronic system.

In the majority of chemical sensors, the receptor interacts with the analyte and, as a result, its physical properties are changed. This alteration is converted into a measurable signal, such as an electronic, photonic, thermal or mass signal, which is amplified, processed and made visible into a display.

In this context a biosensor is a chemical sensor in which the recognition system utilizes a biochemical mechanism [2, 3].

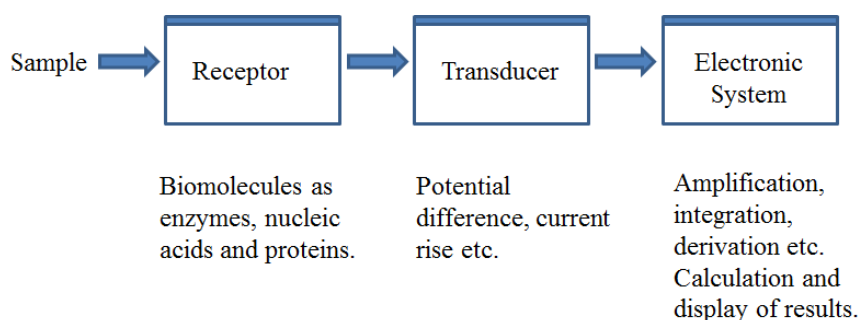


**Figure1 Elements of Biosensor.**

On the base of the typology of the receptor, biosensors can be classified in three classes: molecular biosensors (based on antibodies, nucleic acids, and enzymes), cellular biosensors, and tissue biosensors. Considering the first class of biosensors, they can be further divided in:

- Enzyme biosensors: the receptor is an enzyme that catalyses a reaction in which the analyte is involved;
- Bio-affinity biosensors: the receptor is an antigen or an antibody and the recognition mechanism is based on the antigen-antibody specific interaction. These systems are usually called immunosensor.



Antibodies are classified in different varieties known as isotypes or classes, on the base of structural differences of heavy chain C region, and for antibodies of the same isotype they have the same amino acidic sequence. In mammals there are five antibody isotypes known as IgA, IgD, IgE, IgG, and IgM, which differ in their biological properties, functional locations and ability to deal with different antigens [6]. IgG isotype is the main antibody class in the serum and has a crucial role in protection against invading bacteria and viruses, whereas IgE helps to protect against infection with parasitic helminths and is also responsible for the debilitating symptoms of allergy. IgA, another major serum antibody, arguably has its key role at mucosal surfaces, such as the linings of the lungs and the gastrointestinal tract, where it is the main immunoglobulin in the secretions that bathe these surfaces. IgM, which is restricted mainly to the circulation, due to its large size, is also known to protect against bacterial and fungal infection, whereas the function of IgD remains less clear. The different suffixes of the antibody isotypes denote the different types of heavy chains that antibody contains, with each heavy chain class named alphabetically:  $\alpha$ ,  $\gamma$ ,  $\delta$ ,  $\epsilon$ , and  $\mu$ ; this gives rise to IgA, IgG, IgD, IgE, and IgM, respectively. Furthermore, each isotype is present in a different molecular form, specifically as monomer, dimer or pentamer, depending on the tertiary protein structure that they assume. In humans, IgG exists as four subclasses (IgG1, IgG2, IgG3 and IgG4) and IgA as two (IgA1 and IgA2), in which the heavy chain of each subclass is the product of a different heavy-chain constant (C) region gene, while IgM and IgD are present in only one class (Table 1).

**Table 1 Antibody description.**

ANTIBODY				
ISOTYPE	SUBCLASS	HEAVY CHAIN DESIGNATION	PRIMARY LOCATION	MAIN MOLECULAR FORM
<b>IgA</b>	IgA <sub>1</sub> , IgA <sub>2</sub>	$\alpha$	Serum, seromucous secretions, milk, colostrum and tears	Monomer
<b>IgD</b>	IgD	$\delta$	Serum	Monomer
<b>IgE</b>	IgE	$\epsilon$	Serum	Pentamer
<b>IgG</b>	IgG <sub>1</sub> , IgG <sub>2</sub> , IgG <sub>3</sub> , IgG <sub>4</sub>	$\gamma$	Serum, tissues	Monomer
<b>IgM</b>	IgM	$\mu$	Serum	Dimer

On the base of antibodies immunoreactivity, it is possible to classify them in mono- and poly-clonal, according the ability to bind the corresponding antigen, through one or more recognising epitopes. The nature of antigen-antibody interaction is non-covalent and reversible. Various non-covalent interactions such as electrostatic forces, hydrogen bonds, Van der Waals forces and hydrophobic



interactions are involved in the immuno-recognition process. The contribution of each interaction depends on the antigen and antibody structures. The extent of these interactions can be expressed by an affinity constant ( $K_D$ ), which express the stability of the antigen-antibody complex (Figure 3).

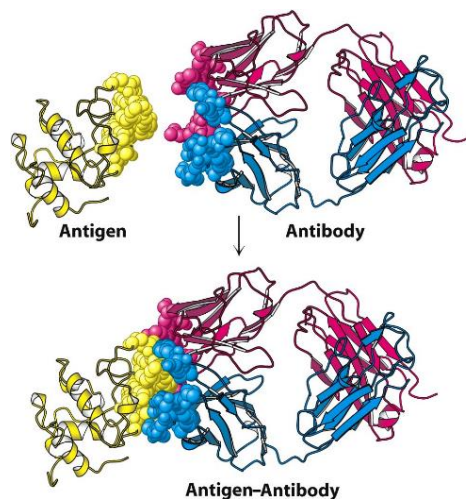


**Figure 3 Antigen-Antibody interaction.**

The specificity and the selectivity of antigen-antibody interaction are the base principle of different immunometric analytical methods, as ELISA and immunosensors, described as follows.

## 1.3 IMMUNOSENSORS AND ELISA TESTS

As previously stated, an immunosensor is a bio-affinity sensor, characterized by a high specificity, due to interaction between the epitope of an antigen and its related binding site on the Fab portion of the antibody, giving a stable complex [7]. On the basis of this working principle, they can be defined as a transposition of the ELISA (Enzyme-Linked Immunosorbent Assay) on a sensing substrate.

ELISA is a plate-based assay (Figure 4), high throughput screening technique, designed for detecting and quantifying substances such as proteins and antibodies [8, 9]. In ELISA the antigen or the antibody is immobilized to a solid surface and the complementary species are complexed and detected. The detection is accomplished by means of a labelled antibody, generally enzyme-conjugated, which activity on an appropriate substrate produces a measureable product, suited for the analytical detection. Specifically, the enzyme reacts with the appropriate substrate and the enzymatic product gives a signal proportional to the concentration of analyte, detectable by optical measurements. The most commonly used enzyme labels are horseradish peroxidase (HRP) and alkaline phosphatase (AP) and a large selection of enzyme substrates is available for performing the ELISA with HRP or AP conjugate.

The choice of substrate depends upon the required assay sensitivity and the instrumentation available for the detection of the signal (spectrophotometer, fluorimeter or luminometer).

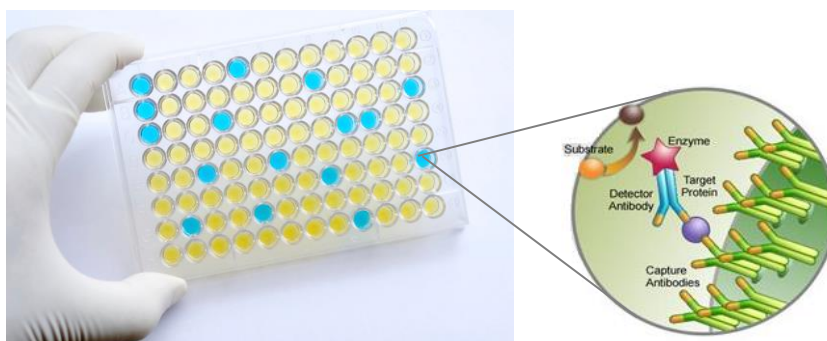


Figure 4 Typical ELISA plate with 96 wells and schematic representation of direct sandwich type working principle.

### 1.3.1 ELISA Formats

ELISAs can be performed with different methodological approaches. There are mainly two types of ELISA assays and each of them can be applied in direct or indirect mode:

- Competitive ELISA
- Sandwich ELISA

Depending on the target analyte (antigen or antibody), ELISA can be competitive, useful for both antigen and antibody detection, or sandwich that is dedicated for antigen detection.

In the first case, the assay is projected for the determination of antibodies as target analytes, but can also be rearranged for the determination of antigens, thanks to an immunocompetitive mechanism.

The antigen is immobilized on the surface of the plate, and during the incubation of the sample the antibody is recognized and subsequently detected by direct enzyme labelling or through a secondary detection antibody (conjugated anti-species antibody), as reported in Figure 5.

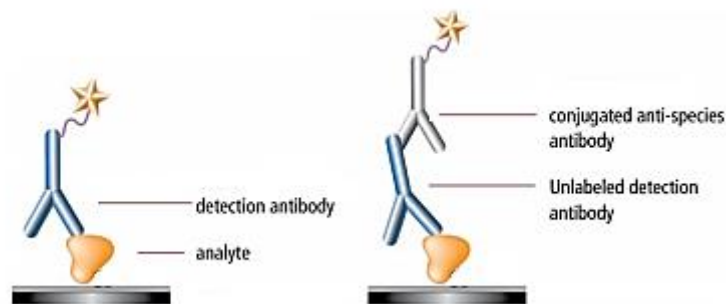


**Figure 5 Direct and Indirect ELISA for antibody detection.**

The antigen-functionalized plate can be also used for competitive determination of the same antigen, through an immunocompetition carried out mixing the specific antibody to the sample containing the target antigen. In this way, the antibody will interact preferentially with the free antigen (when present in the sample) and, only in its absence, it will be adsorbed on the plate surface through interaction with the immobilized antigen. As a result of the immunocompetition, the recorded signal will be high in the absence of target antigen in the sample, showing an inhibition rate proportional to the antigen concentration in sample.

The most powerful ELISA assay format is the sandwich assay, useful for antigen detection. This type of capture assay is called “sandwich” because the analyte to be measured is bound between two antibodies: the capture antibody and the detection (or reading) antibody. The plates are functionalized with the capture antibody and, during the incubation of the sample, the target antigen is recognized and adsorbed. Subsequently, a second (reading) antibody reacts with the antigen through a different epitope, generating the “sandwich” immunocomplex. In direct sandwich assay the reading antibody is directly conjugated with the enzyme label, while for indirect approach a third enzyme-conjugated (secondary anti-antibody) is used (see Figure 6).

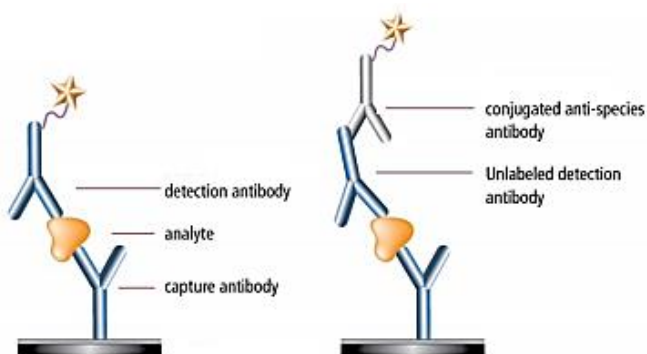


**Figure 6 Direct and Indirect Sandwich ELISA.**

### 1.3.2 Comparison of Direct and Indirect ELISA detection methods

The choice of the proper ELISA protocol is very critical and could be carefully performed on the basis of the analytical purpose and of the required performances. Direct ELISA has the advantage to be fast, because only one antibody and fewer steps for immunoassay development are used, furthermore, cross-reactivity of secondary antibody is avoided. However, immunoreactivity of the primary antibody might be affected by labeling with enzymes or tags.

On the other hand, indirect ELISA present the advantages arising from the wide variety of labeled secondary antibodies commercially available, to be used when a specific enzyme-labelled antibody directed against the target antigen is not available. The main drawback of indirect ELISA is the requirement of an extra incubation in the assay procedure, with consequent worsening increase of the time involved in the process.

### 1.3.3 ELISA detection step

The final stage in all ELISA systems is a detection step, suiting the reactivity of the labelling system, based on the use of enzymatic, fluorescent or radioactive tags. In the first case, this step involves the introduction of an enzyme substrate which is converted into a useful and detectable product. In fact, the intensity of signal produced when the substrate is added is directly proportional to the amount of target analyte.

Enzyme-conjugated antibodies (commonly HRP and AP) offer the most flexibility in detection and documentation methods for ELISA because of the variety of substrates available for chromogenic, chemifluorescent and chemiluminescent imaging.

Although they are not as sensitive as fluorescent or chemiluminescent substrates, chromogenic ELISA substrates allow direct visualization and enable to perform kinetic studies. Furthermore, chromogenic ELISA substrates are detected with standard absorbance plate readers common to many laboratories. On the contrary, fluorescent ELISA substrates are not as common and require a fluorimeter that produces the correct excitation beam to cause signal emission to be generated from the fluorescent tag. Though best used with a luminometer plate reader, chemiluminescent substrates can be detected by various means including digital camera systems. The main drawback of using chemiluminescent substrates is that the signal intensity can vary more with than other substrates.

The above described ELISA tests are high throughput methods, allowing a screening of a large number of samples and multi-target analysis for the same sample, even if the analysis is qualitative or semi-quantitative and, in some instances, they need a confirmatory comparison with other analytical methods. Moreover, they required the use of a dedicated instrumentation for the optical detection step, generally quite unwieldy and not suitable for analysis outside the dedicated laboratory. In this perspective, immunosensors are a good alternative to the ELISA tests, indeed they combine the advantages of the high antigen-antibody specificity and selectivity with the advantage of a cheap and easy-to-use instrumentation, also suitable for *in situ* analysis, thanks to the compactness of the required instrumentation. Furthermore, in most cases it is possible to reach better sensitivity associated to lower Limit Of Detection (LOD), with respect to the corresponding ELISA photometric kit.

## 1.4 AMPEROMETRIC IMMUNOSENSORS

On the basis of their transduction element, immunosensors can be categorized as electrochemical, field-effect transistor, optical, piezoelectric, surface acoustic wave and thermal.

Focusing the attention on the electrochemical sensors, according to the measured variable (voltage, current or resistance) they can be classified in [10]:

- Potentiometric
- Conductometric or impedimetric”
- Amperometric and “coulometric”

Electrochemical immunosensors are mainly based on amperometric transduction, suiting the electroactivity of specific enzymatic substrates.

In the last years amperometric immunosensors have been widely applied in several fields of applications such as medicine, food quality, control, environmental monitoring and research, thanks the possibility to reach high sensitivity, with easy-to-use, cheap and compact instrumentations, allowing *in situ* analysis and testing of small volumes of sample [11]. Their working principle is based on measuring of current that arises from the application of a certain potential, able to induce the oxidation or reduction of an electrochemical species.

Basically, the required instrumentation is composed by a potentiostat connected to a three-electrodes device (Figure 7).

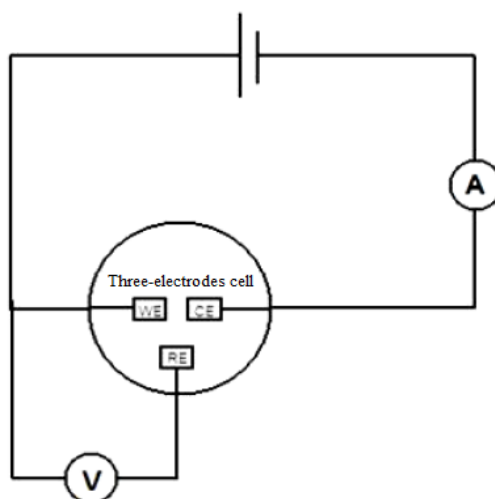


Figure 7 Three-electrodes system.

The potentiostat is the apparatus necessary to apply the potential and to monitor the current arising from the electrode faradic process. Nowadays potentiostats consist of discrete integrated-circuit, operational amplifiers and other digital modules. In many cases, especially in the larger instruments, the potentiostat package also includes electrometer circuits, A/D and D/A converters, and dedicated microprocessors with memory.

The three-electrodes system, connected to the potentiostat, is composed by:

- Working electrode (WE)
- Counter electrode (CE)
- Reference electrode (RE)

Concerning amperometric biosensors, the biological receptor is immobilized on the working electrode surface (generally made with gold, carbon or platinum), the potential applied between the working and the counter reference electrode, and measured *versus* the reference electrode (commonly an Ag/AgCl electrode or Ag pseudo reference) is pre-scanned or kept constant at a certain value, and the current resulting from the oxidation or reduction of the electroactive species, is measured between the working and the counter electrode. However, in some cases, the analyte of interest is not able to attend the redox reaction and it is necessary to use a redox mediator able to give rise to an electrochemical signal indirectly referable to the concentration of the analyte. This is the case of the amperometric immunosensors where the analyte is a protein species, like an antigen or an antibody, and the detection step is performed through electrochemically active labels, usually enzymes. For example, in the case of immunosensors involving AP-conjugated antibodies, the alkaline phosphatase is able to dephosphorylate a phosphate-substrate, such as di-phosphate hydroquinone, natively not electroactive, giving rise to hydroquinone detectable by its oxidation to quinone. The electrochemical signal related to the hydroquinone oxidation is then indirectly referred to the concentration of the target protein.

## 1.5 VOLTAMMETRIC METHODS

The collective term ‘voltammetry’ comprises all methods based on the evaluation of current-potential responses, including the above described amperometric method.

Voltammetry [12, 13] is an electrochemical technique useful to obtain information of analytical (concentration), thermodynamic (redox potentials and equilibrium constants) and kinetics (reaction rate) concern. This technique consists in varying the applied potential and measuring the resulting current.

There are different voltammetric methods:

- Linear Sweep Voltammetry (LSV)
- Rapid Scan Voltammetry-Linear Sweep Voltammetry (LSV)
- Cyclic Voltammetry (CV)
- Differential Pulse Voltammetry (DPV)
- Square Wave Voltammetry (SWV)
- Rotating Disk Voltammetry RDV - Rotating Ring-Disk Voltammetry (RRDV)
- Stripping Voltammetry SV- Anodic Stripping Voltammetry (ASV)
- Cathodic Stripping Voltammetry CSV
- Adsorptive Stripping Voltammetry (AdSV)

Among them, CV and DPV are the most used for several fields of application.

### Cyclic Voltammetry

In CV a triangular potential scan is linearly applied in order to induce and explore a forward process (oxidation or reduction), followed by the related backward process involving the electroactive species (Figure 8). At the end of the first linear potential scan, the direction is inverted and the cycle can be repeated several times.

The obtained curve has a cyclic trend, in which anodic and cathodic signals are equally or asymmetrically represented, as a function of the electrochemically reversibility degree and of the thermodynamic and kinetics features of the studied system (Figure 8b).

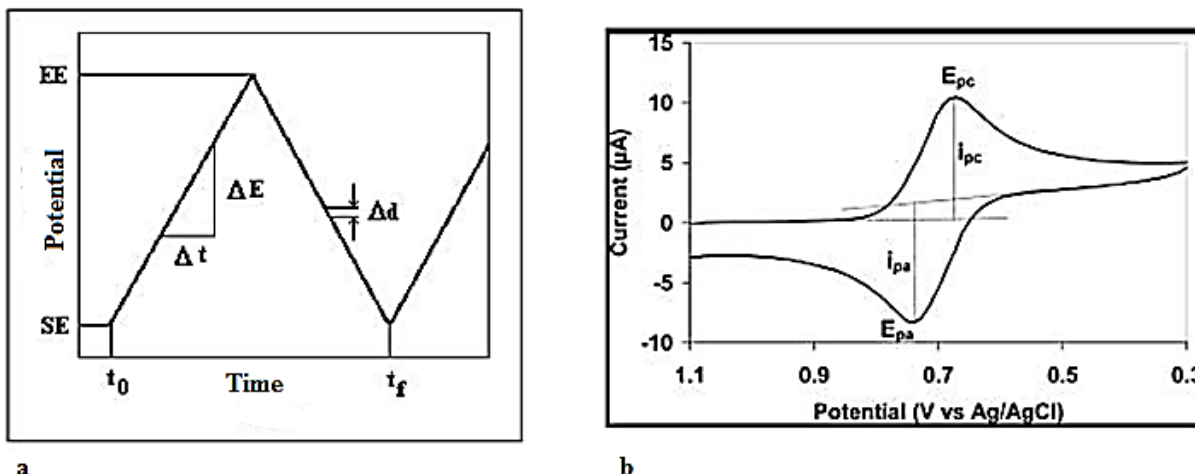


Figure 8 CV: a) Potential anodic scanning, b) Cyclic Voltammogram of a reversible system.

Basically, two fundamental parameters can be gained from a cyclic voltammogram: the ratio of peak currents,  $i_{pa}/i_{pc}$ , and the separation of peak potentials,  $E_{pa}-E_{pc}$  (as shown in Figure 8b).

It is possible to have information about the reversibility of the redox system, in terms of exchanged electrons and standard potential, through these relations:

$$(E_{pa}-E_{pc}) \cong (0.1984 \cdot T)/n$$

$$E^\circ \cong E_{1/2} \cong (E_{pa}+E_{pc})/2$$

$E_{pa}$ ,  $E_{pc}$  = potentials of anodic and cathodic peak (mV)

T= temperature (K)

n= number of exchanged electrons

As all the voltammetric methods, this is a non-destructive method and it requires low volume of samples for the analysis.

Generally, this technique is more used for qualitative analysis than for quantitative aims, allowing a rapid location of redox potentials of electroactive species and providing important information about reaction mechanisms and electrochemical properties of the explored analyte.

### Differential Pulse Voltammetry

In order to reach a signal improvement, enhancing the faradic component of the signal with respect to the capacitive background, the potential scan can be performed applying a periodic series of voltage pulses, with constant duration and amplitude (generally 10 to 100 mV), superimposed on a slowly changing base potential. This is the principle of the differential pulse voltammetry (DPV).



Current is measured at two points for each pulse, the first point just before the application of the pulse and the second at the end. The difference between current measurements at these points, for each pulse, is determined and plotted against the base potential (Figure 9b).

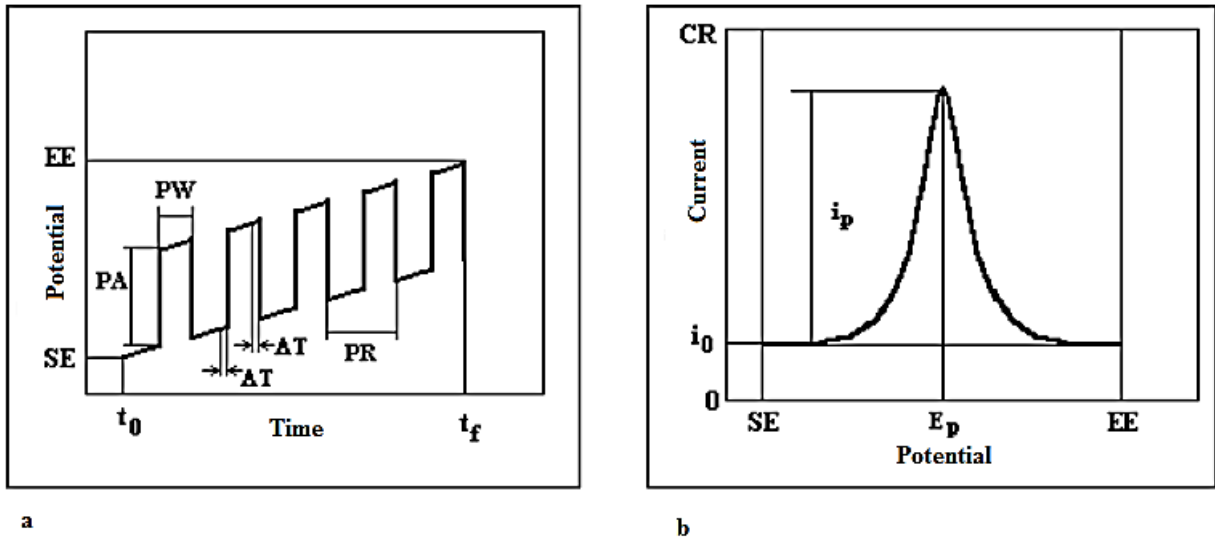


Figure 9 DPV: a) Potential anodic scanning, b) Voltammogramm.

This is a very sensitive technique and it is useful to detect low concentration of samples, where small signals are recorded, with a LOD improvement respect to the CV method.

## 2. ELECTRODES: CHARACTERISTICS AND FUNCTIONALIZATION

### 2.1 SCREEN-PRINTED ELECTRODES

Nowadays biosensors development involves Screen-Printed Electrodes (SPEs) as electrochemical substrates, thanks to their advantageous properties such as disposability, use simplicity, and low volume of samples requested for the analysis (10-50  $\mu\text{L}$ ) [14]. Furthermore, these substrates present compact size, making them successfully utilised for rapid *in situ* analysis in different fields of application, as environmental, clinical or agro-food areas. Another benefit of these electrodic supports is also the low manufacturing cost, allowing their massive production; for these reasons, the homemade fabrication of SPEs in small batches with screen-printing machines is more and more experimented. The formats of SPEs are variable with respect to the requirements for a specific analytical process. In addition, the surface of SPEs can be easily modified to fit multiple purposes. These electrodes are characterized by a ceramic or plastic support on which the three electrodes of the amperometric sensor are printed with different inks, according to the use [15-17]. Figure 10 shows a DropSens® SPE with the description of all the device components. According to the purpose of the immunosensor, it is possible to choose the material of each electrode, using glassy carbon, gold, platinum, and several other inks for WE and silver for RE. CE is usually printed with the same ink employed for WE. Inks based on carbon nanotubes, gold nanoparticles and various composite/nanocomposite materials are also used for the realization of high performance SPEs, particularly suitable for the development of biosensing devices.

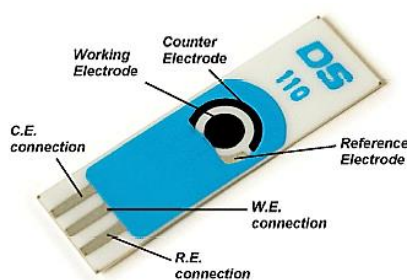


Figure 10 DropSens® SPE.

The choice of the proper electrode substrate for a specific electrochemical immunosensor is fundamental for several reasons as the overall performance of the device (i.e. sensitivity, detection limit, precision etc.), the costs involved in its realization, the use of the assay and the possibility to adopt different approaches for the immobilization of the active bio-receptor [18].

SPEs combine ease of use and portability with simple and inexpensive analytical methods, making them a good alternative with respect to many of commonly used conventional analytical methods. For these reasons, biosensors implemented on SPEs represent a first choice for high-throughput screening analysis of numerous samples of clinical concern.

## 2.2 BIO-RECEPTOR IMMOBILIZATION METHODS

The most critical step in the development of a biosensor is the functionalization of the electrode surface with the bio-receptor and its integration in the transduction system.

In the case of the immunosensors based on antigen-antibody interaction, it is very important to maintain the peculiar features of the immobilized receptor, in terms of preservation of the structural and conformational features, preventing denaturing processes that could change its immunoreactivity. The immobilization methodologies are depending on the physical and chemical characteristics of the transducer element and the environment of the operation. The most used methods of functionalization [19, 20] are:

- Adsorption
- Gel entrapment
- Cross-linking
- Covalent bonding

### **Adsorption**

This is the simplest method, mild conditions are required and the functionalization is generally realized through weak interactions such as Van der Waals forces, dipolar interactions or hydrogen bonds; for this reason, it does not ensure the preservation of the functionalities of the receptor during the following steps. Biosensors based on adsorbed enzyme or proteins have often low sensitivity.

### **Gel Entrapment**

In this case, the protein is immobilized in a gel (polyacrylamide, agar, conductive polymers, polyurethane etc.) where covalent bonds are involved. As the previous case, mild operational conditions are required, although partial loss of the biological material are frequently noticed.

### **Cross-linking**

The fundamental characteristic of this method is the involvement of multifunctional reagents such as glutaraldehyde, bis-isocyanate derivatives or bis-diazobenzidine. These reagents are able to bind with one of their functional group the sensor substrate and with another one the biologically active species. The procedure is simple and it involves a strong chemical binding of the biomolecules, however, the regiochemical control of the immobilization reaction is very critical and fundamental in order to *i*) avoid the involvement of functional groups playing a primary role in the binding properties and *ii*) to preserve the optimal conformational freedom.

## **Covalent bonding**

The nucleophilic moieties of functional groups in the protein structure, such as amines, thiols and carboxyl are involved in the functionalization process. The interaction with substrate can be direct or mediated by a proper linker molecule that acts as a bridge between the substrate and the receptor. This approach guarantees the best performance in terms of stability and operating life of the biosensor, however, a partial or complete loss of the receptor-binding activity, due to the involvement of functional groups necessary for the biological activity, is possible.

## 2.3 NANOSTRUCTURED MATERIALS

Various nanomaterials, including carbon nanotubes, nanoparticles, nanomagnetic beads, and nanocomposites are being used to develop highly sensitive and robust biosensors and biosensing systems [21].

Nanostructured Materials (NsM) are materials with a microstructure of characteristic length scale on the order of a few nanometers (typically  $1\pm 10$ ).

Generally NsM consist of nanometer-size crystallites (e.g. Au or NaCl) showing different crystallographic orientations and/or chemical compositions. The properties of NsM deviate from those of single crystals (or coarse-grained polycrystals) and/or glasses with the same average chemical composition. This deviation results from the reduced size and/or dimensionality of the nanometer-sized crystallites as well as from the numerous interfaces between adjacent crystallites [22].

An important difference between the nanomaterials and the conventional bulk materials is the increase of the surface/volume ratio, with a consequent increase of the available surface area. Concerning the use of NsMs for biosensing applications, the above cited features makes them particularly useful for the efficient functionalization of the electrode surface with high loading capability and significant enhancement of the instrumental responses.

Among these materials, carbon nanotubes are characterized by nanometric diameters, while metal nanoparticles (Au, Ag, Pt, Pd, Ru etc.) are three-dimensionally nano-sized.

### 2.3.1 Carbon Nanotubes (CNTs)

Nanotubes can be defined as one of the allotropic forms of carbon. In these structures, one or more superimposed graphite sheets are folded to form a hollow cylindrical structure, with resulting properties, which depend on the atomic arrangement, the diameter and the length of the tubes. CNTs can be classified principally in two types (Figure 11b, 11c):

- Single-Walled Carbon Nanotubes (SWCNTs): constituted by a single graphitic sheet wrapped on itself;
- Multi-Walled Carbon Nanotubes (MWCNTs): formed from multiple sheets wrapped coaxially on each other.

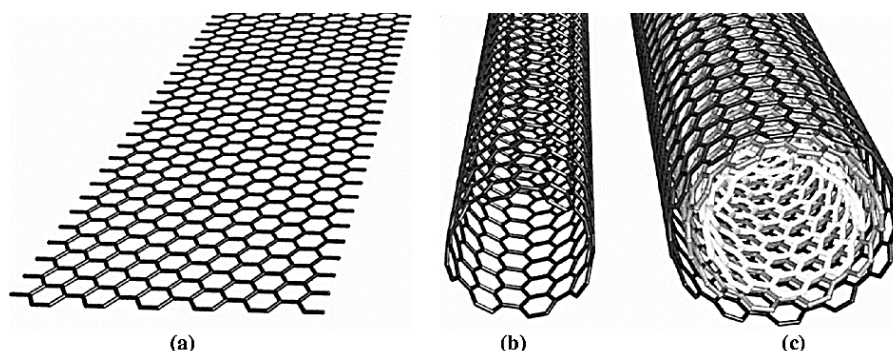


Figure 11 a) Graphite sheet, b) SWCNT, c) MWCNT [23].

The body of the nanotube is formed by only hexagons, whereas hexagons and pentagons form the closure structures. For this conformation of hexagons and pentagons, nanotubes often have structural defects or imperfections leading to deformations of the cylindrical structure. The diameter of a nanotube is between a minimum of 0.7 nm and a maximum of 10 nm. The very high length to diameter ratio (in the order of  $10^4$ ) allows considering them as virtually one-dimensional nanostructures with peculiar properties.

The study of the physical properties of SWCNTs and MWCNTs showed exceptional properties for several different potential applications in medicine, ranging from cancer radiation therapy and drug delivery to biosensors and tissue engineering.

Their curved structure and the hybridization of the carbons involved in the network, give them greater mechanical strength, thermal and electrical conductivity, along with the ability to be more active biologically and chemically compared to a single graphite sheet (Figure 11a).

From the electrical point of view, carbon nanotubes have some interesting properties: depending on their diameter and geometry, they may behave as current conductors, like metals, or as semiconductors, like silicon. This is important from the point of view of their application in biosensing, considering that such materials are able to improve the electrons transfer phenomena, involved in the electrochemical detection, thanks to the enhancement of the electrodic active area suitable for the immobilization of the receptors, and for the establishment of the electron transfer process.

### **2.3.2 Metal Nonoparticles**

The term nanoparticle normally identifies particles composed by atomic or molecular aggregates with a diameter approximately between 2 and 200 nm.

Metal nanoparticles are used for several application because of the advantages related to their mechanical strength, light weight, chemical and physical stability, conductivity and biocompatibility. These structures show very peculiar optical, electronic and magnetic properties, as a function of their size and specific composition.

Gold nanoparticles (AuNPs) are the mostly used metal nanoparticles in the field of biosensors, thanks to their high biocompatibility, stability, catalytic properties, and good performance in the enhancement of electronic transfer, concerning electrochemical devices.

AuNPs are optimal substrates for the immobilization of bio-receptors on the electrode surface, thanks to the high affinity of gold with the sulfur and nitrogen atoms carried on the of the cysteine- and lysine- moieties of all proteins; moreover, the enhanced surface area allows the immobilization of a larger amount of receptor. The chemisorption of enzymes, antibodies and other protein receptors on gold nanostructures takes place, in more cases, with retention of the biological activity of the receptor, maintaining a good conformational freedom.

A further advantage making AuNPs widely used for several applications is the simplicity of their chemical synthesis, requiring inexpensive instrumentation, simple procedures and low reaction times [24]. Concerning the use of AuNPs as electrodic substrates, Glassy Carbon Screen-Printed Electrodes (GC-SPEs) can be easily derivatized by potentiostatic or potentiodynamic electrodeposition of nanogold, starting from tetrachloroauric acid ( $\text{HAuCl}_4$ ). Although the electrodeposition of nanogold is a highly reproducible and standardized procedure, commercially available and ready to use Gold NanoParticles-functionalized Screen-Printed Electrodes (GNP-SPEs) are also used as nanostructured

substrates, as for the experiments discussed in the present thesis where Dropsens® GNP-SPEs were used (Figure 12).

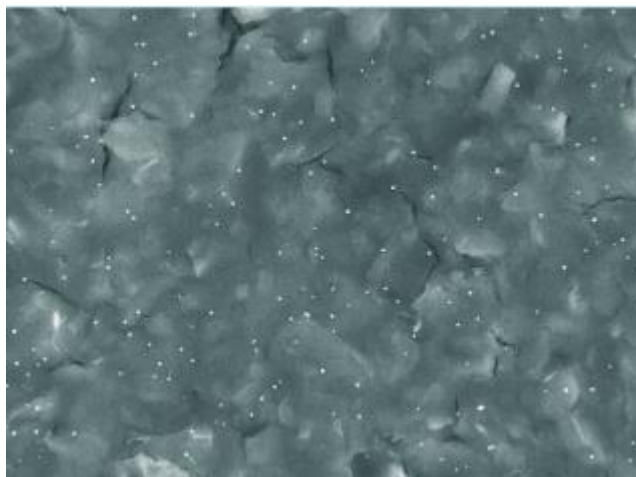


**Figure 12 SEM images of DropSens® GC-SPE working electrode.**

## 2.4 ANTIGEN AND ANTIBODY IMMOBILIZATION

As previous stated, (Chapter 2.2), the most critical step in biosensors development is the functionalization of the electrode with the bio-receptor. Concerning the immunosensors, the methodological approaches for the immobilization of antigens of antibodies are summarized as follows:

### 2.4.1 Antibody immobilization: direct and protein-assisted orientation

The easiest method for antibody immobilization is the adsorption on a solid substrate, through hydrophilic and/or hydrophobic interactions. However, in most cases the adsorbed antibodies are randomly oriented with consequent alteration of the binding properties for the target antigen [25].

In order to allow the recognition of one or more epitopes of the corresponding antigen, the proper orientation of the antibodies can be induced promoting the linkage via the Fc fraction, using auxiliary proteins such as protein A and G. They are able to specifically bind the Fc fraction of the antibody, ensuring the good exposition of the FAb fraction for the immunoreactivity. Depending on the specie and class of the antibody, it is possible to choose the auxiliary protein, on the basis of the best binding affinity, as reported in Table 2:

**Table 2: Relative affinity of Immobilized Protein A and Protein G for various antibody species and subclasses of IgGs.**

SPECIES	ANTIBODY CLASS	PROTEIN A	PROTEIN G
Mouse	Total IgG	++++	++++
	IgG <sub>1</sub>	+	+++
	IgG <sub>2a</sub>	++++	++++
	IgG <sub>2b</sub>	++++	++++
	IgG <sub>3</sub>	+++	+++
Human	Total IgG	++++	++++
	IgG <sub>1</sub>	++++	++++
	IgG <sub>2</sub>	++++	++++
	IgG <sub>3</sub>	+	++++
	IgG <sub>4</sub>	++++	++++
Rat	Total IgG	+	++
	IgG <sub>1</sub>	-	+
	IgG <sub>2a</sub>	-	++++
	IgG <sub>2b</sub>	-	++
	IgG <sub>2c</sub>	++	+++
Hamster	Total IgG	++	++
Guinea Pig	Total IgG	++++	++
Rabbit	Total IgG	++++	+++
Horse	Total IgG	++	++++
Cow	Total IgG	++	++++
Pig	Total IgG	+++	++
Sheep	Total IgG	+	++
Goat	Total IgG	+	++
Chicken	Total IgG	-	-



### 2.4.2 Antibody immobilization through covalent immobilization- Self assembled-monolayer

Covalent cross-linking of antibodies on chemically activated solid surface is another common method for antibody immobilization. Amino- or carboxyl- groups of the amino-acids located on the “side chains” of the antibody can be coupled with the complementary functional groups, previously immobilized on the solid support. Self Assembled-Monolayers (SAMs) are very efficient and versatile scaffolds for the orientated immobilization of bio-receptors.

SAMs are generated through a spontaneous process consisting in the organization of heterobifunctional molecules in stable aggregates with structures stabilized by non-covalent bonds. The linking is established by a head group with high affinity for the substrate where the layer is going to be realized, while a tail group is generally located at the end of an aliphatic chain (Figure 13).

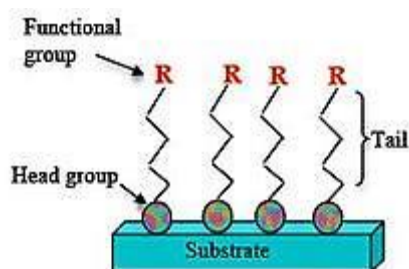


Figure 13 SAM structure.

These aggregates are created by the chemisorption of head groups onto the substrate, followed by a slow organization of tail groups. Initially, adsorbed molecules form a disordered mass, subsequently rearranged in the “slow stage” of the process, where the tail groups assemble together, through Van der Waals interactions, with a subsequent organization of a three-dimensional crystalline or semi-crystalline structure on the substrate surface. The functional tail-groups (R) play an active role in the covalent linking of the target biomolecule through amide bonds, with optimal spacing from the electrodic substrate, tunable as a function of the length and orientation of the hydrocarbon spacer chain.

This method is widely used for biosensing applications for the mild conditions required and easiness of preparation, based on simple drop casting of a solution of the heterobifunctional cross-linker on the active surface (i.e. working electrode).

An example of SAM-mediated immobilization of antibodies involves a mercapto-carboxylic acid, with variable hydrocarbon chain length, and N-Ethyl-N'-(3-(dimethylamino)propyl)carbodiimide (EDC) associated N-hydroxysuccinimide (NHS) as coupling reagents promoting the covalent linking via amide bonds [26, 27].

The thiol -group of the linker play the role of head group, necessary for the interaction with the gold substrate. After the immobilization of the SAM, the carboxylic groups linked to the electrode surface, are activated with EDC forming an active O-acylisourea intermediate that is easily displaced by nucleophilic attack from the amino amino groups of the target molecule to be anchored. Considering that the O-acylisourea intermediate is unstable in aqueous solutions, being easily hydrolysed, the reaction is co-assisted by NHS, forming an intermediate ester that is considerably more stable than

the O-acylisourea intermediate, allowing for an efficient conjugation to primary amines at physiologic pH. The mechanism of the EDC/NHS-assisted coupling reaction is described in Figure 14.

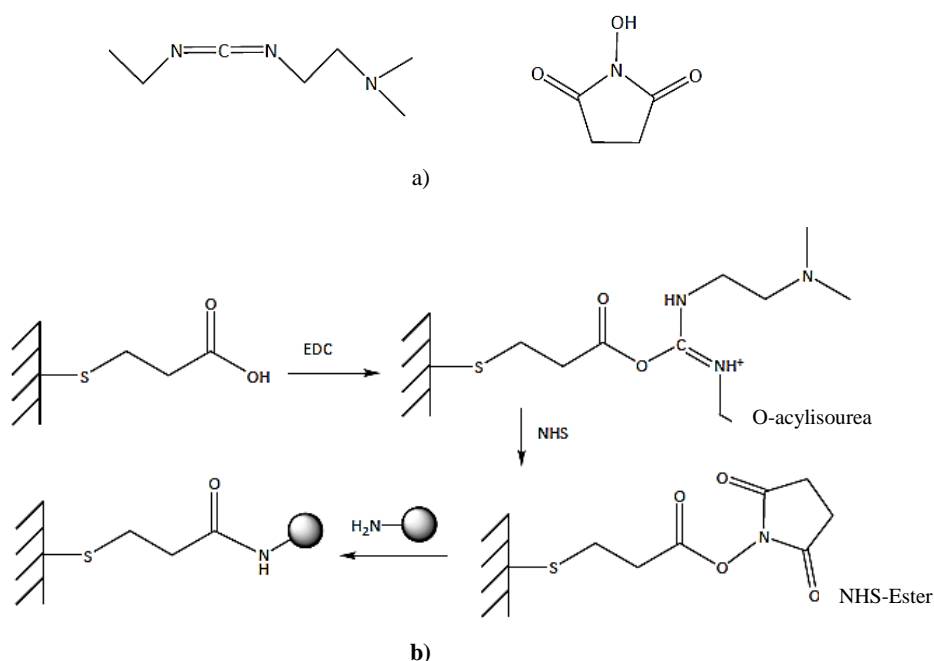


Figure 14 a) EDC and NHS molecular structures, b) EDC/NHS-assisted coupling reaction.

Although this approach ensures the stability of the covalent linking, it does not guarantee the proper orientation of the antibody. For this reason, the combination of SAMs with auxiliary proteins is frequently used [28].

### 2.4.3 Direct immobilization of antigen

The above discussed linking methodologies can analogously be used also for the functionalization of the electrode surface with antigen proteins, choosing the strategy suitable for the electrodic material (glassy carbon, gold nanoparticles, carbon nanotubes, etc.) and according to the performance required to the sensor.

If the antigen is directly chemisorbed on the surface of the working electrode (Figure 15), the linkage is allowed through the interaction between sulfur and/or nitrogen donor atoms of the protein and nanostructured or flat gold [29, 30] of the electrode substrate. As for immunosensors, the direct approach is frequently critical because the chemisorption could involve functional groups included in the epitopes participating to the immunochemical recognition.

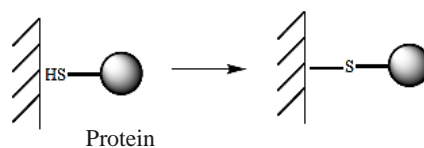


**Figure 15 Direct electrode functionalization with the bio-receptor.**

In order to overcome these problems, bi-functional linkers, as the above described SAMs, can be successfully suited also for the regio-controlled immobilization of the antigen proteins, aimed to prevent the involvement of the immuno-reactive antigen moieties.

#### 2.4.4 Antigen immobilization through SAM system

As previously described for antibody immobilization, also for antigen it is possible to use the SAM approach. In this case, the length of the spacer arm of the heterobifunctional linker plays a key role. In fact, if the aliphatic chain is too long, folding phenomena could partial or completely shield the receptor, decreasing or inhibiting its reactivity with the target antibody. Conversely, a too short spacer does not allow the conformational freedom requested for the immunoreactivity.

#### 2.4.5 Chitosan/glutaraldehyde system

A recently investigated cross-linking approach, alternative to deposition of SAMs on gold substrates, is provided by the combined use of chitosan (CH) and glutaraldehyde (GA) on gold-free carbon electrodic substrates.

Chitosan is a linear polysaccharide composed of randomly distributed  $\beta$ -(1,4)-linked D-glucosamine and N-acetyl-D-glucosamine. It is produced by treating the chitin shells of shrimp and other crustaceans with an alkali, like sodium hydroxide; its structure is not well defined and may differ in molecular weight, degree of acetylation and the sequence of the monomers. The peculiar feature of CH is the presence of a primary amino group at C-2 position of the glucose-amine residues, as shown in Figure 16.

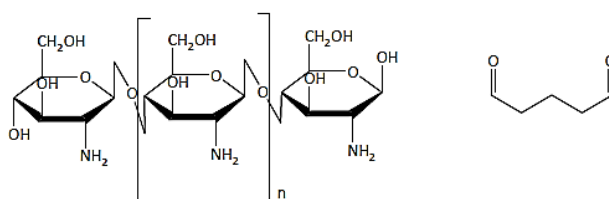


**Figure 16 Chitosan and glutaraldehyde structures.**

Chitosan is chemisorbed on carbon substrates, while glutaraldehyde is used as cross-linker for covalent binding of bio-receptors [31-33].

The aldehyde (GA), acts as bridging molecule, connecting the chitosan backbone with the bio-receptor, using the two terminal carbonyl groups, giving raise to imidic bonds. The cross-linking reaction is schematized in Figure 17:

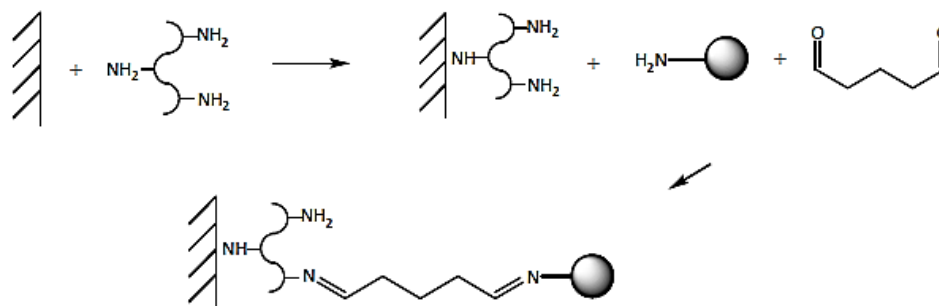


**Figure 17 Reactions involved in chitosan/glutaraldehyde system.**

This immobilization method allows a better functionalization of the electrode surface, ensuring an ordered layer that promotes a good exposure of the antigen epitopes for reaction with the antibody, thanks to the presence of two imide bonds and a relatively short hydrocarbon chain, allowing the proper conformational freedom and preventing folding phenomena.

Chemical-physical and biologic properties of chitosan, are related to its molecular weight and deacetylation degree [34, 35], with effects on the binding ability, as a function of the extent of available amino-groups.

As for the behaviour of glutaraldehyde as cross-link agent, the pH of the solution used for the derivatization of the electrode plays a fundamental role [36]. The more versatile formulation of GA is commercially available as ready to use acidic aqueous solutions (pH 3.0–4.0) with concentration ranging from 2% to 70% (w/v), packaged in sealed vials due to high self-reactivity of the reagent.

The cross-linking capability of GA is strongly dependent on its polymerization degree, since it can exist in solution not only as monomeric di-aldehyde, but also as a dimer, trimer, and other oligomers, as reported in Figure 18.

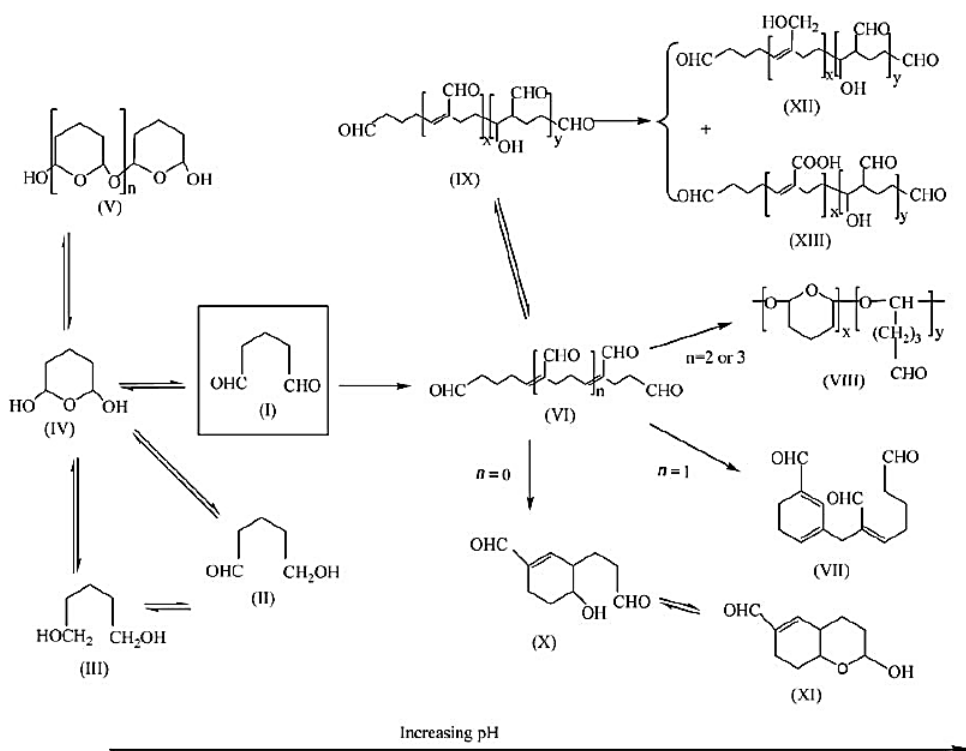


**Figure 18** Summary of the possible forms of glutaraldehyde in aqueous solution.

Some studies [37] reported that upon dilution, the polymerized glutaraldehyde is slowly converted to monomers, thus inducing a great variation in the relative abundances of monomeric and polymeric species, according to the glutaraldehyde concentration. The findings of these studies indicate that in dilute solutions and in the at pH values ranging from 3.0 to 8.0, glutaraldehyde is almost monomeric, predominantly in cyclic hemiacetal form (structure IV). In 1997, the same authors [38] found that glutaraldehyde structure was similar for aqueous solutions up to 10% (w/v).

On the basis of the above considerations, the experimental conditions in terms of pH and GA concentration have to be carefully set in order to improve the number of useful monomers for the cross-linking reaction.

## **AIM AND SCOPE OF THE PhD THESIS**

The aim of the present thesis project was the development and validation of sensing devices implemented on Screen-Printed Electrodes (SPCEs) based on different electrodic materials, with applications in the fields of biomedical diagnosis and food safety control.

We challenged different goals, focusing the attention on competitive immunosensor for early and rapid diagnosis of HIV and HCV infections (*see Chapters 3 and 4*), use of micro- and nano- materials for biosensing applications (*Chapter 5*) and development and validation of a competitive immunosensor for quality assurance of foods and dietary products specially formulated for celiac disease patients (*Chapter 6*) .

## 3. HIV AND HCV

### 3.1 HIV

The Human Immunodeficiency Virus (HIV) is responsible for the Acquired ImmunoDeficiency Syndrome (AIDS), considered a pandemic disease by the World Health Organization (WHO) [39-40]. HIV is a retrovirus (virus able to replicate in a host cell through the process of reverse transcription) belonging to the lentivirus type, which is characterized by a long incubation period [41]. As lentivirus, it is able to give rise to a chronic infection, which is insensitive to the immune response, showing a slow but progressive evolution with fatal outcome, in the absence of proper treatments.

HIV occurs in two serotypes, HIV-1 and HIV-2, the first of which is the most common, more virulent and infective respect to the second one [42]. Globally, it is the cause of the majority of HIV infections and it is particularly common in Europe, America and central Africa. The HIV-2, on the contrary, is more common in western Africa and Asia, and is related to a much more moderate syndrome.

The pathogenic course, from infection to AIDS, which is the acute phase, can be divided into three stages:

- the acute infection
- the clinical latency stage
- the symptomatic stage (immunodeficiency expression)

The acute infection is characterized by the rapid and massive viral replication, with progressive increases of the viral load, reaching values of millions of RNA copies/mL.

The acute phase ceases with the beginning of the immune response, which requires from 2 to 8 weeks and leads to the production of anti-HIV antibodies. Antibodies have neutralizing activity and are able to inactivate a large amount of free and circulating virus. The end of the acute phase is characterized by a significant reduction of the viral load.

The immune response is followed by the so-called clinical latency stage, characterized by a variable duration, ranging from a few years up to more than fifteen years. During the clinical latency, the virological pathway is still on, with HIV replication particularly noticed in the lymphatic tissues, contained and controlled by the immune response.

#### 3.1.1 HIV virion morphology

HIV virion is characterized by a spherical structure, with a diameter of about 100-120 nm. It consists of two outer membranes (pericapsid) that involve an external structure, called envelope, and a cone shaped membrane. The envelope is composed of two layers of phospholipids and a viral glycoprotein complex, called Env, composed of a cap with three molecules of glycoprotein gp120 and a stem which consists of three molecules of gp41, that anchor the complex to the envelope. The glycoproteins gp120 and gp41 are responsible for the binding and the access of the virus in the host cell.

The virion integrity is ensured by a matrix composed of p17 proteins that surrounds the conic structure, called capsid or viral core, containing p24 proteins [43].

In the core of the virion cell, there are two copies of positive single-stranded RNA (mRNA) which code for the virus genes. These two copies are strongly bound to the nucleus-capsid proteins where are also the reverse transcriptase enzymes (DNA polymerase and RNA-dependent), protease and integrase enzymes (Figure 19).

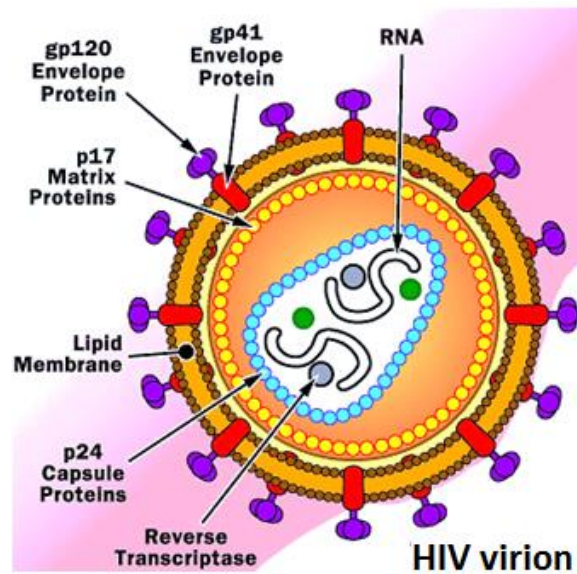


Figure 19 Schematic representation of HIV virion.



## **3.2 HCV**

Hepatitis C Virus (HCV) is a Hepacivirus of the Flaviviridae family and it is responsible for the liver disease Hepatitis C [44-46]. It was discovered in 1989 with occurrence of six different viral variants identified, named from 1 to 6, differing for the genotype (the content of genetic information) with more than 90 subtypes (named a, b, c, etc.) [47]. The 6 genotypes are differently distributed in the world, with a prevalence of type 1 [48].

The target organ of HCV is the liver, through activation of the host immune system, causing structural and functional damage also very serious. Specifically, the infection causes the death of liver cells (liver necrosis), which are replaced by a new repair-healing tissue, so as to determine the process of hepatic fibrosis. This scar tissue might replace all or most of the healthy part of the liver, which leads to severe impairment of its activities, evolving, as the last stage, to liver cirrhosis.

A high proportion of asymptomatic forms characterizes hepatitis C. Clinically, in most cases, the onset of the disease is asymptomatic, in fact, the majority of HCV-positive people are unaware of being infected, becoming aware of their own state only by accident. The clinically evident acute episode, which is not very frequent, can be characterized by the appearance of jaundice, pain in the right hip, feeling sick and tiredness as well as an important increase in transaminases.

The symptoms can be present predominantly after two or three months after infection, at the peak of transaminases and of the appearance of HCV-related RNA.

About 15-45% of infected people spontaneously clear the virus within six months of infection without any therapeutic treatment. The remaining percentage of people develop chronic HCV infection and, beyond them, the risk of cirrhosis is between 15-30% within twenty years.

### **3.2.1 HCV virion morphology**

As HIV, HCV virion is characterized by a spherical structure, but with a smaller diameter of 55-65 nm. It consists of a pericapsid with a predominantly lipid composition and an icosahedral capsid containing molecule of single stranded RNA with positive polarity [49].

In the pericapsid areas, it is possible to identify two glycoproteins (E1 and E2), characterized by hypervariable regions, responsible for the great antigenic variability of the virus, and other proteins: among which NS4A and NS4B, cofactors of the NS3 protease, and NS5A (a protein able to regulate the interferons) (Figure 20).

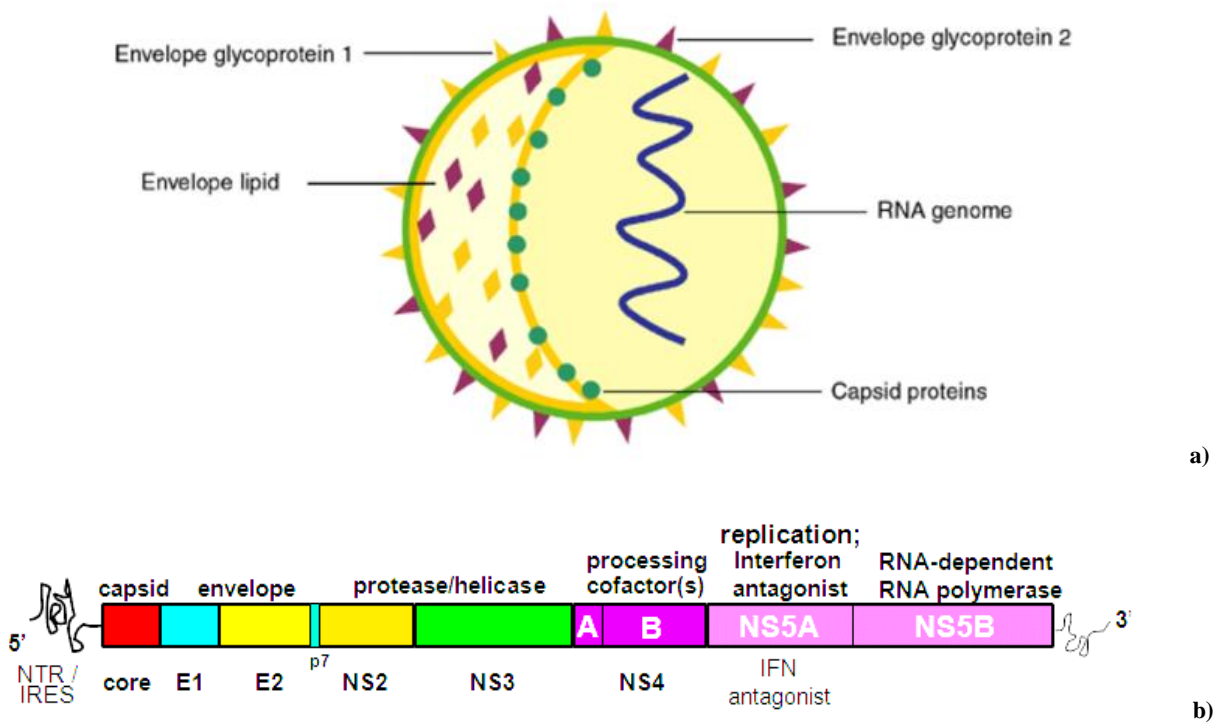


Figure 20 HCV: a) Model structure and b) Genome organization.

### 3.3 HIV-HCV ROUTE OF TRANSMISSION

Both HIV and HCV can be transmitted by exposure to infected blood, through sexual intercourse and from a mother to her infant. However, the percentage of transmission through these shared routes is different between the two viruses.

HCV is approximately 10 times more infectious than HIV through blood exposures [50]. About sexual transmission, between heterosexual partners, HIV is more transmissible than HCV [51], indeed, this route of transmission for HCV is uncommon, but may be more likely in persons with partners who are co-infected with HIV and HCV. However, although more prospective studies of HCV male homosexual couples are needed to clarify the risk, the existing data indicate that intercourse is a more efficient mode of transmitting HIV than HCV.

Concerning HIV, vertical transmission, from mother to infant, without antiretroviral treatment, occurs in 20% to 30% of infants born to HIV infected mothers. Conversely, this way of transmission is uncommon for HCV infection, which occurs in approximately 2% to 5% of infants born from HCV positive mothers. In most studies, the incidence of HCV transmission from mother to infant increases if the mother is co-infected with HIV [52, 53].

### 3.4 HIV–HCV CO-INFECTION

It is estimated that about 4.5 million people are living with HIV -HCV co-infection in the world. In Italy people with co-infection are about 33,000 but considering also not aware population, this number rises to more than 50,000. In other words, in Italy about 40% of HIV-positive people are also co-infected by HCV [54].

Co-infection is common because of similarities in the routes of transmission [55, 56] and the early diagnosis is a crucial aspect for each of these viruses [57, 58]. Co-infection by HIV accelerates the progression of HCV liver disease to cirrhosis and hepatocellular carcinoma [59-61], significantly increasing the mortality rate, with respect to patients infected by only HCV [62, 63]. Analogously, it seems that HCV is one of the causes leading to death in HIV-positive populations, affecting one third of third of them [64]. HCV might promote the HIV disease progression according to different pathways: it may enhance the virus replication, favour the CD4 T-cell (cell type playing a key-role in the immune system, particularly in the adaptive immune system) and deplete the effectiveness of antiretroviral therapy, increasing the toxicity of drugs. However, clinical studies that examined the influence of HCV on HIV disease progression show conflicting results [65-70]; not all studies evidence an association between HCV infection and faster HIV disease progression.

### 3.5 METHOD OF DIAGNOSIS

In view of the above described effects, arising from the co-infection, a timely diagnosis is necessary in order to monitor the consequences of the HIV/HCV co-presence.

The methods available to diagnose the occurrence of these infections are summarized as follows:

- Methods based on antibodies: requiring a “window period” (4-8 weeks) to be detectable in blood stream, as a results of the time necessary for their production by the immune system;
- Methods based on the research of viral nucleic acids: the so-called NAT methods (Nucleic Acid Test), which, however, are expensive tests that also require the use of sophisticated instrumentation, expert technicians, making them less suitable for routine analysis in laboratory;
- Methods based on the determination of the viral proteins: like the capsid protein. These proteins are expressed intracellularly and detectable in the serum of subjects infected earlier than antibodies, through an easy-to-use instrumentation and with low cost analysis. The capsid proteins are expressed in the viral core cell and enter in blood-circulation since the first few weeks after infection contraction, this make them useful markers for an early diagnosis. These proteins are respectively p24 for HIV and NS4 for HCV.

### 3.5.1 HIV methods of diagnosis

To date, no drug or vaccine [71] has become available to treat or stop the onset of disease [72]; therefore, prevention is the primary strategy to control HIV. Diagnosis of HIV infection, through laboratory analysis, is a fundamental aspect and a sensitive and practical detection method to monitor, diagnose, and screen HIV infection is especially important for controlling AIDS [73].

In recent years, the World Health Organization (WHO) underlined that effective treatment prevents onward transmission of HIV, thus, an improvement of testing coverage is fundamental, especially where it is hard to reach people with diagnostic instrumentation, in resource-limited regions (e.g. poor area of Africa). For this reason the research attention is focused on new testing approaches, to facilitate greater uptake, earlier diagnosis, and greater access to prevention, care and treatment services [74].

Among the diagnosis methods available, as previously introduced, HIV-antibody detection is not suitable for timely diagnosis of HIV-infection, requiring a too long “window period” to be detectable. The ‘window period’ describes a stage between immediate acute HIV infection and serum conversion of virus specific antibodies that normally develop within 4 to 8 weeks, but sometimes up to 6 months after infection, depending on the individual [75, 76]. During this period it is possible to have false negative results, even though a person is infected with HIV.

There are principally two types of assays for IgG antibodies detection: first and second Indirect Enzyme Immunoassays (EIAs) that detect antibodies to viral lysate and recombinant or synthetic peptide antigens, respectively. As alternative to exclusively IgG antibodies detection, it is possible to detect both IgG and IgM antibodies, with the 3rd generation antibody assays [77]. These are EIAs based an antigen-sandwich format, increasing their ability to detect all HIV antibodies isotypes. Furthermore, 3rd generation assays reduces the serological window to approximately 3 weeks [78], because IgM is usually expressed before IgG in response to the infection.

Methods based on the research of viral nucleic acids, as PCR (Polymerase Chain Reaction), also known as Nucleic Acid Amplification Test (NAAT), which detects viral RNA or DNA, are useful for early diagnosis of HIV infection [79, 80], with the advantage to detect the HIV during its initial incubation stage. NAAT has significantly narrowed the time-gap between initial infection and its detection, through amplification of viral nucleic acid rather than detecting the presence of antibody following seroconversion [73]. However, these are laborious methods and require specialist and expensive instrumentations, with limitation in the applicability, especially in resource-limited regions and point-of-care service providers [81].

Nowadays, the requirement of simple, rapid, sensitive, specific, and inexpensive HIV screening method, also supported by a portable instruments to prevent and control AIDS propagation, is strongly increased, because this infectious disease is one of the global-health burden, especially in resource-limited settings.

As previously introduced, the HIV-1 capsid protein p24 plays a primary diagnostic role for early diagnosis, entering in blood circulation since the following weeks of HIV exposure and being detectable earlier than the antibodies [82, 83], furthermore it is used to develop sensitive assays, comparable in sensitivity to PCR, but with easy-to-use instrumentations, suitable for routine analysis. In addition, this protein plays a fundamental role also in the acute phase of the disease, AIDS, because its blood concentration is closely related with the viral load, and 30 viruses/mL equates to

approximately 3 fg/mL of p24. For this reason it can also be used for monitoring the effectiveness of antiretroviral therapy [84], as biomarker for follow-up purposes (Figure 21). As a consequence, an increasing attention have been recently focused on development of p24-based assays, beside the already available 4th generation EIA assays, able to detect both p24 and HIV antibodies (IgG/IgM).

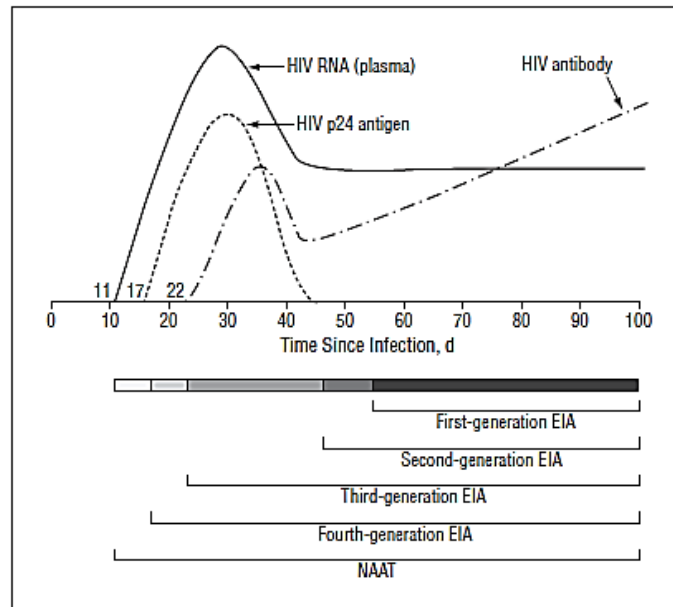


Figure 21 Window of detection of HIV markers in early infection and window period of different EIAs compared to NAAT [85].

### 3.5.2 HCV methods of diagnosis

HCV infection is a global health problem for which, in the absence of vaccine availability, prevention is the only way to reduce the possibility of infection. However, an early infection diagnosis is fundamental for the establishment of an appropriate follow-up protocol, as well as for limitation of the virus transmission to other persons. WHO suggests specific screening programs for people potentially exposed to risk of infection, such as:

- people using narcotic drugs through intravenous administration ;
- people using intranasal drugs;
- people exposed to contacts with blood-contaminated materials or carrying out invasive procedures in health-care facilities with inadequate infection control practices;
- children born to mothers infected with HCV;
- people acting risky sexual practices with occasional (potentially infected) partners;
- people with HIV infection;
- people who have had tattoos or piercings.

As previously described, Hepatitis C is characterized by a high proportion of asymptomatic forms, as the most part of people are not aware to be HCV-positive and only few of them are diagnosed during the acute phase of the infection. Indeed, chronic hepatitis is asymptomatic and until decades after infection, when it becomes symptomatic and it develops to liver damage, people discover to be infected. For these reasons people who may be exposed to high risk of infection should be screened as soon as possible.

Nowadays hepatitis C diagnosis is based on two main blood tests [86, 87]:

- the detection of specific antibodies against HCV;
- the identification of viral particles through the examination of the HCV-RNA (qualitative analysis) and viral load determination (quantitative analysis).

Specifically, the second test it is necessary if the antibody-test is positive, in order to confirm chronic infection. In fact, about 15–45% of people infected by HCV undergoes spontaneous immuno-mediated clearance of the infection, keeping a positive response to anti-HCV antibodies blood screening. Thus, detection of anti-HCV antibody cannot distinguish between a current or past infection; in addition, this kind of test might provide false negative results because the window period required for antibodies detection is of about 45-68 days. On the other hand, the test based on HCV-RNA allows to discriminate between past and current infection, however false positive results are possible due to contaminations. Anyway, nucleic acid-tests are labour-intensive and expensive for routine use [88, 89], as previously discussed.

In the last years there was a great interest on the detection of HCV core antigens, since they appear earlier than antibodies and may be detected within 1 or 2 days following the appearance of HCV RNA in serum [90-92]. Furthermore, in the acute phase of the infection, it has been reported a significant correlation between core antigens levels and RNA [93, 94], making them valuable indirect markers of HCV replication, with many advantages in terms of costs and simplicity of the analysis method, with respect to RNA-based approaches [95-98].

Under confirmation of HCV infection, it is possible to use some clinical tests, such as liver biopsy or liver elastography in order to evaluate the liver damage (FibroScan). Furthermore, the identification of the HCV genotype (multiple infection with more than one genotype is frequently observed) is necessary to begin the proper drug therapy, because they respond differently to the therapeutically treatment.

### 3.5.3 HIV and HCV biosensors: state of the art

In recent years there was a more and more increasing interest on development of biosensors for an early diagnosis of HIV and HCV infections, as alternative to methods already available, and previously described.

Literature data extensively report about immunosensors aimed to determine the viral capsid proteins, in order to reduce the diagnostic window period, through easy-to-use and inexpensive instrumentations, with performances comparable, even better, to ELISA assays and NAAT methods. To the best of our knowledge, sandwich or competitive immunosensors for diagnosis of HIV/HCV co-infection, through capsid protein detection, have not yet been investigated. Currently, immunosensing devices for co-infection are mainly based on antibodies detection. For example, Lochhead et al [99] developed a multiplex fluorescence immunoassay for simultaneous serodiagnosis of HIV-1 and co-infections, among which HCV. The system combines disposable assay cartridges with a reading instrument, implemented on a USB-connected device, powered and driven by a laptop computer. Fluorescence responses are imaged using a multimode waveguide technology. The immunoassay principle is the immuno-recognition of the target anti-HIV antibodies, subsequently detected by a dye-conjugated secondary antibody.

Zhao and Liu [100] also developed a paper-based electrochemical immunosensor for detecting HIV and HCV antibodies in serum. The paper device includes 8 electrochemical immunosensors, and each sensor consists of a circular reaction zone (patterned on chromatography paper via wax printing) and a group of sensing electrodes (WE, CE, and RE) patterned on the reaction zone, through screen-printing. The handheld potentiostat, constructed using a microcontroller-based electronic circuit, has 8 signal readout channels to interface with the 8 sensors. A multi-channel pipette can be used to add fluid samples to the array device. In this system the electrode surfaces are functionalized with antigens and the samples with different concentrations of antibody are incubated and detected by using an AP-labelled secondary antibody (Figure 22).

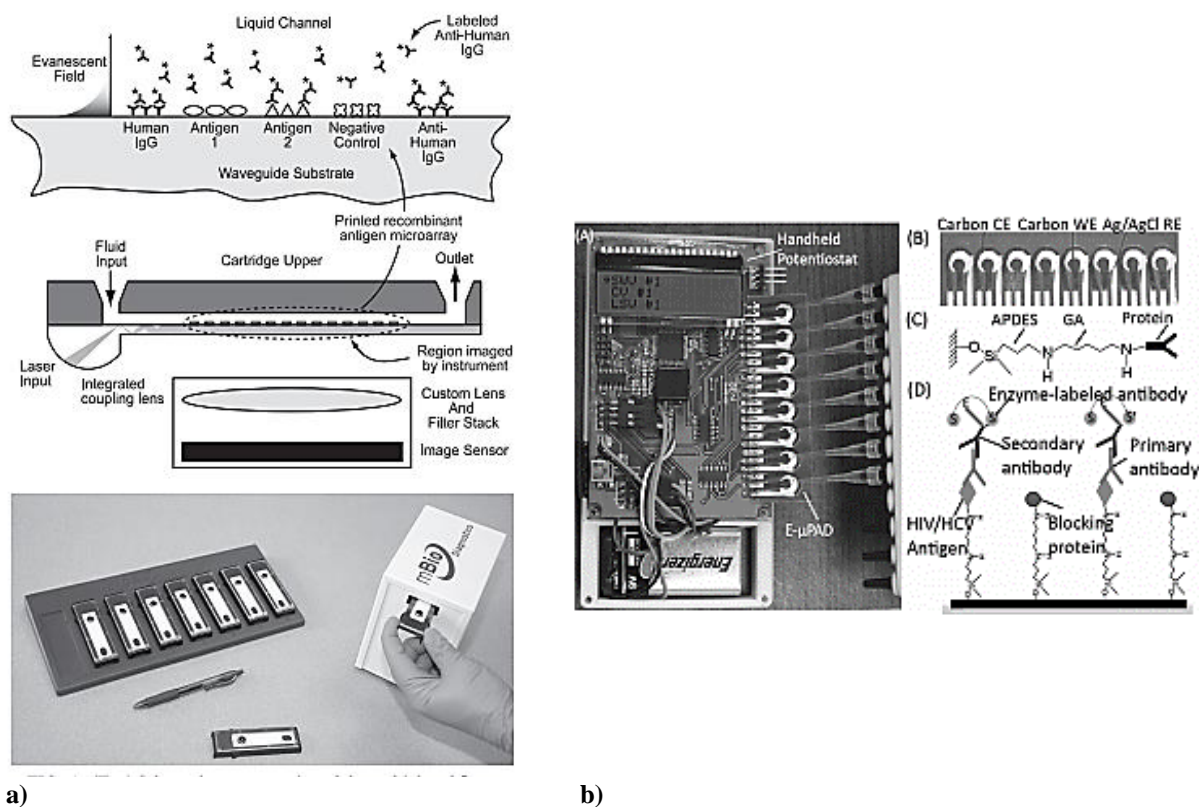


**Figure 22 a) Multiplexed immunoassay for HIV-1 and b) co-infections and Paper-based immunosensors for HIV and HCV markers.**

Concerning the immunosensing devices aimed to single diagnosis of HIV or HCV infection, several works were focused on detection of capsid proteins as reliable early biomarkers of infection.

Focusing the attention on HIV diagnosis, Zheng et al [73] realized a sandwich HIV p24 immunosensor, implemented on gold nanoparticles-coated glassy carbon electrodes, functionalized with anti-p24 antibodies. The amperometric signal showed a linear relationship with the concentration of p24, ranging from 0.01 ng/mL to 100 ng/mL and a detection limit of 0.008 ng/mL. Lower by more than two orders of magnitude with respect to the corresponding photometric ELISA.

Chang et al [101] developed a simple and low-cost, digital immunoassay for p24, based on trapping enzyme-labeled immunocomplexes in high-density arrays of femtoliter microwells and constraining the diffusion of the enzyme–substrate reaction. The digital immunoassay was evaluated in terms of analytical sensitivity for HIV capsid protein p24, and compared with commercially available NAT methods and immunoassays for p24, including 4th-generation antibody/antigen combo assays, for early detection of HIV in infected individuals. The digital immunoassay was found to exhibit 2000–3000-fold greater analytical sensitivity than conventional immunoassays reactive for p24, and comparable sensitivity to NAT methods. Assaying serial samples from 10 HIV-infected individuals, the digital immunoassay detected acute HIV infection as early as NAT methods, and 7–10 days earlier than conventional immunoassays. Comparison of assay results between the digital immunoassay and a quantitative NAT method from HIV infected serum exhibited a linear correlation.

More recently, Zhou and co-workers [102], developed an RGO@Au@Ru-SiO<sub>2</sub> composite (combination of Ru(bpy)<sub>3</sub><sup>2+</sup>-doped silica (Ru-SiO<sub>2</sub>) nanoparticles and gold-nanoparticle-decorated



graphene (P-RGO@Au)) -based sandwich-type electrochemiluminescence immunosensor for the analysis of HIV-1 p24 antigen. The composite worked as carrier to immobilize target antibody and to build a sandwich-type immunosensor through an interaction between antigen and antibody. Taking advantage of both Ru-SiO<sub>2</sub> nanoparticles and the P-RGO@Au composite, the proposed immunosensor exhibited a linear range from 10<sup>-9</sup> to 10<sup>-5</sup> mg/mL, with a detection limit of 1.0 × 10<sup>9</sup> mg/mL of p24.

In 2016, Zhang and collaborators [103] developed a system of magnetic beads (MBs) coupled with catalytic fluorescent immunoassay for rapid and sensitive determination of p24. Antibodies immobilized on MBs captured the antigen, and the biotin-tagged reading antibodies were detected by a horseradish peroxidase-streptavidin conjugate, catalysing the oxidation of o-phenylenediamine (OPD) to produce a fluorescent molecule. This is the first reported utilization of the fluorescence of OPD oxidation product catalysed by HRP for immunoassay. Optimization of conditions afforded a low detection limit of 0.5 pg/mL for p24 with a linear range of 1.4–90.0 pg/mL.

Concerning HCV infection, a minor amount of papers are reported in literature, with respect to HIV. Among capsid-protein-based immunosensors, Ma et al [104] reported the construction of a label-free electrochemical immunosensor for detecting the HCV core antigen. The sensor was developed on glassy carbon electrodes modified with a nanocomposite from gold nanoparticles, zirconia nanoparticles and chitosan. In parallel, a nanocomposite was synthesized from AuNPs, silica nanoparticles and chitosan, and conjugated to a secondary antibody. The sandwich type immunosensor displayed high sensitivity to the HCV core antigen in the concentration range between 2 and 512 ng/mL, with a detection limit of 0.17 ng/mL.

The same authors [105] developed an electrochemical immunosensor, consisting of graphitized mesoporous carbon–methylene blue (GMCs–MB) nanocomposite as an electrode modified material and a horseradish peroxidase-DNA-coated carboxyl multi-wall carbon nanotubes (CMWNTs) as a secondary antibody layer. After modification of the electrode with GMCs–MB nanocomposite, Au nanoparticles were electrodeposited on to the electrode to immobilize the captured antibodies. The bridging probe and secondary antibodies linked to the CMWNTs, and DNA concatamers were obtained by hybridization of the biotin-tagged signal and auxiliary probes. In addition, in this case the reading of the assay was varied out through a horseradish peroxidase-streptavidin conjugate. The reduction current of MBs were generated in the presence of hydrogen peroxide and monitored by square wave voltammetry. Under optimum conditions, the amperometric signal increased linearly with the core antigen concentration (0.25 pg/mL to 300 pg/mL). The immunosensor exhibited a detection limit of 0.01 pg/mL, associated to a high selectivity.

## 4. PROJECT PURPOSE

### 4.1 DEVELOPEMENT OF AN INNOVATIVE IMMUNOSENSOR FOR CO-DETERMINATION OF HIV AND HCV SERUM BIOMARKERS

The initial aim of the thesis project was the design and implementation of a bi-plexed immunosensor for the simultaneous determination of Human Immunodeficiency Virus (HIV) and Hepatitis C Virus (HCV) protein biomarkers, as simple, easy-to-use and robust device to be applied for early infection and co-infection diagnosis.

The simultaneous determination of p24 and NS4 was evaluated to be developed on dual-SPEs platforms, with different functionalization of each of the two elliptic working electrodes with the proper bio-receptors, i.e. capture antibodies or capsid proteins, for sandwich or competitive systems, respectively. In both cases, the signals arising from the two electrodes are simultaneously transmitted over independent channels for reading through simple, inexpensive and compact bi-potentiostat (Figure 23).

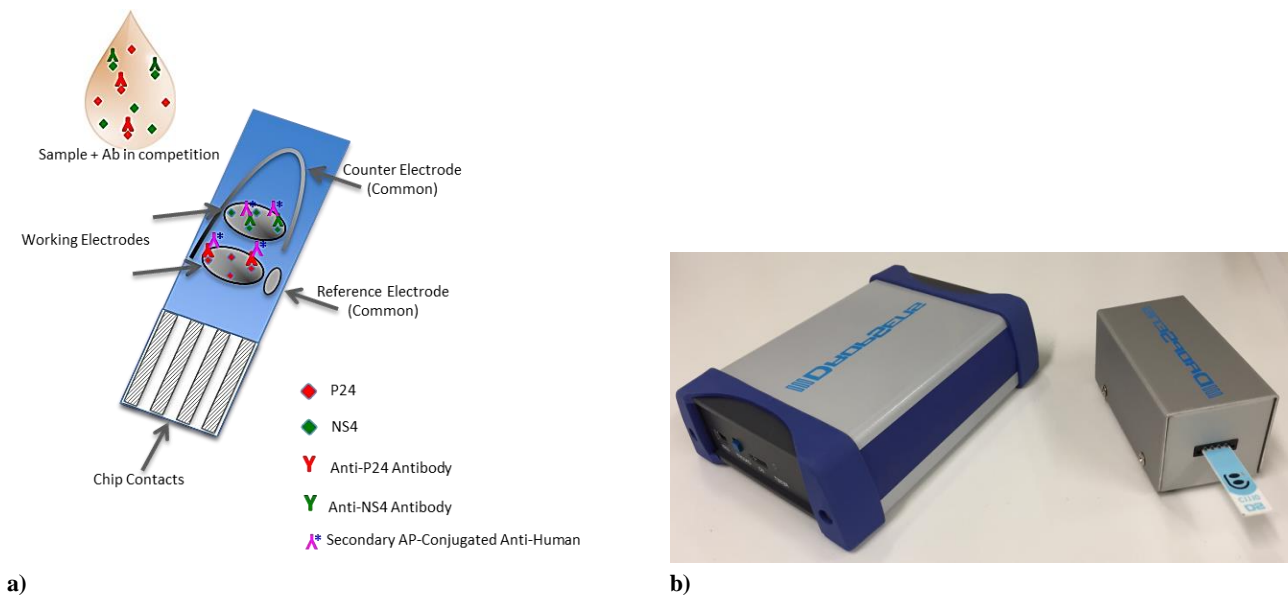


**Figure 23 a) Schematic representation of dual-SPCE functionalization and principle behavior, b) Used bi-potentiostat and dual-chip SPE.**

Concerning the typology of the working electrode material, different options were considered, such as glassy carbon, gold nanoparticles on glassy carbon or carbon nanotubes [106, 107], in order to evaluate and compare their performances.

A crucial aspect was the strategy adopted for the immobilization of the bio-receptor on the electrode surface, chosen on the basis of the features of both electrodic substrate and biological receptor. For the sandwich assay, in a first approach the linking of the capture antibody was implemented by direct chemisorption on gold nanoparticles-functionalized substrates. The obtained results evidenced that the direct exploitation of the reactivity of cysteine moieties present on the side chains

conformationally limits the effectiveness of the interaction of the antibody with its specific antigen. This aspect was improved by using proteins A and G, as linkers able to specifically bind the Fc fraction of the antibody, in such a way to expose the receptor Fab fraction, directly implicated in the interaction with the antigen. However, this type of functionalization not ensure a robust linkage of the antibody, being a non-covalent binding. Thus, a covalent linkage was evaluated to reach a more efficient functionalization of the electrode, using SAM from heterobifunctional molecules, alone or in combination with protein G. Also in these cases a not useful antibody orientation was achieved. For these reasons, a competitive strategy was then investigated, exploiting and comparing both non-covalent and covalent methods for electrode functionalization with capsid virial antigens. The amperometric transduction required the use of reading antibodies conjugated with Alkaline Phosphatase (AP), to generate a current signal indirectly correlated with the concentration of the analyte in the previously incubated sample. The amperometric signal is obtained in the presence of Hydroquinone Diphosphate (HQDP) as enzymatic substrate. HQDP is not natively electroactive, but is enzymatically dephosphorylated and then electrochemically oxidized to Quinone (Figure 24).

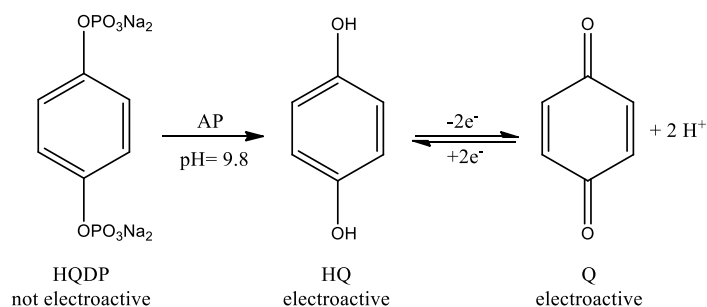


**Figure 24 AP enzymatic reaction on HQDP: dephosphorilation and oxidation to HQ.**

This enzyme substrate, useful in case of mono-WE electrodes, present a drawback when applied to multi-sensor platforms, evidencing the so-called "cross-talk" phenomena taking place because of diffusion of the electroactive indicator to adjacent electrodes and giving rise to false positive results. This problem, frequently observed when the electroactive redox mediator dissolved in the reading solution is revealed by diffusion, can be overcome with the use of an alternative enzymatic substrate as 3-indoxyl phosphate (3-IP), in co-presence of a silver salt [108,109]. In this case, AP is able to catalyse the dephosphorylation of 3-IP, giving an intermediate product able to reduce silver ions in solution into a metallic deposit, which is localized where the enzymatic label AP is attached (Figure 25). The deposited silver can be electrochemically stripped into solution and detected by anodic stripping voltammetry.

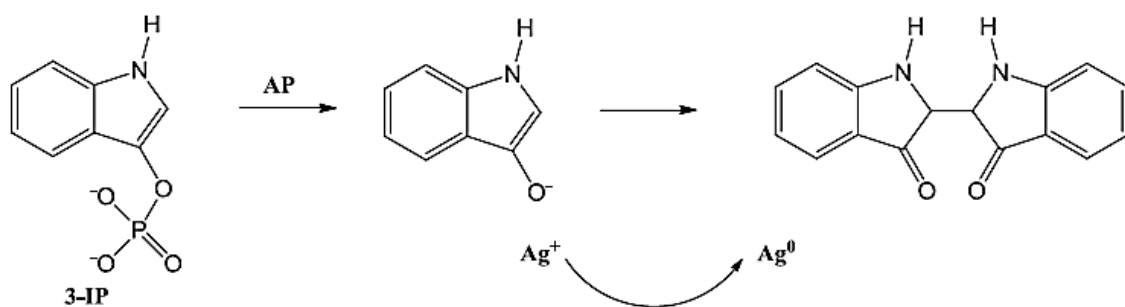


Figure 25 AP enzymatic reaction on 3-IP: dephosphorilation and Ag reduction.

All the above discussed aspects were thoroughly studied and the experimental conditions were properly evaluated, to reach the goal of development of practical, robust, cheap and easy-to-apply devices suitable for HCV and HIV diagnosis in clinical laboratories.

However, before approaching the dual devices, p24 and NS4 systems were individually studied on conventional mono-screen-printed electrodes, in order to assess their response to the sensing devices and optimize the setup for each system.

## 4.2 DEVELOPEMENT OF AN IMMUNOSENSOR FOR THE DETECTION OF HIV CAPSID PROTEIN p24

The attention was initially paid to the development of an immunosensor for the determination of p24 capsid protein as HIV serum biomarker.

At first, sandwich-type assay was investigated, using a mouse monoclonal capture antibody in combination with another mouse monoclonal reading antibody (different target epitopes) and a secondary rabbit-anti mouse AP-conjugated antibody. However, the best results (see discussion) were obtained following a competitive approach, in which the electrode surface is functionalized with the capsid protein itself, with subsequent incubation with an anti-p24 mouse monoclonal antibody and the same secondary rabbit-anti mouse AP-conjugated antibody (Figure 26).

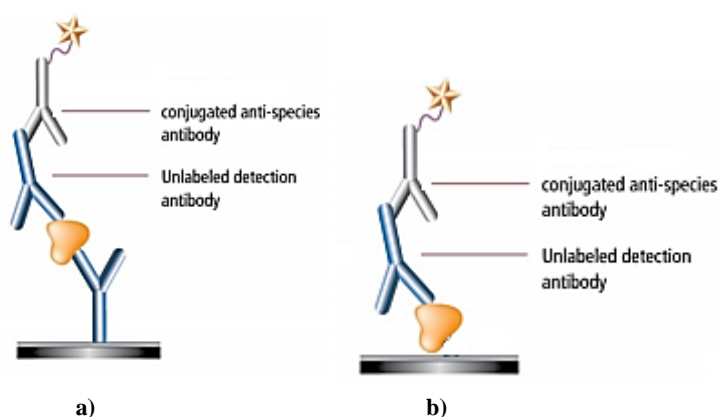


Figure 26 Working principle of a) sandwich and b) competitive assay.

### 4.2.1 Reagents and solutions

Triethanolamine, Dimethyl pimelimidate dihydrochloride (DMP), ethanolamine, 11-Mercapto-undecanoic acid, 95% (MUA), N-hydroxysuccinimide (NHS), N-(3-Dimethylaminopropyl)-N'-ethylcarbodiimide hydrochloride, 98% (EDC), Trizma® base, Tween-20, Bovine Serum Albumin (BSA), chitosan (CS, medium molecular weight), glutaraldehyde (GA, 25% in aqueous solution),  $\alpha$ -Casein from bovine milk and acetic acid (99-100% puriss.) were purchased from Sigma-Aldrich (Milan, Italy).

Proteins A and G, Recombinant (*E. coli*) HIV-1 p24 full-length protein, Mouse monoclonal anti-HIV-1 p24 IgG1 [39/5.4A], mouse monoclonal anti-HIV-1 p24 IgG1 [39/6.14] and Alkaline Phosphatase-conjugated rabbit anti-mouse IgG (Ab-AP) were purchased from abcam® (Cambridge, UK).

Sodium Phosphate Bibasic, Potassium Phosphate Monobasic and Magnesium Chloride were purchased from Carlo Erba (Milan, Italy). Hydroquinone Diphosphate (HQDP) and Dropsens® screen-printed electrodes were purchased from Metrohm Italiana (Origgio-VA, Italy).

Deionized water was obtained from an in-house Milli-Q water purification system Alpha Q-Water (Millipore, Billerica, MA, USA).

Phosphate-buffered saline (PBS 10×) was prepared according to the following composition: 1.37 M NaCl, 0.027 M KCl, 0.015 M KH<sub>2</sub>PO<sub>4</sub> and 0.08 M Na<sub>2</sub>HPO<sub>4</sub> (pH 7.4).

Diluted Phosphate buffered (PBS 1 x) was prepared by dilution of PBS 10 X in water.

The washing buffer PBS-T consisted of PBS containing 0.05 % of the surfactant Tween-20.

The cross-linking buffer was prepared with 0.2 M of triethanolamine in water, pH= 8.2.

The quenching buffer consisted of 0.1 M ethanolamine in PBS (1x), pH= 8.0.

TRIS buffer was prepared according to the following composition: 0.1 M Trizma® base, 0.02 M MgCl<sub>2</sub> (pH 7.4), and the washing buffer TRIS-T consisted of TRIS containing 0.05 % of the surfactant Tween-20.

“Reading buffer” (RB) has the same composition of TRIS buffer but pH = 9.8.

## 4.2.2 Apparatus and electrodes

The immunosensors were realized using DropSens® disposable screen-printed electrodes, assembled on ceramic substrate (L 33 x W 10 x H 0.5 mm), with 4 mm-diameter working electrode, counter electrode of the same material of WE and silver reference electrode.

The readings of the electrochemical assays were performed by Differential Pulse Voltammetry (DPV) or Cyclic Voltammetry (CV), scanning the potential between -0.5 V and +0.3 V, with a scan rate of 0.05 V/s for CV and, in case of DPV, with a pulse amplitude of 0.05 V, a step potential of 0.005 V and a pulse time of 0.1 s. Nonelectroactive HQDP was used as enzymatic substrate. A 1 mg/mL solution of HQDP dissolved in RB was used as reading solution. After drop-casting of the reading solution on the sensor, an equilibration time of 90 s and a preconditioning stage of 30s at -0.5 V were applied prior to run CV or DPV, in order to reach an exhaustive enzymatic reaction and to pre-concentrate HQ in its reduced form, respectively.

All electrochemical measurements were performed with a μAutolab III electrochemical workstation (EcoChemie, Utrecht, NL) equipped with GPES 4.0 version customized software.

## 4.2.3 Methods

### 4.2.3.1 Sandwich indirect immunoassay

The immobilization of the capture anti-p24 antibody was investigated according to the methodological approaches already described in Section 2.4 (direct chemisorption, protein A/G-assisted linking, SAM-assisted linking, and SAM-assisted linking combined with protein G).

#### 4.2.3.1.1 Direct functionalization on Gold Nanoparticles- Screen -Printed Carbon Electrodes (GNP-SPCEs)

GNP-SPCEs were functionalized by drop casting with 30 μL of 10 μg/mL solution of mouse monoclonal anti-HIV-1 p24 IgG1 [39/5.4A], as capture antibody, dissolved in PBS, at room

temperature, for 1h. After removal of unreacted antibody, by accurate washing with PBS-T and PBS, a blocking treatment was carried out with 30  $\mu$ L of a 10 mg/mL solution of BSA, dissolved in PBS, for 1h at room temperature, followed by washing with PBS-T and PBS buffer. All washing steps were repeated 3 times. Then, a volume of 30  $\mu$ L of p24 standard solution (5  $\mu$ g/mL) was transferred on the working electrode and the incubation was allowed to take place for 1h at room temperature. After antigen incubation, the electrode was carefully washed with PBS-T and PBS, as previously described. Subsequently, 30  $\mu$ L of a 10  $\mu$ g/mL solution of mouse monoclonal anti-HIV-1 p24 IgG1 [39/6.14], used as secondary antibody were incubated at room temperature for 1h. In order to detect the secondary antibody, each immunosensor was incubated for 1h, at room temperature, with 30  $\mu$ L of a solution of the Ab-AP, diluted 1:500 in TRIS buffer. After washings with TRIS-T and TRIS, the voltammetric signal was acquired in HQDP solution, in RB.

#### **4.2.3.1.2 Auxiliary protein A for GNP-SPCEs functionalization**

In this case, in order to promote a correct antibody orientation, for its subsequent interaction with the antigen, GNP-SPCEs were functionalized with 30  $\mu$ L of a 200  $\mu$ g/mL solution of protein A, dissolved in PBS, at 4  $^{\circ}$ C, overnight.

After removal of unreacted antibody, by accurate washing with PBS-T and PBS, 30  $\mu$ L of capture antibody solution (10  $\mu$ g/mL) were deposited on the electrode surface, at room temperature for 1h. After the usual washings, the cross-linking was performed by reaction with 30  $\mu$ L of 25 mM DMP, dissolved in cross-linking buffer, for 30 minutes at room temperature, followed by washings with cross-linking buffer.

Then, 30  $\mu$ L of quenching buffer were allowed to react for 15 minutes at room temperature. After washing with PBS, a blocking treatment was carried out with 30  $\mu$ L of a 10 mg/mL solution of BSA dissolved in PBS, for 1h at room temperature, followed by final washings with PBS.

30  $\mu$ L of p24 standard solution (5  $\mu$ g/mL) were transferred on the working electrode and the incubation was allowed to take place for 1h, at room temperature. After antigen incubation, the electrode was carefully washed with TRIS-T and TRIS and 30  $\mu$ L of secondary antibody solution (10  $\mu$ g/mL) were incubated at room temperature for 1h, followed by final washings with TRIS-T and TRIS.

In order to detect the secondary antibody, each immunosensor was incubated for 1h, at room temperature, with 30  $\mu$ L of a solution of the Ab-AP, diluted 1:500 in TRIS buffer. After washings with TRIS-T and TRIS, the voltammetric signal was acquired in HQDP solution, in RB.

#### **4.2.3.1.3 Auxiliary protein G for GNP-SPCEs functionalization**

As previously reported (Table 2), protein G has a higher expected affinity than protein A to IgG1. For this reason the experiments described in Section 4.2.3.1.2 were analogously replicated, under replacement of protein A with protein G.

#### **4.2.3.1.4 Covalent Linking – SAM/Protein G for GNP-SPCEs functionalization**

With the aim of promoting a robust functionalization of the electrode surface, together with a correct orientation of the antibody, GNP-SPCEs were functionalized through SAM method combined with protein G. Therefore, 30  $\mu\text{L}$  of 14 mM MUA solution in absolute ethanol were deposited at 4  $^{\circ}\text{C}$  overnight on the electrode surface. After removal of MUA excess, by accurate washing with absolute ethanol, an activation treatment was carried out with 30  $\mu\text{L}$  of a mixture of 0.2 M EDC and 0.05 M NHS, in ethanol. This activation was performed for 2h at room temperature, followed by washing with absolute ethanol and water [110]. All washing steps were repeated 3 times. After removal of reagents excess, the experiments described in Section 4.2.3.1.3 were analogously repeated.

#### **4.2.3.2 Competitive indirect immunoassay**

##### **4.2.3.2.1 Direct functionalization of GNP-SPCEs with p24**

GNP-SPCEs were functionalized by drop casting with 30  $\mu\text{L}$  of a 10  $\mu\text{g}/\text{mL}$  solution of p24 protein, in PBS at 4  $^{\circ}\text{C}$ , overnight. After removal of unreacted protein and accurate washing, a blocking treatment was carried out with 30  $\mu\text{L}$  of a 10 mg/mL solution of BSA dissolved in PBS-T, for 1h at room temperature, followed by washing with PBS-T and PBS buffer. All washing steps were repeated 3 times. Therefore, 30  $\mu\text{L}$  of mouse monoclonal anti-HIV-1 p24 IgG1 [39/5.4A] (10  $\mu\text{g}/\text{mL}$ ) were casted to the working electrode and allowed to react for 1h at room temperature. Then, in order to detect the anti-p24 antibody, each immunosensor was incubated for 1h at room temperature with 30  $\mu\text{L}$  of a solution of the Ab-AP, diluted 1:500 in TRIS buffer. After washings with TRIS-T and TRIS, the voltammetric signal was acquired in HQDP solution, in RB.

##### **4.2.3.2.2 SAM-mediated p24 linking on GNP-SPCEs**

In this case, before incubating p24 protein, the electrode surface was functionalized with a SAM, from MUA, according to the previous described procedure, Section 4.2.3.1.4. The following steps are the same of the previous described for the direct functionalization with p24 (Section 4.2.3.2.1).

##### **4.2.3.2.3 p24 linking on gold-free GC-SPCEs and SWCNTSPEs via Chitosan/glutaraldehyde**

In this case, the competitive amperometric immunosensor was developed on gold-free Glassy Carbon Screen-Printed Electrodes (GC-SPCEs) or Single Walled-Carbon NanoTubes Screen-Printed Electrodes (SWCNTSPEs), previously functionalized with chitosan, and suiting the cross-linking properties of glutaraldehyde. In this way, a covalent and efficient immobilization of the viral capsid protein p24 was realized.

SPCEs were coated with 15  $\mu\text{L}$  of a 0.05 mg/mL solution of CS in 0.1 M acetic acid and allowed to dry at room temperature. The reactive amino- functionalities of CS were then activated with 0.05 M



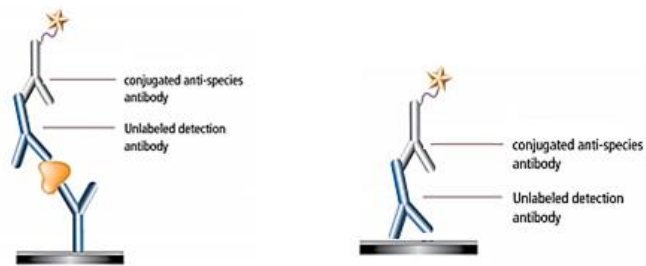
GA, dissolved in PBS, for 2 h, followed by washing with deionized water. Therefore, 30  $\mu\text{L}$  of a 10  $\mu\text{g}/\text{mL}$  solution of p24 protein were casted on the working electrode, allowed to react at room temperature for 1h, and then kept at 4  $^{\circ}\text{C}$  overnight.

After removal of unreacted p24 by accurate washing with PBS-T and PBS, a blocking treatment was carried out with 30  $\mu\text{L}$  of a 20  $\text{mg}/\text{mL}$  solution of  $\alpha$ -Casein dissolved in PBS-T for 1 hour at room temperature, followed by washing with TRIS-T and TRIS buffer. All washing steps were repeated 3 times. The p24-modified-SPCEs are ready to use as substrates for the development of the competitive electrochemical immunoassay. Hence, 30  $\mu\text{L}$  of p24 solutions with different concentrations were mixed with 30  $\mu\text{L}$  of a solution of mouse monoclonal anti-HIV-1 p24 IgG1 [39/5.4A], dissolved in TRIS at optimized concentration levels, as discussed in Section 4.2.4.2.2. The mixture was transferred on the working electrode of the immunosensor and the competition reaction was allowed to take place for 1 hour at room temperature. After immunocompetition, the sensors were carefully washed with TRIS-T and TRIS to remove unspecifically bound material. In order to detect the Ab Anti-HIV-1 p24 immobilized on the electrodes surface, each immunosensor was incubated for 1hour at room temperature with 30  $\mu\text{L}$  of a solution of the Ab-AP, diluted 1:500 in TRIS (1x). After washings, the readings of the electrochemical assays were performed in HQDP solution, by DPV measurements.

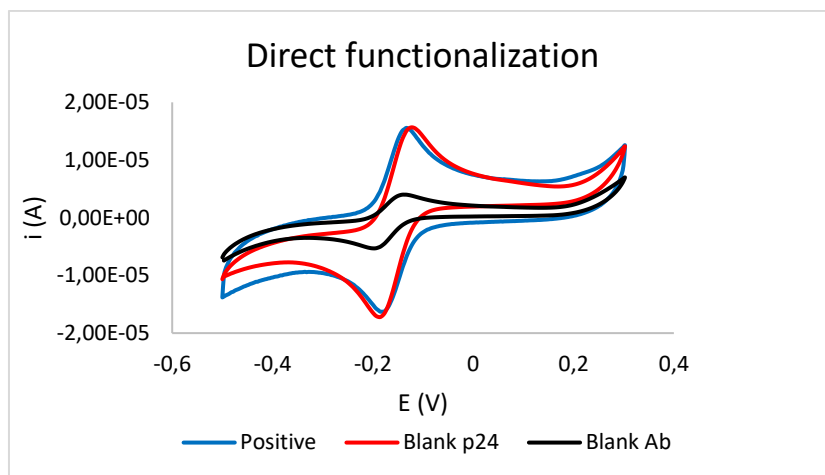
## **4.2.4 Results discussion**

### **4.2.4.1 Sandwich indirect immunoassay**

Although it is the easiest approach, the direct functionalization of the electrode surface with the anti-p24 antibodies did not ensure the correct orientation for the immunorecognition. This was confirmed through electrochemical measurements, showing comparable signals for blank and positive experiments (PBS and p24 standard solution, respectively). In order to confirm the hypothesis of the uncorrected orientation of the antibodies, further experiments were carried out also in the absence of anti-p24 antibodies. Significantly lower signals were obtained, confirming that the comparable CV curves with and without antigen are ascribable to the interaction of the AP-conjugated reading antibody with the Fc of bottom-oriented anti-p24 (See Figures 27a and 27b).



a)



b)

**Figure 27: a) Correct and wrong orientation of the capture antibody, b) CV signals obtained with different combination of p24 antigen and anti-p24 antibody.**

Similar results were obtained using proteins A and G as linkers for the immobilization of anti-p24 antibodies. Although higher responses were obtained with protein G respect to protein A, in both cases not significant differences were noticed between the blank and positive samples (with or without p24) (Figure 28).

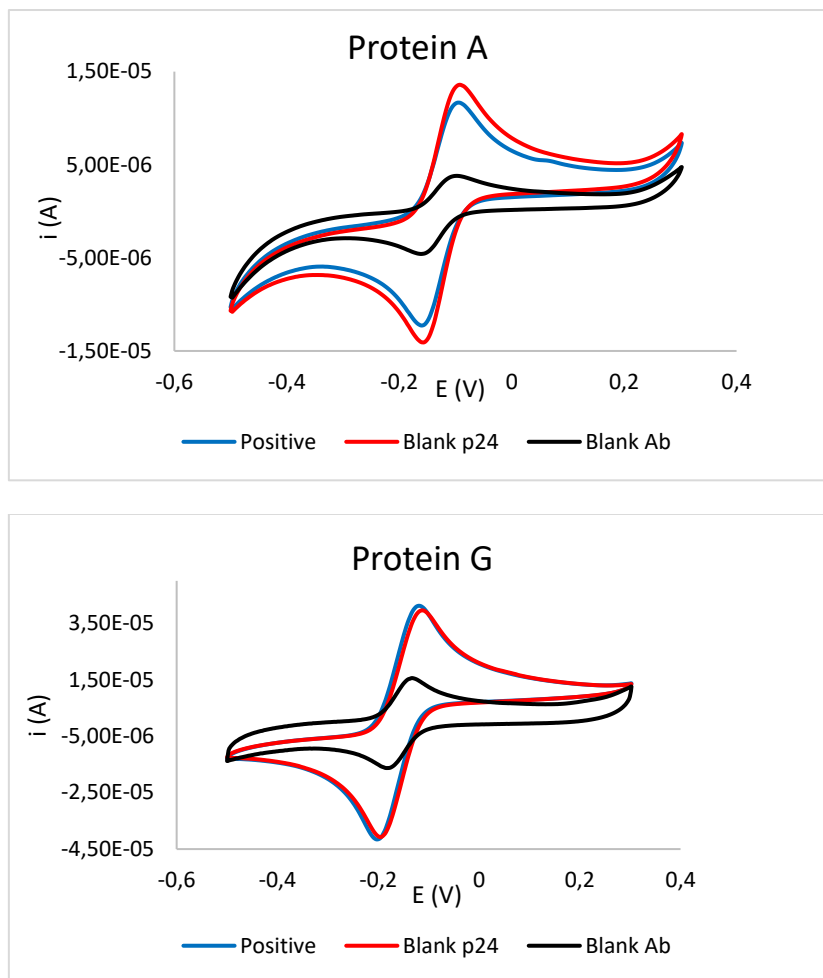
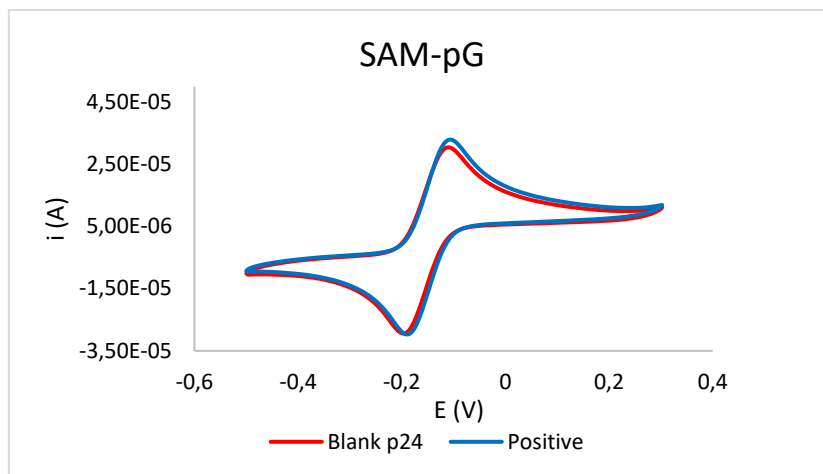


Figure 28: CV signals obtained using proteins A and G as linkers for the immobilization of anti-p24 antibodies.

These experimental data were interpreted taking into account not only the not appropriate orientation reached upon immobilization of the antibodies, but also the possibility of a poor suitability of the selected antibody “pair”, in terms of inadequate regio-chemistry of the epitopes involved in the immunoreactivity of the capsid protein with the two exploited antibodies. Furthermore, in order to improve the conformational freedom of the system the combined use of a SAM from MUA and protein G was also tested, however, giving unsatisfying results, as shown in Figure 29.



**Figure 29: CV signals obtained under combination of a SAM from MUA and protein G as linkers for the immobilization of anti-p24 antibodies.**

On the basis of these findings, our efforts were switched to a competitive approach, also considering that studies concerning the development of competitive immunosensors for p24 determination have not yet been published in the literature. According to this approach, the electrode surface was functionalized with the p24 antigen. In this case an immunocompetition process is involved in order to quantify the antigen in the sample. The sample containing p24 is loaded on the sensing substrates functionalized with the same antigen and a fixed amount of a unique anti-p24 antibody is added for all standards and/or samples. The antibody will preferentially react with the free antigen present in the sample, while it is less favored the interaction with the immobilized p24, which takes place in the absence of the free antigen or at its low concentrations. In this way, the high “blank” signal recorded in the absence of p24 undergoes progressive inhibition because the increase of p24 concentration will reduce the amount of antibodies bound to functionalized sensor surface.

Competitive assays have the advantages to require only one antibody, resulting in shorter analysis time, and lower cost and higher simplicity in electrode functionalization; furthermore, the same sensing device can be employed also for the determination of the antibody, when the immunocompetition with the antigen is not carried out.

Different methods of functionalization of screen-printed electrodes with p24 were explored, in order to individuate the best one.

#### 4.2.4.2 Competitive indirect immunoassay

##### 4.2.4.2.1 Immobilization of p24 on GNP-SPCEs

Preliminary experiments were carried out by direct chemisorption of p24 antigen on gold substrates, in order to evaluate if this kind of immobilization allows to maintain the immunoreactivity towards the antibody. Figure 30 shows a comparison between the responses obtained upon chemisorption of p24 and subsequent incubation with 10  $\mu\text{g/mL}$  solution of anti-p24 or PBS, as blank reference. Not significant differences were noticed, together to very low signals, so evidencing the not proper immobilization strategy.

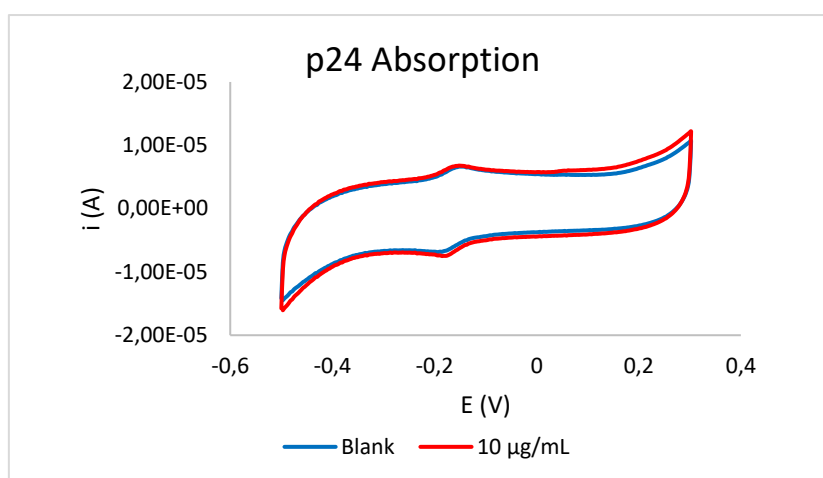


Figure 30 CV responses for anti-p24 (10  $\mu\text{g/mL}$ ) and PBS (Blank) incubation on GNP-SPCEs, after direct chemisorption of p24.

This result can be explained considering that the cysteine moieties, involved in the interaction with gold substrates, are probably included in the epitope domain necessary for the immunoreactivity with the antibody. This hypothesis was confirmed by means of targeted measurements performed on a Quartz Crystal Microbalance (QCM).

The working principle of this type of measurement is based on properties of Piezoelectric Quartz Crystals (PQC). Piezoelectric crystals are well known to be quite sensitive to pressure and any mass change on their surfaces. They can be used in microbalances for thin film technology and trace quantitative analysis. The oscillating frequency of a piezoelectric crystal decreases with the adsorption of foreign substances on the surface. The variation of vibrational frequency  $\Delta f$  (Hz), related to a mass change  $\Delta m$  (g) of an adsorbed substance onto the piezoelectric crystal surface with area  $A$  ( $\text{cm}^2$ ), density  $\rho_q$ , shear modulus of quartz  $\mu_q$  (for AT-cut crystal) and fundamental frequency ( $f_0$ ) can be evaluated from Sauerbrey's equation (1).

$$\Delta f = \frac{2f_0^2}{A\sqrt{\rho_q \mu_q}} \cdot \Delta m \quad (1)$$

The substrate used for the measurements consists of a quartz plate and a gold electrode (both in upper and lower side), as reported in Figure 31.

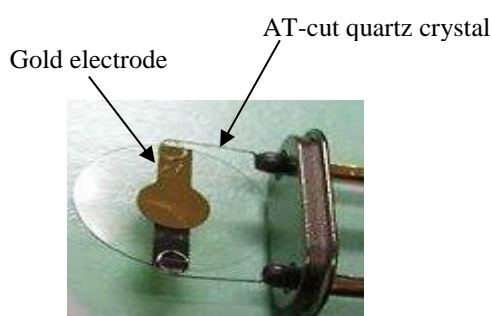


**Figure 31 Gold-coated PQC.**

The surfaces of the chip are patterned with electrodes, which serve two purposes: drive the crystal into oscillation or resonance electrically and provide a sensor surface on which bio-receptor binding takes place. The most pronounced oscillation or resonance mode is the shear mode (displacement along the chip surface). The resonance frequency decreases upon adsorption of species onto the sensor surface. On the base of this, the sensor was directly functionalized with p24, and the frequency shift was monitored during the whole process.

The measurements were carried out in a dynamic flow-cell (70  $\mu$ L) driven by a computer-controlled peristaltic pump.

A pronounced frequency shift was noticed during the incubation of p24 on gold, as well as during the following blocking with BSA. As confirmation of the voltammetric findings, the incubation of anti-p24 antibody was not associated to significant frequency shifts, due to the unavailability of the active epitopes of the so immobilized p24 (Figure 32).

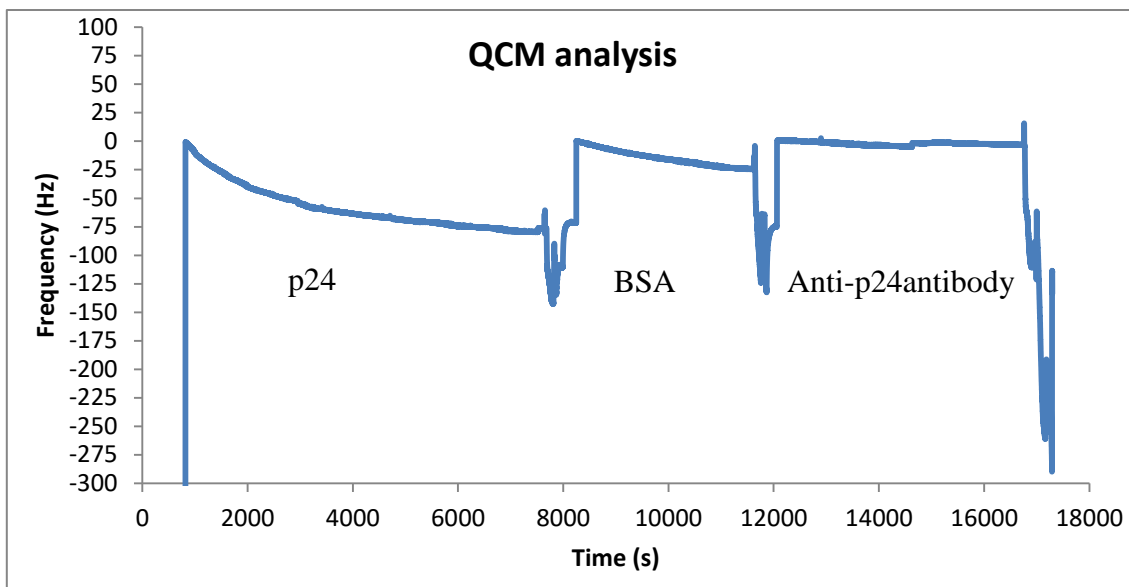


Figure 32 Frequencygram recorded during subsequent incubation of p24, BSA and anti-p24 on gold-coated PQC. The signal was zero-reset at the end of each washing procedure.

Analogous results were obtained using the SAM from MUA (Figure 33) as linker for the immobilization of antigen on gold electrodes.

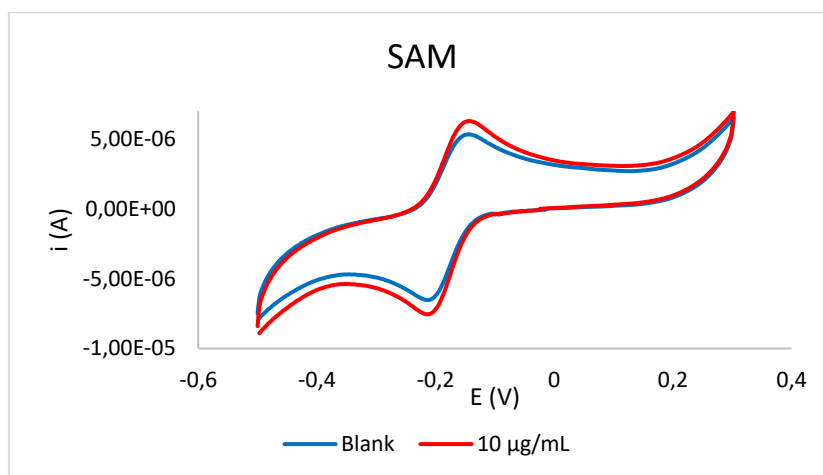


Figure 33 CV responses for anti-p24 (10 µg/mL) and PBS (Blank) incubation on GNP-SPCEs, after direct covalent linking of p24, using SAM.

On the basis of these results we changed the electrodic substrate moving to gold-free carbon screen-printed electrodes, using chitosan as active layer and glutaraldehyde as cross-linker, as described in Section 4.2.3.2.3.

#### 4.2.4.2.2 Immobilization of p24 on gold-free GC-SPCEs

Preliminary experiments were carried out in order to check the proper immobilization of p24 on chitosan-modified GC-SPEs and to evaluate the immunoreactivity towards the antibody.

For this purpose, immobilized p24 versus anti-p24 "titrations" were carried out, to identify the experimental dynamic domain for the optimization of the immunocompetition. A first set of experiments was performed fixing at 100  $\mu\text{g/mL}$  the concentration of the p24 solution used for functionalization of the GC-SPCEs and incubating the so obtained electrodes firstly with solutions of anti-p24 ranging from 0 (no antibody) to 117  $\mu\text{g/mL}$  (maximum concentration from standard) and subsequently with Ab-AP secondary antibody. Analogous experiments were performed varying the concentration of the p24 solution used for functionalization of the GC-SPCEs from zero to 100  $\mu\text{g/mL}$  and keeping constant the concentration of anti-p24 at 117  $\mu\text{g/mL}$ . In both cases, our findings evidenced DPV signals increasing versus anti-p24 and p24 concentration, respectively. Very weak background signals were recorded in the absence of both anti-p24 and p24, evidencing the proper immobilization of the bio-receptor as well as the non-occurrence of nonspecific binding phenomena (Figure 34).

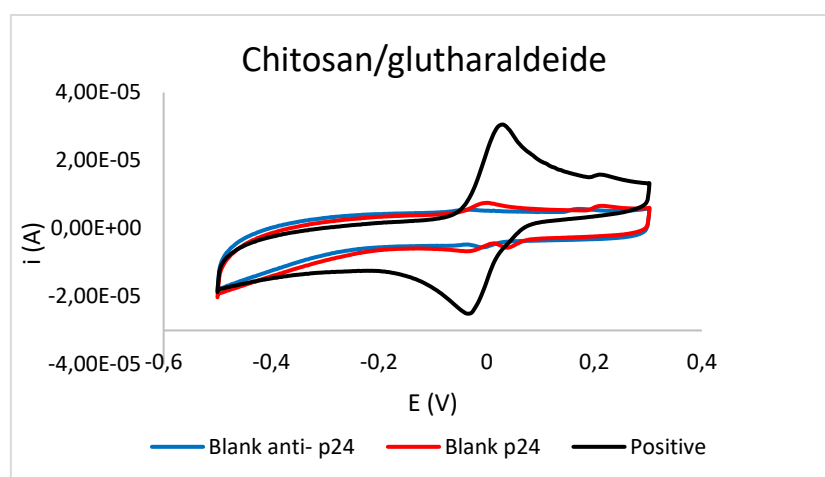


Figure 34 CV responses for no anti-p24 (PBS as blank), no p24 (PBS as blank) and immunoreaction of p24 and anti-p24 both at 10  $\mu\text{g/mL}$ , using chitosan/ glutaraldehyde as GC-SPCEs functionalization system.

On the basis of these results, the optimal concentrations of *i*) the immobilized p24 and *ii*) the anti-p24 antibody were assessed by means of a two-factors and 3-levels experimental design procedure.

For this purpose, immunocompetition experiments were carried out keeping constant the concentration of p24 in competition at 10  $\mu\text{g/mL}$  and varying the concentrations of immobilized p24 and anti-p24 added to the sample. The target variable to be optimized (maximized) was the signal inhibition rate, associated to the fixed concentration of the antigen in competition.

The experimental domain explored for the optimization is reported in Table 3.



**Table 3 Concentration of immobilized p24 and anti-p24 antibody assessed by means of a two-factors and 3-levels experimental design procedure.**

<b>Experiment Number</b>	<b>p24 (µg/mL)</b>	<b>anti-p24 (µg/mL)</b>
1	100 (+)	117 (+)
2	100 (+)	30 (0)
3	100 (+)	3 (-)
4	10 (0)	117 (+)
5	10(0)	30 (0)
6	10(0)	3 (-)
7	1 (-)	117 (+)
8	1 (-)	30 (0)
9	1 (-)	3 (-)

The dataset from the experimental design was elaborated by means of 2-ways ANalysis Of Variance (ANOVA) with interactions. ANOVA was carried out using the Statgraphics Centurion XV statistical software. The obtained interaction plot shows how variables interact each other and how they affect the response (Figure 35). The best inhibition rate values were noticed for the lowest anti-p24 concentration (3 µg/mL) and for both medium and low concentrations of p24 solution: due to the better signal to noise ratio, we chose for p24 solution the 10 µg/mL concentration value.

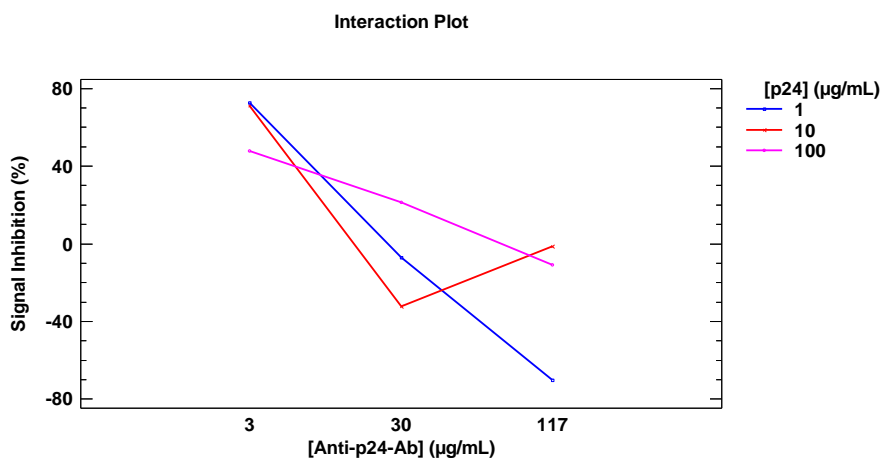


**Figure 35 Interaction plot from 2-ways ANOVA with interaction, carried out on the dataset from the experimental design.**

As p24 present in the sample inhibits antibody binding to the immobilized p24, increasing analyte concentration will reduce the amount of anti-p24 bound to the modified surface of the sensor, as reported in the following voltammograms, recorded varying the concentration of p24 in competition from 0 to 25 µg/mL (Figure 36)

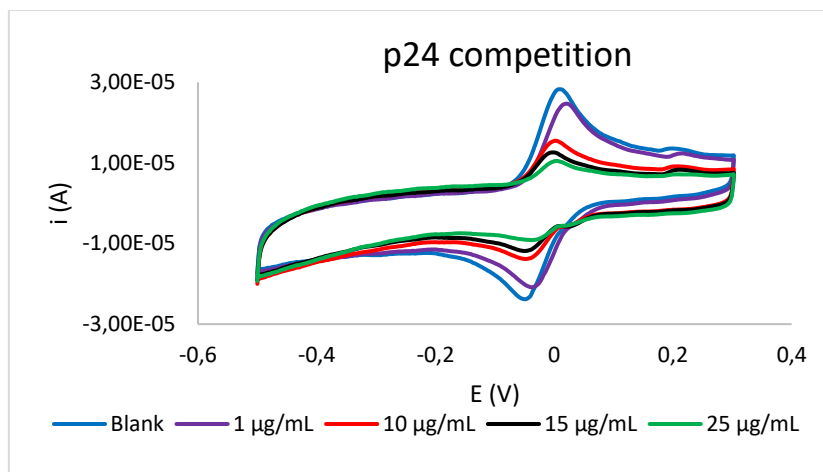


**Figure 36** Selected CV responses from immunocompetition experiments carried out varying the concentration of p24 in competition from 0 to 25 µg/mL.

The voltammetric responses were blank-normalized by dividing the current values observed for each concentration ( $S$ ) by the signal from blanks ( $S_0$ ), obtained with only anti-p24, without antigen in competition. The normalized signals, expressed as percentage values ( $S/S_0 \cdot 100$ ), were plotted *versus* the logarithm of the p24 concentration and fitted using a four-parameter logistic function (2), as conventional for competitive immunoassays [111,112]:

$$S/S_0 = S_{min} + \frac{(S_{max} - S_{min})}{1 + ([C]/I_{50})^B} \quad (2)$$

Where  $S_{min}$  and  $S_{max}$  are the asymptotic minimum and maximum, respectively ( $S_{max}$  is recorded in the absence of analyte) and  $B$  is the curve slope at the inflection point  $I_{50}$ , corresponding to the p24 concentration  $[C]$  giving a 50% of signal inhibition. Data fitting was performed by means of Microcalc Origin software.

The fitted immunocompetition curve is reported in Figure 37:

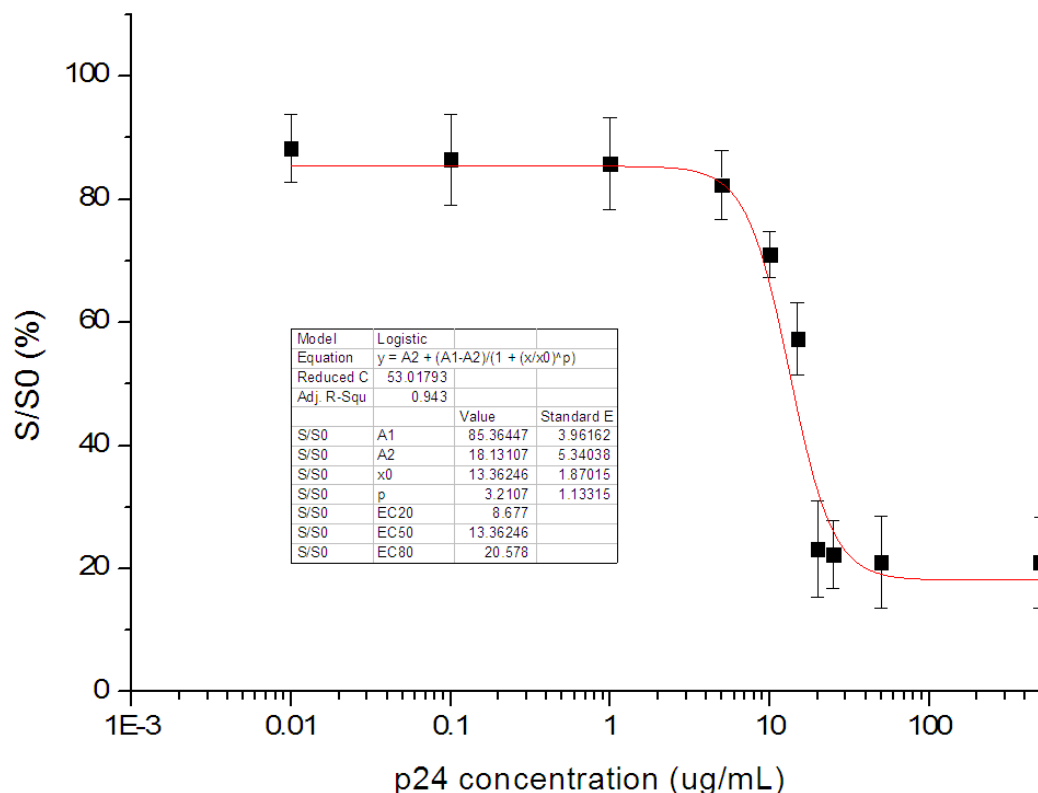


**Figure 37 Immunocompetition curve obtained over the 0.001-500  $\mu\text{g/mL}$  range, fitted with the four-parameter logistic function. Optimized parameters in the inset table.**

These encouraging results demonstrated the suitability of the competitive approach for the development of amperometric immunosensors for determination of p24 HIV-1 related capsid antigen. The main limitation in the performance of the developed device is the narrow dynamic response range, located in a concentration range too high for its suitability for diagnostic purposes.

In order to improve the performance of this device, the whole procedure was reproduced and re-optimized on Single-Walled Carbon Nanotubes-functionalized Screen-Printed Electrodes (SWCNT-SPEs), on the basis of the well-known peculiar properties of SWCNTs in terms of enhancement of electrochemical active area, more efficient immobilization of bio-receptors and improvement of the electronic transfer process, aimed to a signal enhancement.

The immobilization strategy for p24 antigen, based on chitosan/glutaraldehyde, was maintained, whereas the previously optimized experimental conditions were re-tuned, in terms of anti-p24 and Ab-AP secondary antibody concentrations.

Keeping constant at 10  $\mu\text{g/mL}$  the concentration of the p24 solution used for the functionalization of the electrode, the concentration of anti-p24 used during the immunocompetition process was adjusted in order to improve the inhibition rate for a fixed concentration of p24 antigen (0.5  $\mu\text{g/mL}$ )

The starting conditions were as from optimization studies carried out on conventional carbon SPEs, and we decided to avoid the implementation of a new complete multifactorial experimental design, also considering the costs of the reagents and of the nanostructured electrodic substrates. In order to evaluate the effect of the anti-p24 concentration, the previously optimized value (3  $\mu\text{g/mL}$ ) was only subjected to a decrease, considering the working principles of the competitive immunoassays.

The new explored concentration (1  $\mu\text{g/mL}$ ) was chosen in the same order of magnitude. The findings of these experiments evidenced the extreme sensitivity of the immunocompetition processes, strongly depending from the concentration of the antibody. As expected, a lower concentration of anti-p24 resulted into a lower DPV signal recorded for “blank” experiment, in the absence of p24. Nevertheless, a higher inhibition rate was observed in the presence of 0.5  $\mu\text{g/mL}$  of p24, so demonstrating the improved sensitivity reachable under these conditions, that we considered as optimal. (Figure 38).

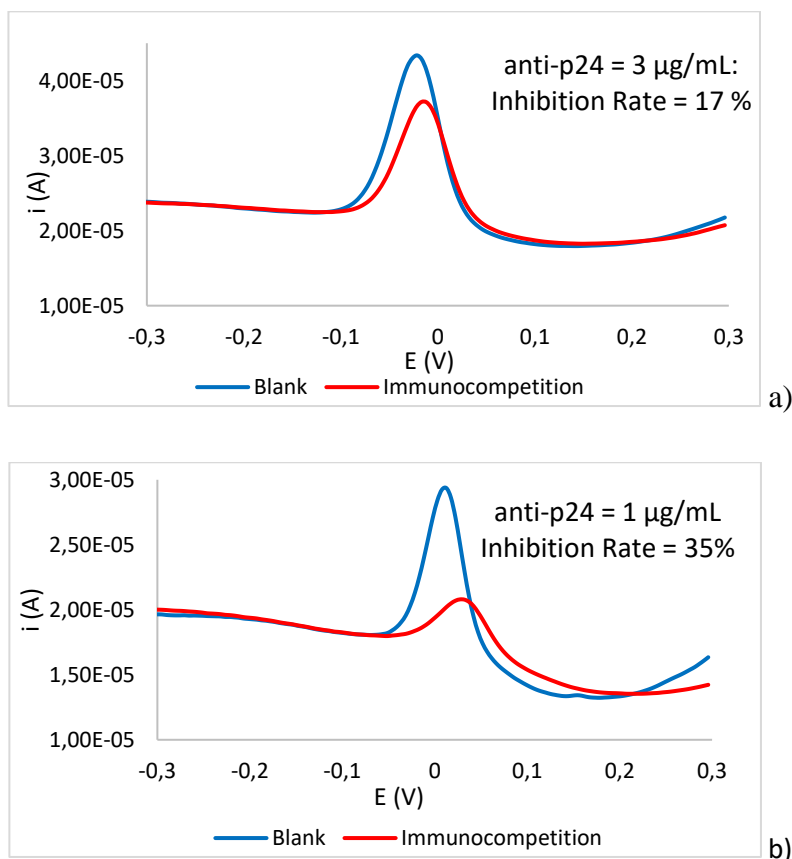


**Figure 38** DPV responses obtained under immunocompetition experiments carried out at fixed concentration of p24 (0.5  $\mu\text{g/mL}$ ) varying the concentration of anti-p24 from a) 3  $\mu\text{g/mL}$  to b) 1  $\mu\text{g/mL}$ .

Another experimental aspect strongly influencing the performance of the electrochemical competitive immunoassay is the concentration of the secondary enzyme-labeled reading antibody (Ab-AP). Although this reagent has to be even in excess, too high concentrations frequently lead to unspecific binding of the signalling antibody. In order to assess the dilution factor of the commercial standard, leading to the best sensitivity, in term of signal to noise (S/N) ratio, we carried out two set of experiments using 1:250 and 1:500 as dilution factors. For each dilution factor we acquired the signals obtained in the presence and in the absence of anti-p24. (Figure 39).

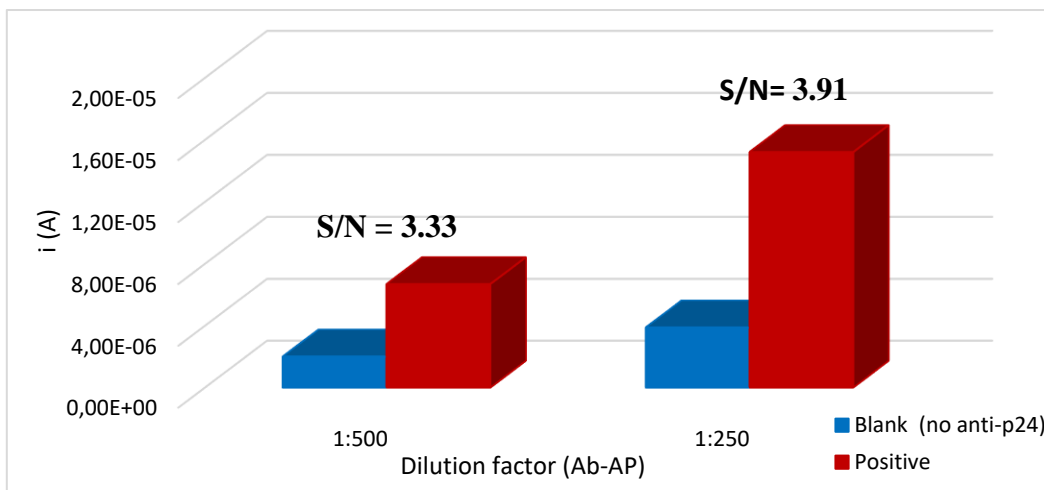


**Figure 39** Effect of different dilution factor of Ab-AP (1:250 and 1:500), on signal to noise (S/N) ratio.

On the basis of these findings, best inhibition rates were obtained performing the immunocompetition experiments fixing the anti-p24 concentration at 1  $\mu\text{g}/\text{mL}$  and diluting the Ab-AP reading antibody by a 1:250 factor, with respect to the commercial stock solution. A remarkable improvement of the performance of the immunoassay was noticed, obtaining a device able to work in an extended concentration range (Figure 40), with higher sensitivity and strongly improved limits of detection (LOD) and quantification (LOQ), assessed at 95  $\text{pg}/\text{mL}$  and 2.6  $\text{ng}/\text{mL}$ , respectively. The LOD and LOQ were assessed as the concentration of analyte giving a signal that is  $2t_{s_b}$  and  $10s_b$  above the mean blank signal, respectively, where  $s_b$  is the standard deviation of the blank signal obtained from ten independent blank measurements and  $t$  is the constant of the t-Student distribution (one-tailed) at 95 % confidence level. At least three replicate measurements (independent immunoassays carried out with different p24-modified SWCNT-SPEs) were carried out for all samples.

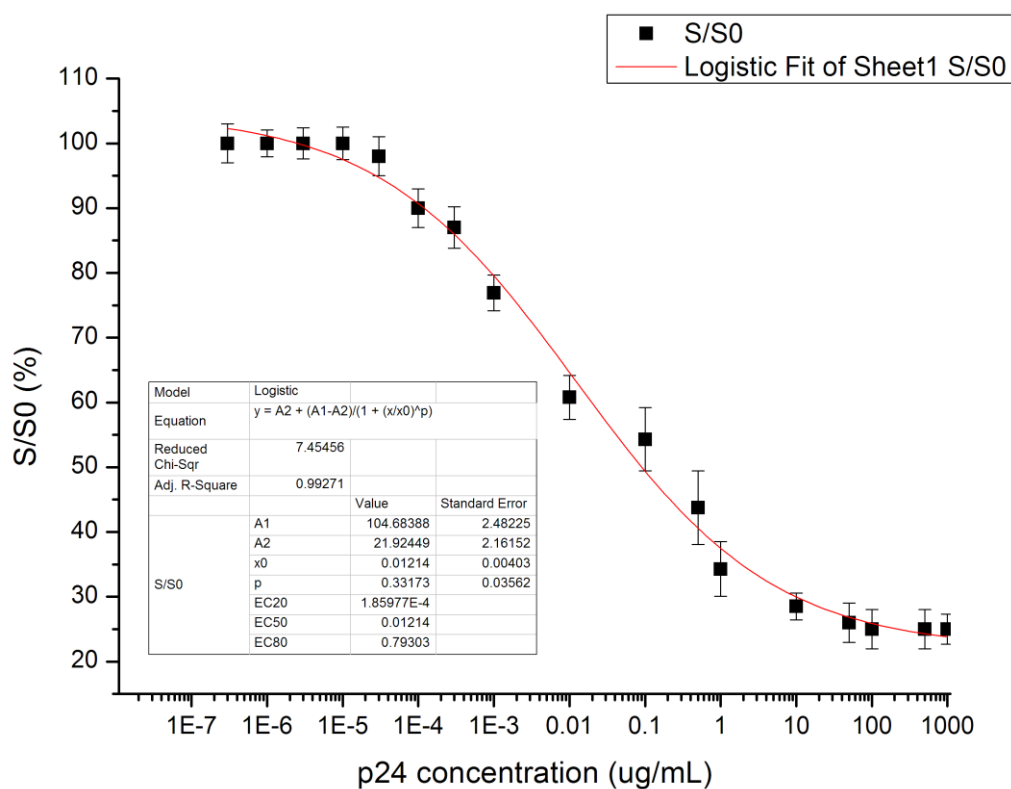


**Figure 40 Immunocompetition curve obtained on SWCNT-SPCEs, over the 1 pg/mL - 1 mg/mL p24 concentration range, fitted with the four-parameter logistic function. Optimized parameters in the inset table.**

These results confirm the exceptional enhancing properties offered by carbon nanotubes and allow us to consider the concrete perspective of applicability of the immunodevice for rapid and easy screening programs aimed to early diagnosis of HIV infection. In order to evaluate the reliability and the analytical robustness of the immunosensor for clinical purposes, a full validation procedure, carried out in real matrix of interest (serum samples) is currently under development.

### 4.3 DEVELOPEMENT OF A COMPETITIVE IMMUNOSENSOR FOR THE DETECTION OF HCV CAPSID PROTEIN NS4

Analogously to the sensor for HIV, the development of a competitive immunosensor for the determination of capsid protein NS4, aimed to diagnosis of HCV infection, was preliminarily investigated.

NS4 is a more complex system, resulting in a combination of NS4A and NS4B proteins, located in the cell virial core. Specifically, the NS4 protein used in this study is a recombinant protein, generated in *Escherichia coli*, containing the HCV immunodominant regions, corresponding to amino acids 1691-1710, 1712-1733 and 1921-1940, fused with a Glutathione-S-Transferase (GST) tag at N-terminus. NS4A corresponds to amino acids 1658-1711 and NS4B to 1712-1972.

On the basis of the results obtained for the development of the immunosensor for HIV-1 p24 protein, the protocol for the immunodevice was characterized by the use of carbon SPEs substrates, on which NS4 was covalently linked, through chitosan/glutaraldehyde system. Also in this case, the anti-NS4 antibodies immunosorbed as a result of the immunocompetition, were detected by an alkaline phosphatase-tagged secondary anti-mouse antibody (Ab-AP).

The first experiments were aimed to evaluate the response of the NS4/anti-NS4 antibody system to the electrochemical assay, in order to proceed to the setup of the competitive immunodevice.

#### 4.3.1 Reagents and solutions

Trizma® base, Tween-20, chitosan (CS, medium molecular weight), glutaraldehyde (GA, 25% in aqueous solution),  $\alpha$ -Casein from bovine milk and acetic acid (99-100% puriss.) were purchased from Sigma–Aldrich (Milan, Italy).

Recombinant (*E. coli*) Hepatitis C Virus Genotype 1 NS4 protein, Mouse monoclonal Anti-Hepatitis C Virus IgG1 [5D4/10E7] (anti-NS4 antibody) and Alkaline Phosphatase-conjugated rabbit anti-mouse IgG (Ab-AP) were purchased from abcam® (Cambridge, UK).

Sodium Phosphate Bibasic, Potassium Phosphate Monobasic and Magnesium Chloride were purchased from Carlo Erba (Milan, Italy).

Hydroquinone Diphosphate (HQDP) and Dropsens® screen-printed electrodes were purchased from Metrohm Italiana (Origgio-VA, Italy).

Deionized water was obtained from an in-house Milli-Q water purification system Alpha Q-Water (Millipore, Billerica, MA, USA).

Phosphate-buffered saline (PBS 10×) was prepared according to the following composition: 1.37 M NaCl, 0.027 M KCl, 0.015 M KH<sub>2</sub>PO<sub>4</sub> and 0.08 M Na<sub>2</sub>HPO<sub>4</sub> (pH 7.4).

Diluted Phosphate buffered (PBS 1 x) was prepared by dilution of PBS 10 X in water.

The washing buffer PBS-T consisted of PBS containing 0.05 % of the surfactant Tween-20.

TRIS buffer was prepared according to the following composition: 0.1 M Trizma® base, 0.02 M MgCl<sub>2</sub> (pH 7.4), and the washing buffer TRIS-T consisted of TRIS containing 0.05 % of the surfactant Tween-20.

“Reading buffer” (RB) has the same composition of TRIS buffer but pH 9.8.

### 4.3.2 Apparatus and electrodes

The immunosensors were realized using DropSens® disposable screen-printed electrodes, assembled on ceramic substrate (L 33 x W 10 x H 0.5 mm), with 4 mm-diameter working electrode, counter electrode of the same material of WE and silver reference electrode.

The readings of the electrochemical assays were performed by CV, for the electrochemical characterization of the HCV/NS4 anti-NS4 system, and by DPV for the preliminary studies of the competitive immunosystem. Electrochemical measurements were performed scanning the potential between -0.5 V and +0.3 V, with a scan rate of 0.05 V/s, for CV, and, in case of DPV, with a pulse amplitude of 0.05 V, a step potential of 0.005 V and a pulse time of 0.1 s. Nonelectroactive HQDP (1 mg/mL) was used as enzymatic substrate. All electrochemical measurements were performed with a  $\mu$ Autolab III electrochemical workstation (EcoChemie, Utrecht, NL) equipped with GPES 4.0 version customized software.

### 4.3.3 Methods

#### 4.3.3.1 Electrochemical characterization of the HCV NS4/anti-NS4 antibody system

GC-SPCEs were functionalized with 15  $\mu$ L of 0.05 mg/mL CS in acetic acid (0.1 M) and dried at room temperature, then the modified electrode was activated with 2.5% GA (in 0.05 M, PBS 1x) for 2 h and, after activation, washed with deionized water. Therefore, 30  $\mu$ L of HCV NS4 protein (10  $\mu$ g/mL) were applied to the working electrode, reacted at room temperature for 1h and then kept at 4 °C overnight.

After removal of unreacted NS4, by accurate washing with PBS-T and PBS, a blocking treatment was carried out with 30  $\mu$ L of a 20 mg/mL solution of  $\alpha$ -Casein dissolved in PBS-T on each electrode for 1h at room temperature, followed by washing with TRIS-T and TRIS buffer. All washing steps were repeated 3 times.

Then 30  $\mu$ L of anti-NS4 antibody IgG1 at different concentration (0  $\mu$ g/mL, 1  $\mu$ g/mL, 10  $\mu$ g/mL, 100  $\mu$ g/mL respectively), were incubated at room temperature, for 1h.

After removal of unreacted antibody, by accurate washing with TRIS-T and TRIS (1x), each electrode was incubated for 1h, at room temperature, with 30  $\mu$ L of a solution of the Ab-AP, diluted 1:500 in TRIS (1x). This step is followed by accurate washings with TRIS-T and RB, to remove unreacted enzyme, and detection, through CV measurements, in order to detect the secondary antibody.

#### 4.3.3.2 Competitive immunoassay

The NS4-modified-SPCEs are ready to use as substrates for the development of the competitive electrochemical immunoassay. Hence, 30  $\mu$ L of NS4 solution at different concentrations (1, 10 and 100  $\mu$ g/mL) were mixed with different concentrations of a solution of Ab anti-NS4 in TRIS (1 x), (in the range: 1  $\mu$ g/mL-100  $\mu$ g/mL). The mixture was transferred on the working electrode of the immunosensor and the competition reaction was allowed to take place for 1h at room temperature. After the immunocompetition, the sensors were carefully washed with TRIS-T and TRIS to remove unspecifically bound material. In order to detect the anti-NS4 antibodies immunosorbed on the



electrode surface, each immunosensor was incubated for 1 hour at room temperature with 30  $\mu\text{L}$  of a solution of the Ab-AP diluted 1:500 in TRIS. After washings, the readings of the electrochemical assays were performed in HQDP solution by DPV.

#### 4.3.4 Preliminary Results

CV responses reported in Figure 41 show a proper trend of the signals, which increase with the concentration of anti-NS4 antibody, with a very low unspecific signal recorded for the blank (PBS 1 x).

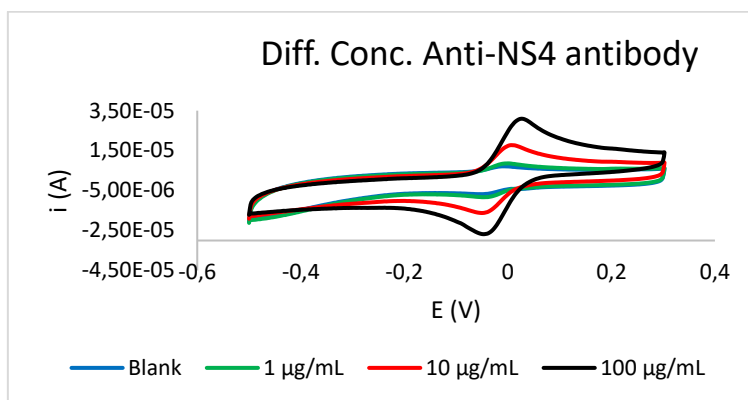


Figure 41 CV responses obtained under incubation of anti-HCV antibody at different concentration, from 0 to 100  $\mu\text{g/mL}$ , on NS4-modified carbon screen-printed electrodes.

On the basis of these results, preliminary immunocompetition experiments were undertaken, showing promising results currently under consolidation. Figure 42 shows signal recorded in DPV for CG-SPEs functionalized with 10  $\mu\text{g/mL}$  of NS4, after incubation of 1  $\mu\text{g/mL}$  of anti-NS4, in absence (Blank) and in presence of NS4 at 1  $\mu\text{g/mL}$  in competition, corresponding to 25% of inhibition rate.

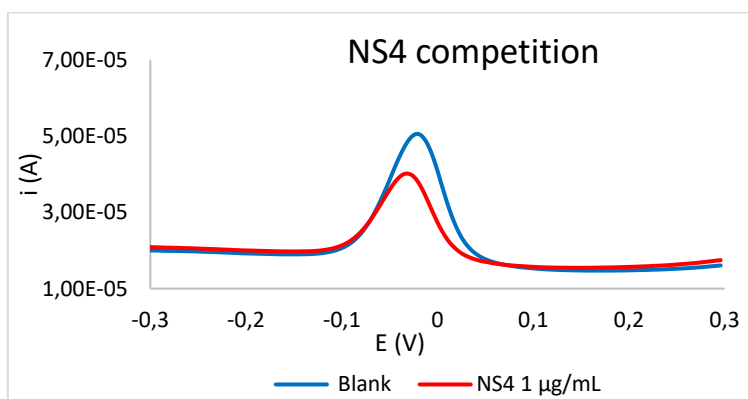


Figure 42 DPV responses from immunocompetition experiments carried out varying the concentration of NS4 in competition from 0 to 1  $\mu\text{g/mL}$ .

#### 4.4 PRELIMINARY STUDIES ON DUAL-CHIP DEVICE

In the perspective of the implementation of a dual-WE system for the simultaneous determination of the capsid proteins related to HIV and HCV, some preliminary studies were performed with p24 protein, on the basis of the promising results obtained for the development of the competitive immunosensor for p24 determination on single-WE screen-printed electrodes.

As previously mentioned in Section 4.1.1, the main limiting factor when using dual devices is the so-called cross-talk phenomenon, due to the diffusion of electroactive species between the two working electrodes, with the risk of false positives in test response. To overcome this problem, a transduction system based on the use of 3-Indoxyl-Phosphate (3-IP) in combination with a silver salt ( $\text{AgNO}_3$ ) was proved [113, 114]. In the presence of alkaline phosphatase, 3-IP is dephosphorylated and the obtained intermediate is able to reduce silver ions in solution into a metallic deposit, which is localized where the enzymatic label AP is attached. Meanwhile the intermediate, which suffers of keto-enolic tautomerism, is oxidized in presence of atmospheric oxygen to produce a product called indigo blue (Figure 43). Then, the deposited silver can be electrochemically stripped into solution and detected by anodic stripping voltammetry.

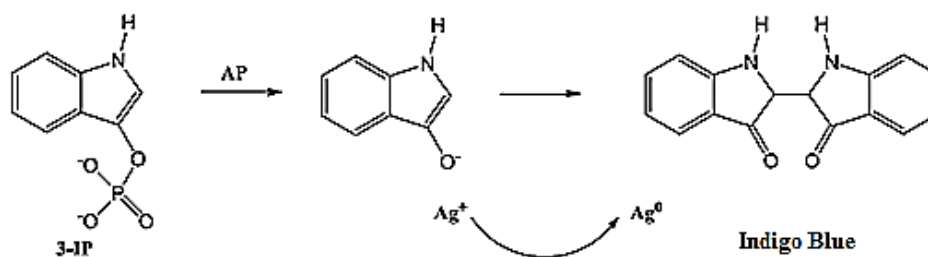


Figure 43 Transduction system based on the use of 3-IP in combination  $\text{AgNO}_3$ : AP enzymatic reaction on 3-IP and Ag reduction.

#### 4.4.1 Reagents and solutions

Reagents and solution used for HIV p24 immunosensor development (Section 4.2.1) were used also in this protocol, with the addition of:

Magnesium nitrate hexahydrate ( $\text{MgNO}_3 \cdot 6 \text{H}_2\text{O}$ ), Indoxyl phosphate disodium salt (3-IP), silver nitrate ( $\text{AgNO}_3$ ), purchased from Sigma-Aldrich (Milan-Italy).

TRIS- $\text{HNO}_3$  buffer was prepared according to the following composition: 0.1 M Trizma® base, 0.02 M  $\text{MgNO}_3 \cdot 6 \text{H}_2\text{O}$  (pH 7.4).

“Reading buffer” (RB) consists of 0.1 M Trizma® base, 0.02 M  $\text{MgNO}_3 \cdot 6 \text{H}_2\text{O}$  (pH 9.8), containing 0.005 M 3-IP and 0,0004 M  $\text{AgNO}_3$ , stored in dark flasks at +4°C.

#### 4.4.2 Apparatus and electrodes

The immunosensor was realized using DropSens® disposable dual-SPCEs, assembled on ceramic substrate, with two elliptic carbon working electrodes, one carbon counter electrode and a silver reference electrode.

The readings of the electrochemical assays were performed by CV or DPV, scanning the potential between -0.2 V and +0.5 V and with a scan rate of 0.05 V/s. Nonelectroactive 3-IP/ $\text{AgNO}_3$  was used as enzymatic substrate. 1mL of 3-IP/ $\text{AgNO}_3$  containing RB was incubated in darkness for the necessary time, until the end of enzymatic reaction.

All electrochemical measurements were performed with  $\mu\text{Stat}$  400 portable bipotentiostat, allowing to simultaneously read the signals from the two WEs, driven by the *Drop View 8400* customized software.

#### 4.4.3 Method and results discussion

Electrode functionalization with p24 and following incubations were carried out analogously to the experimental procedure reported in Section 4.2.3.2.3, until incubation of antibody AP-conjugated.

Concerning the use of 3-IP/ $\text{AgNO}_3$  as enzyme substrates, a preliminary study was carried in order to assess the time required to reach an exhaustive enzymatic reaction. Specifically, three different reaction times (5, 15 and 20 minutes) were evaluated on conventional one-WE SPEs, functionalized with p24, and incubated with TRIS buffer (blank) and anti p24 solutions at 3 and 30  $\mu\text{g}/\text{mL}$ . All electrodes were finally incubated with 1:500 diluted Ab-AP (Figure 44).

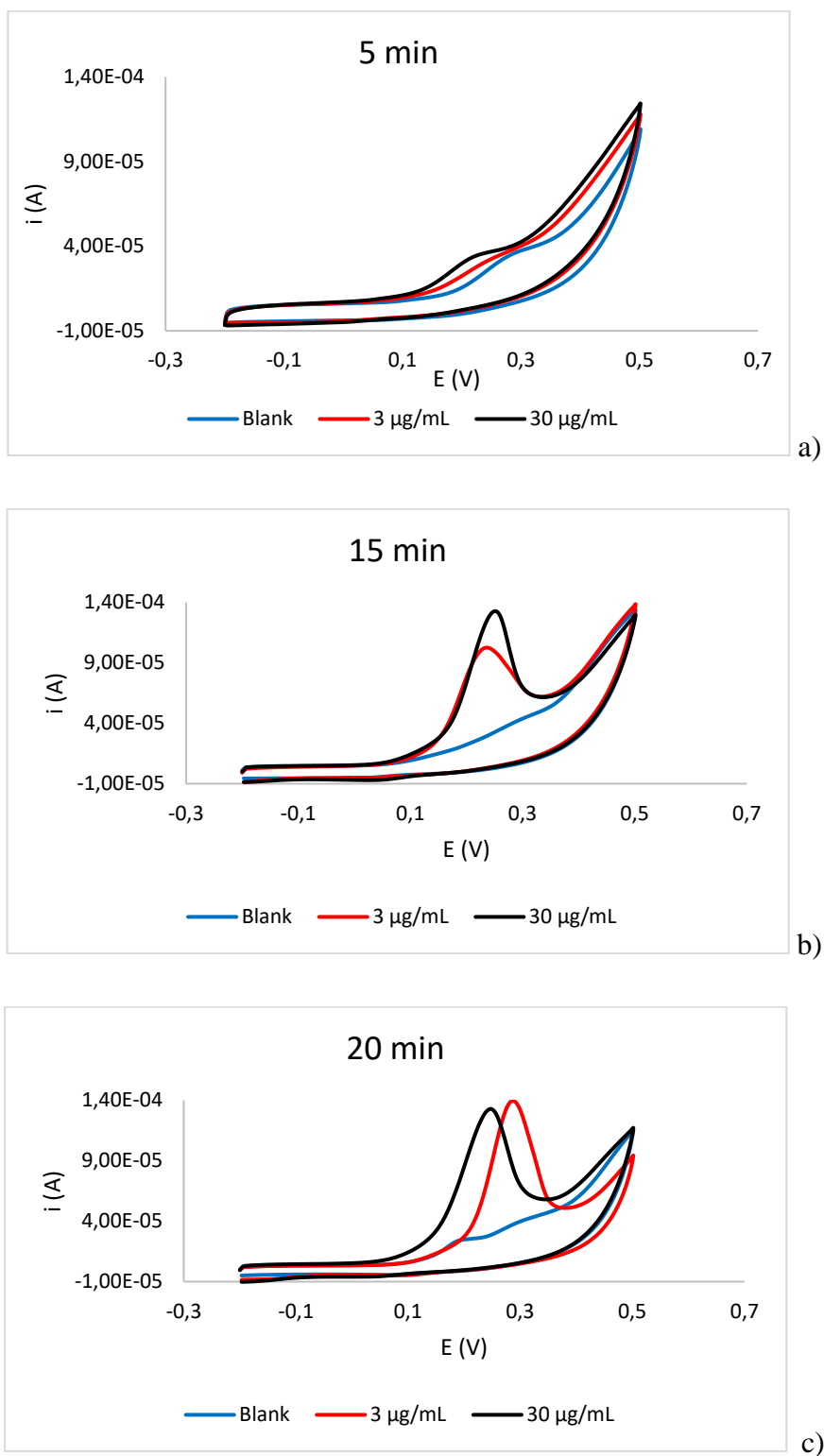


**Figure 44** CV responses obtained under incubation of different concentrations of anti-p24 antibody on p24-modified glassy carbon screen-printed electrodes, at different incubation time of 3-IP/AgNO<sub>3</sub>: a) 5, b) 15 and c) 20 minutes.

As shown in the above voltammograms, 5 minutes of incubation time are not enough to allow the enzyme reaction, while 20 minutes led to superimposable responses for different concentration of anti-p24. Best results were obtained with an incubation time of 15 minutes, allowing to discriminate the responses from different concentrations of anti-p24.

To evaluate the extent of the cross-talk phenomenon, some measurements were performed with dual-SPCEs previously functionalized with chitosan and activated with glutaraldehyde, using both HQDP and 3-IP/AgNO<sub>3</sub> as enzyme substrates.

Each WE of the dual SPCEs was functionalized with 10  $\mu$ L of a 10  $\mu$ g/mL p24 solution, then one electrode was incubated with 10  $\mu$ L of TRIS buffer (blank) and the other electrode with 30  $\mu$ g/mL anti-p24 antibody (Figure 45). Finally, 50  $\mu$ L of 1:500-diluted Ab-AP was incubated (in a single drop, covering both WEs) and the reading was performed on the two independent channels.

The finding of these experiments evidenced very weak and undifferentiated signals from the two WEs, when using HQDP as reading substrate. Conversely, a moderate but significant difference between the two signals was observed using the 3-IP/AgNO<sub>3</sub> system (Figure 45).

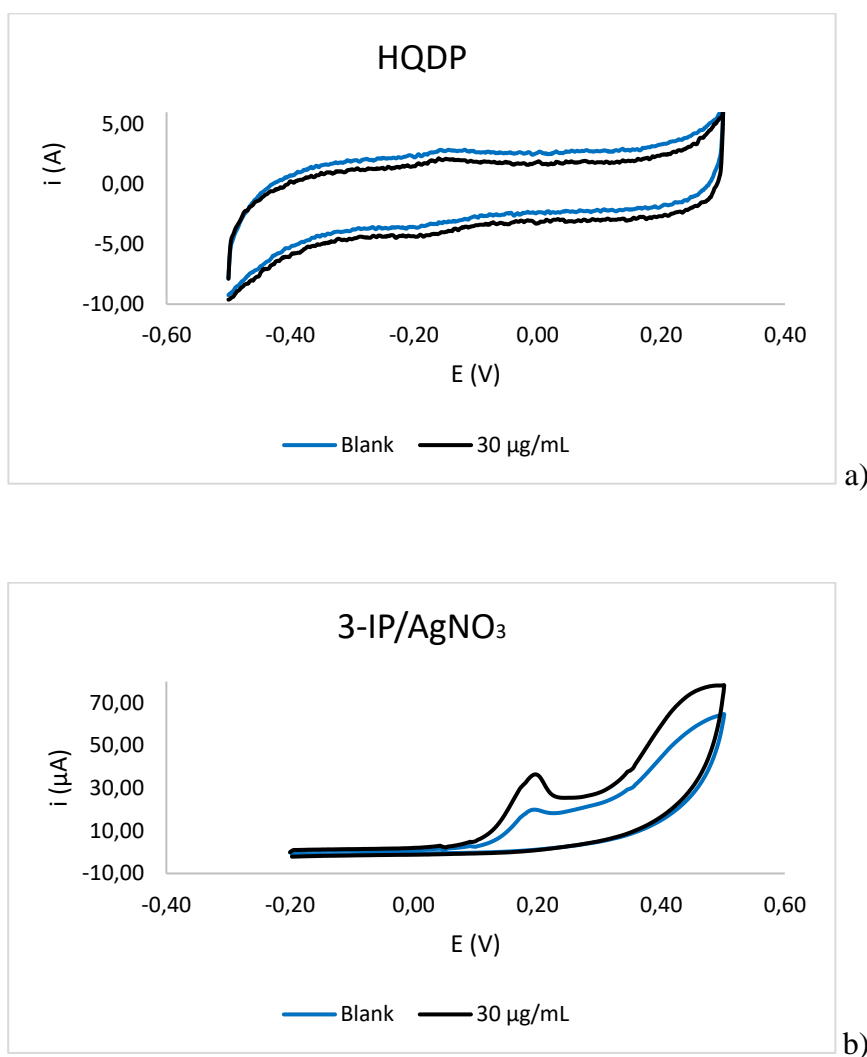


**Figure 45** CV responses obtained under incubation of anti-p24 antibody at 30  $\mu$ g/mL (reading channel 1) and PBS, as blank, (reading channel 2) on p24-modified glassy carbon screen-printed electrodes, using a) HQDP and b) (3-IP/AgNO<sub>3</sub>) as transduction systems.

The signal recorded for “blank channel”, although lower with respect to the “positive channel”, is probably due to contamination between the two drops, occurring during the incubation. This unspecific response represents a critical issue arising from the contiguity of the two electrodes, also considering the absence of concavity that could help the confinement of the solution used for the differential functionalization of the sensing platforms.

On the basis of these findings, also considering the high level of criticality experimented and demonstrated for the immunocompetitive approach involving complex proteins such as p24 antigen (potentially occurring as oligomeric aggregates, with different immunoreactivity), we decided to focus our attention on the consolidation of the results singularly concerning the two infection biomarker proteins, postponing the combination of the systems onto a dual device to a future project.

## **5. MAGNETOIMMUNOSENSOR BASED ON GOLD/SILVER BI-METALLIC NANOPARTICLES FOR SENSITIVE DETECTION OF HIV CAPSID PROTEIN p24**

This project was carried out at Catalan Institute of Nanoscience and Nanotechnology (ICN2), located at Autonomous University of Barcelona (UAB) campus (Bellaterra), in Nanobioelectronics & Biosensors Group, directed by Professor Arben Merkoçi.

### **Abstract**

The aim of the present project is the development of a competitive immunoassay, implemented on Screen-Printed Electrodes (SPCEs), involving gold/silver bi-metallic nanoparticles (BNPs) as electroactive tags, for a sensitive detection of p24 antigen, as Human Immunodeficiency Virus (HIV) biomarker. To reach this purpose, magnetic beads (MBs) and BNPs were used.

Thanks to MBs it is possible to reach an improvement in sensitivity and selectivity, due to the pre-concentration of the sample and to the minimization of matrix effects. The gold present on BNPs allows a good bio-functionalization, associated to a catalytic effect in silver oxidation.

The aim of this part of the project was the application of the above described micro- and nano-materials as pre-concentration substrates and enzyme-free labeling systems, respectively. In this perspective, the already promising performance of the devices discussed in Section 4.2.4.2.2 could be further improved.

## **5.1 INTRODUCTION**

### **5.1.1 Metal nanoparticles for immunosensing applications**

In the last years, the increasing interest on nanoparticles is mostly due to their unique chemical, physics and electronics properties, different from their bulk materials, which can be successfully exploited for construction and improvement of sensors and biosensors (as mentioned in Section 2.3.2).

The peculiar properties of metal nanoparticles (MNPs) are strongly dependent on their synthesis, fundamental for MNPs quality, as well as on their modification through chemical or biological methods. They can play different roles [115, 116] in different field of applications, such as:

- Direct involvement in chemical/physical reaction (as reactants)
- Biomolecules immobilization
- Electrochemical catalysis
- Electron transfer enhancement
- Biomolecules labeling

Focusing the attention on the labeling properties for biomolecules (antigen, antibody or DNA), MNPs can be studied and employed for the development of high sensitive electrochemical biosensors. In this way, biomolecules maintain their immunoreactivity towards their counterpart and the concentration of the target analyte can be determined through direct or indirect electrochemical detection of MNPs.

In the first case, MNPs are directly detected, without any preliminary step of dissolution. This method requires a direct contact between particles and electrode surface, in order to avoid the loss of “non-touching” particles during detection; it is characterized by rapid response and considerable LOD.

Very sensitive MNPs detection can be reached with indirect voltammetric methods, requiring metal nanoparticles dissolution for detection of their corresponding ions, through stripping analysis. However, these methods have the disadvantage of requiring toxic or concentrated chemical agents for metal dissolution.

Despite the high sensitivity of stripping analysis, different strategies have been studied to reach a further improvement in sensitivity of metallo-immunoassay, including methods based on silver involvement.

In most applications, the enhancement given by silver relies on its reduction on AuNPs surface, followed by anodic-stripping measurements. However, this procedure is time-consuming and its sensitivity is sometimes compromised by non-specific silver deposition. Alternatively, De la Escosura- Muñiz et al [117] reported for the first time the silver electrodeposition process for electrochemical immunoassay detection with AuNPs label. In this case, silver is electrochemically deposited on AuNPs surface for their electrochemical detection, with an improvement in sensitivity and signal enhancement given by the catalytic role played by gold (deposited on the electrode surface) in silver reduction. However, this method required the use of a silver-ammonia complex as starting reagent, inducing an electrode damage in the case of SPCEs.

In order to take advantage of both silver enhancement process and gold catalysis, in this project BNPs were used for electrochemical biosensing, as alternative approach to the methods already available.

#### **5.1.1.1 Gold/silver bimetallic nanoparticles (BNPs) for biosensors development**

The aim of this project was the investigation of the electrochemical properties of BNPs in order to reach an improvement in sensitivity and signal enhancement thanks to gold and silver combination. Specifically, the key purpose was the combination of the biocompatibility of gold NPs, allowing their conjugation with antibodies, with their catalytic activity toward redox process involving silver. In fact, in order to avoid silver reduction or electrodeposition, followed by stripping analysis, the silver natively included in the BNPs is directly involved in the analytical detection of the target

In the perspective of the development of a BNPs-based magnetoimmunosensor for detection of HIV capsid protein p24, a preliminary study aimed to electrochemical characterization of BNPs was carried out.



## **5.2 GOLD/SILVER BI-METALLIC NANOPARTICLES (BNPs): ELECTROCHEMICAL CHARACTERIZATION**

### **5.2.1 Experimental**

#### **5.2.1.1 Reagents and solutions**

Phosphate buffered saline tablets were purchased from Sigma–Aldrich Química (Spain).

60 nm-sized gold/silver bi-metallic nanoparticles (BNPs) and 60 nm-sized silver nanoparticles (AgNPs) were synthesized and optically characterized by Mr. Lorenzo Russo, member of Inorganic Nanoparticles Group at ICN2, directed by Professor Victor Puntes.

Deionized water, obtained using a Milli-Q system, produced from Millipore, was used for preparation of samples.

Phosphate buffered saline (consisting on 10 mM phosphates, 1.37 mM NaCl and 3 mM KCl, pH= 7.4) was prepared by dissolution of 1 PBS tablet in 200 mL of water.

#### **5.2.1.2 Apparatus and electrodes**

The electrochemical transducers were homemade Screen-Printed Carbon Electrodes (SPCEs) and all electrochemical measurements were performed using an Autolab 20 (EcoChemie) device.

Furthermore, the electrochemical evaluation of different BNPs and AgNPs were performed by Cyclic Voltammetry (CV), scanning the potential between -0.9 V and +0.9 V, with a scan rate of 0.05 V/s. After drop-casting of the BNPs sample on the sensor, an equilibration time of 30 s and a preconditioning stage of 60 s at -0.8 V were applied prior to run CV, in order to reach an exhaustive reduction and to pre-concentrate Ag.

Then, the evaluation of different reduction potential both with BNPs and AgNPs was performed by Differential Pulse Voltammetry (DPV), scanning the potential between -0.3 V and +0.3 V, with pulse amplitude of 0.05 V, step potential of 0.001 V and a pulse time of 0.1 s. After drop-casting of the BNPs on the sensor, an equilibration time of 30 s and a preconditioning stage of 60 s, at -0.8, -0.4 or -0.2 V for BNPs and -0.8, or 0.2V for AgNPs, was applied prior to run DPV.

### 5.2.1.3 Methods

#### 5.2.1.4 Electrochemical evaluation and characterization of BNPs

Different types of BNPs at different Au/Ag ratio (called "200", "260" and "500", respectively) were evaluated (Figure 46). On the basis of the preliminary results, BNPs with best performance were selected for the following studies and applications.

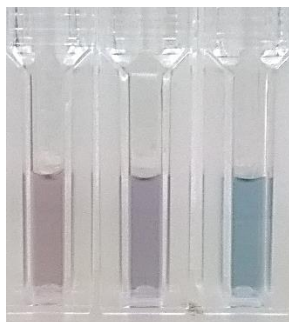


Figure 46 Different types of BNPs: "200", "260" and "500", from left to right.

Prior to the electrochemical characterization, the colloidal nanoparticles were washed by centrifugation at 8000 rcf for 10 minutes at room temperature, followed by resuspension in milliQ water. Then they were properly diluted in PBS buffer and electrochemically studied.

### 5.2.2 Results and discussion

A characterization of BNPs in PBS buffer showed a singular behavior: the chloride ions contained in the buffer preliminary induce the oxidation of silver to  $\text{Ag}^+$  ions and the following silver reduction is catalyzed by gold. (Figure 47).

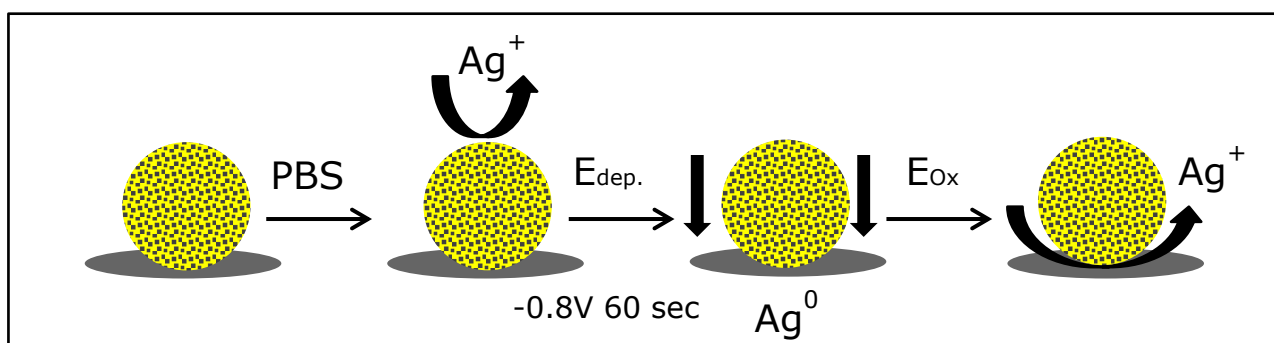


Figure 47 Schematic representation of redox process involving silver of BNPs.

Due to the preliminary oxidation step, for silver detection it is necessary to apply a deposition potential of  $-0.8\text{ V}$ , in order to allow  $\text{Ag}^+$  reduction. This process is catalytically assisted by gold,

allowing to reach the silver reduction at potential values less negative than -0.8 V, followed by oxidation of the pre-reduced silver. Voltammograms reported in Figure 48 show the trend observed as a function of the Au/Ag ratio of the studied BNPs: as the amount of gold increases, switching from “200” to “500” BNPs (i.e. increasing Au/Ag ratio), the half-wave potential (corresponding to silver reduction) shifts to less negative potentials, together with an increase in the peak current intensity, corresponding to silver re-oxidation, as confirmation of the establishment of a electrocatalytic process.

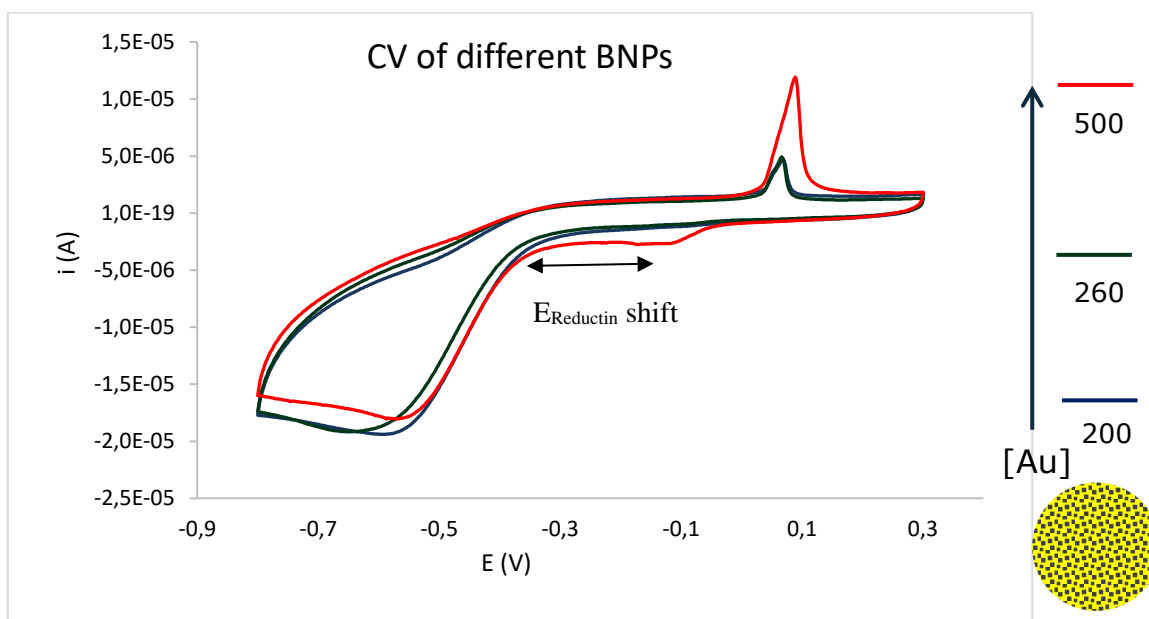


Figure 48 CV responses for different types of BNPs (“200”, “260” and “500”) at different gold/silver ratio.

These preliminary measurements in PBS buffer were analogously performed also in chloride-free PB buffer, in order to confirm the role played by chloride ions in the silver oxidation step. The measurements were performed with “500” BNPs (the highest gold content). Moreover, the behavior of mono-metallic AgNPs has been also investigated as reference comparison (Figure 49).

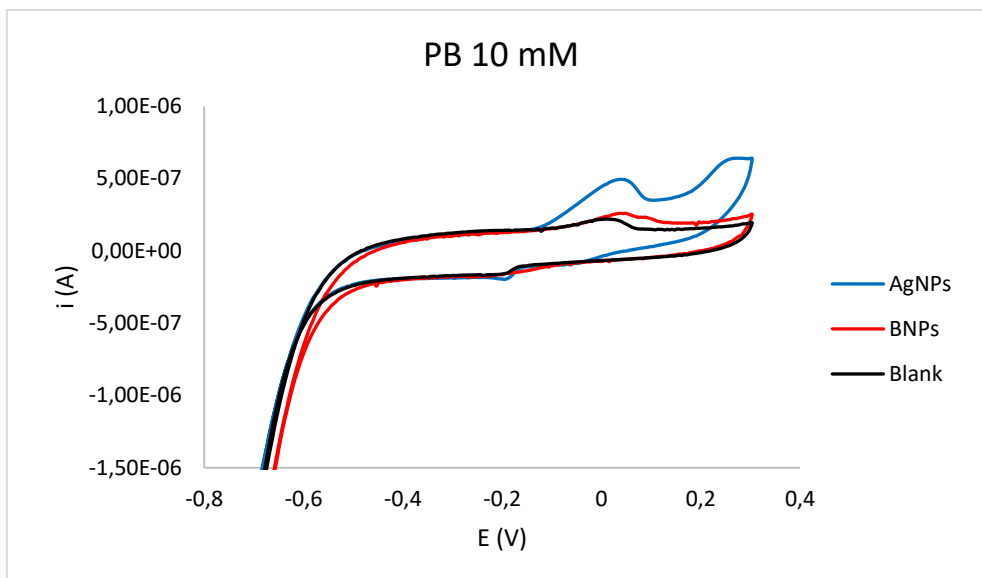


Figure 49 CV signals obtained with AgNPs, BNPs and PB (as blank), in PB 10 mM.

Then, in order to confirm the catalysis by gold, the same measurements were performed also in PBS. Voltammograms reported in Figure 50 show that in PBS it is possible to observe the potential reduction shift only for BNPs, confirming the gold catalytic role in silver reduction.

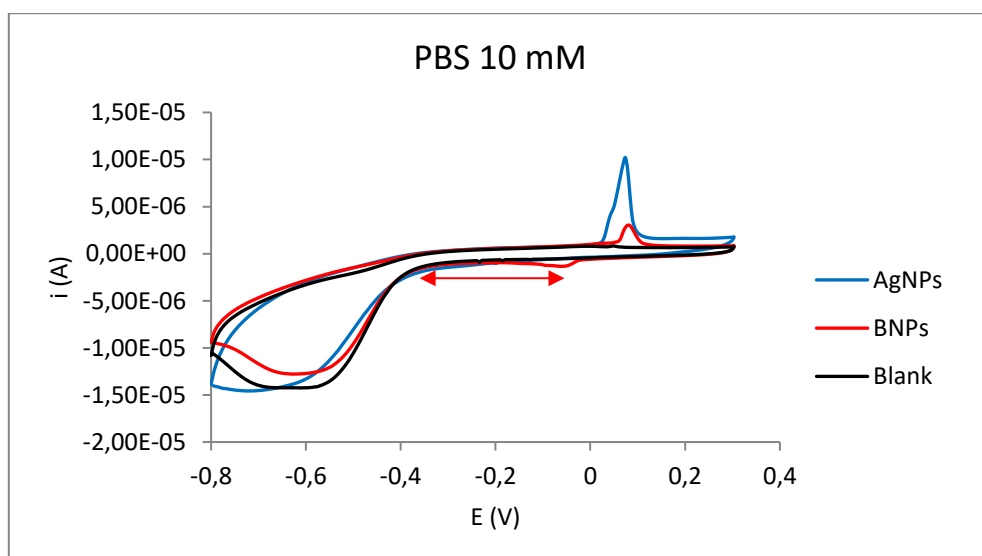


Figure 50 CV signals obtained with AgNPs, BNPs and PBS (as blank), in PBS 10 mM.

On the basis of these findings, it was decided to evaluate different deposition potentials, i.e. -0.8 V, -0.4 V and -0.2 V, performing measurements through DPV in order to enhance the faradic component of the signal with respect to the capacitive background (as described in Section 1.5) and to evaluate lower BNPs concentration. The intensity of the oxidation signal from BNPs was related to the applied deposition potentials. For each deposition potential, the oxidation current trend was evaluated as a

function of BNPs concentration, in order to assess the quantitative relationship. Figure 51 shows DPV responses obtained in the presence ( $1.66 \cdot 10^{-11}$  M) and in the absence of BNPs (PBS). More concentration levels were further explored, giving the results summarized in the bar diagrams reported in Figure 51.

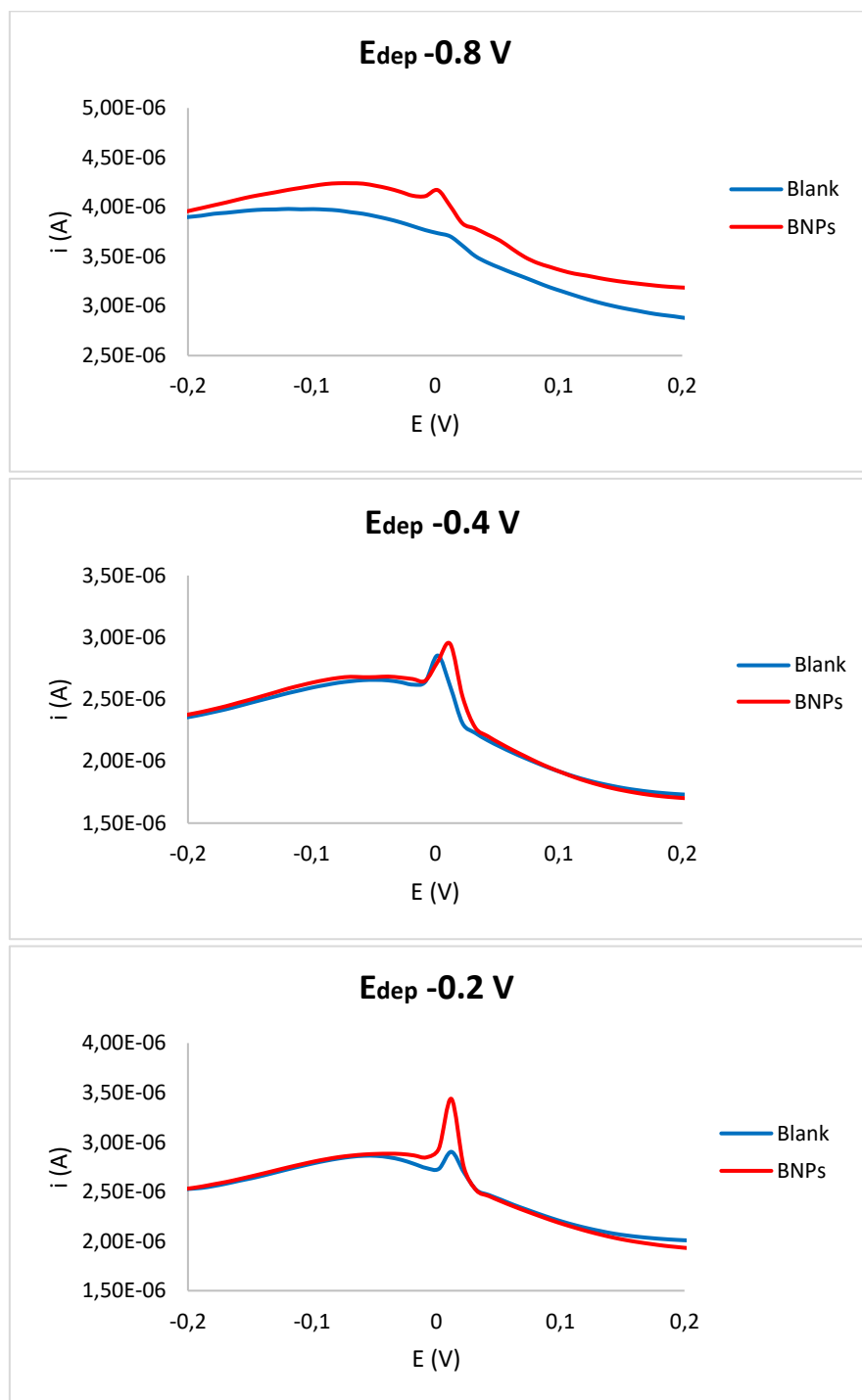


Figure 51 CV signals obtained with BNPs ( $1.66 \cdot 10^{-11}$  M) and PBS (as blank) under application of different deposition potentials: -0.8 V, -0.4 V and -0.2V.

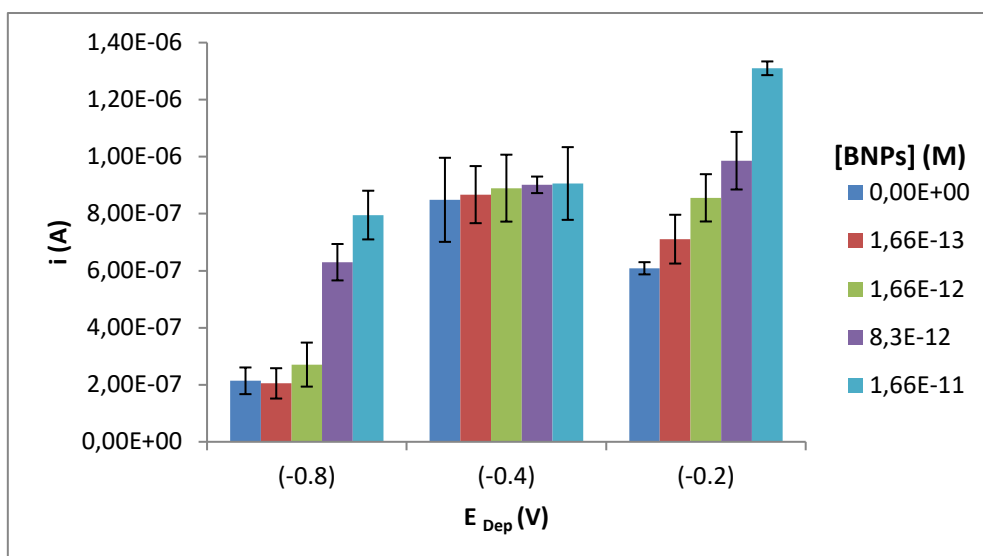


Figure 52 Signals obtained exploring different deposition potential, -0.2 V, -0.4 V and -0.8 V, for BNPs from 0 to  $11.66 \cdot 10^{-11}$  M.

From Figure 52 it can be observed that, thanks to the catalytic effect of gold it is possible to reduce silver at less negative potentials, also obtaining a current signal enhancement, with respect to the usual potential of -0.8 V, necessary for uncatalyzed silver reduction. Under these conditions ( $E_{dep} = -0.2$  V) a relationship between the oxidation current and the BNPs concentration was found, ranging from  $1.66 \cdot 10^{-13}$  M to  $1.66 \cdot 10^{-11}$  M (Figure 53).

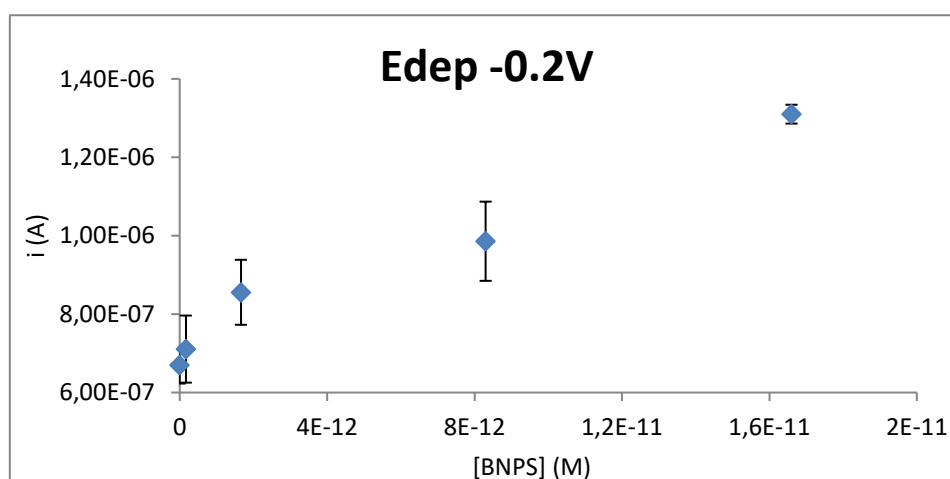


Figure 53 Calibration curve recorded at -0.2 V for BNPs concentration from 0 to  $1.66 \cdot 10^{-11}$  M (three replicate measurements were carried out for each BNPs concentration).

The catalytic effect of gold was further confirmed, performing some measurements with AgNPs, at the same concentration ( $1.66 \cdot 10^{-11}$  M) and size (60 nm) of BNPs, evidencing no reduction at -0.2 V, as showed below (Figure 54).

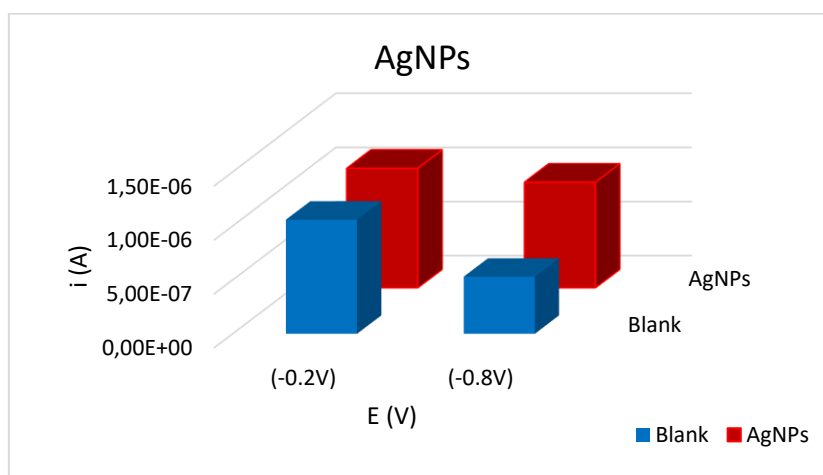


Figure 54 Comparison between signal recorded at -0.2 V and -0.8 V for AgNPs and PBS (as blank).

As reported, at -0.2 V there is no significant difference between blank and positive signals, while at -0.8 V two distinct signals can be found, confirming that catalysis of gold is fundamental to promote reduction of silver at less negative potentials.

### 5.2.3 Conclusions

In this study, BNPs were electrochemically characterized for the first time. They showed useful properties for biosensing application, combining the tag properties of silver with the catalytic properties of gold. Specifically, thanks to preliminary silver oxidation induced by chloride ions of the used PBS buffer, it is possible to observe the fundamental role of gold in silver reduction, which allowed to reach silver reduction at less negative potential, with respect to the usual value of -0.8 V, in association to a significant signal enhancement. This effect was further confirmed through measurements performed in chloride-free PB and with mono-metallic AgNPs as comparison. BNPs allow to overcome problems related to silver-enhanced systems, generally based on its reduction on AuNPs surface, followed by anodic stripping measurements or in silver electrodeposition process. In fact, BNPs present the advantages of both silver enhancement process and gold catalysis, without any additional analytical steps, being silver of particles directly involved in analytical detection. These findings allowed to start preliminary studies for HIV immunosensing development.

### 5.3 STUDY FOR DEVELOPMENT OF MAGNETOIMMUNOSENSOR FOR SENSITIVE DETECTION OF HIV CAPSID PROTEIN p24

After electrochemical characterization of BNPs it was decided to apply them for development of a magnetoimmunosensor for sensitive diagnosis of HIV infection, through detection of its capsid protein p24.

To reach this purpose, the experimental approach is quite different with respect to the setup of the competitive immunosensor described in Chapter 4. In order to improve the performance of the sensing devices, exploiting the peculiar properties of nanomaterials, we used magnetic beads as immun-concentration substrate, in order to perform the assay “away from the electrode”, carrying out all functionalization and immunoreaction steps in solution, and subsequently transferring the magnetic material on SPCEs, only for the final reading step.

Magnetic beads (MBs) are widely applied as supports in biosensing applications having interesting properties, such as biocompatibility, large surface area, simplicity of functionalization and easy transferability, modulated by magnetic fields. This last aspect is especially useful when they are applied for analyses involving complex matrices, allowing a minimization of its effect on test response.

The specific aim of this project is to develop a competitive amperometric immunosensor based on p24-functionalized MBs for rapid detection of HIV infection in serum samples. According to the working principle of competitive immunoassay, the presence of p24 in the sample inhibits antibody binding to the immobilized p24, thus the increase of analyte concentration will reduce the amount of antibody anti-p24 bound to the modified surface of the MBs, resulting in a signal decrement.

The immunosorption capabilities of p24-functionalized MBs will be associated to the high sensitive BNPs, after their conjugation with anti-p24 antibodies, to realize a competitive enzyme-free magnetoimmunosensor with working principle depicted in Figure 55.

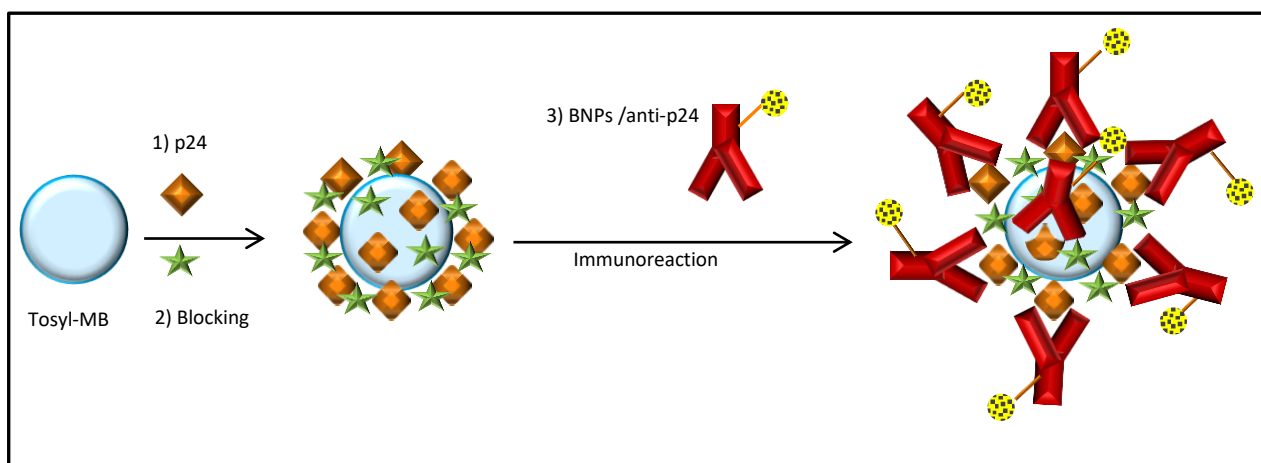


Figure 55 Magnetoimmunosensor setup.

Although this project is currently under development, the voltammetric response of the BNPs/anti-p24 conjugated and the immunoreaction with the corresponding antigen p24, immobilized on MBs, were preliminary evaluated, in perspective of their application for immunoassay development.



### 5.3.1 Experimental

#### 5.3.1.1 Reagents and solutions

Phosphate buffered saline tablets, sodium phosphate bibasic, sodium phosphate monobasic, Tween-20, Bovine Serum Albumin (BSA) were purchased from Sigma–Aldrich Química (Spain).

Tosyl-activated Magnetic Beads (MBs), 2.8µm sized, were purchased from Dynal Biotech (M-280, Invitrogen, Spain).

Recombinant (*E. coli*) HIV-1 p24 full-length protein, Mouse monoclonal anti-HIV-1 p24 IgG1 [39/5.4A] were purchased from abcam® (Cambridge, UK).

MilliQ water, obtained using a Milli-Q system, produced from Millipore, was used for preparation of samples.

60 nm sized gold/silver bi-metallic nanoparticles (BNPs) were synthesized and optically characterized by Mr. Lorenzo Russo, member of Inorganic Nanoparticles Group at ICN2, directed by Professor Victor Puntes.

Phosphate buffered saline (consisting of 10 mM phosphates, 1.37 mM NaCl and 3 mM KCl, pH= 7.4) was prepared by dissolution of 1 PBS tablet in 200 mL of water.

Phosphate buffered (PB) (consisting of 10 mM of phosphates, pH= 7.4) was prepared according to the following composition: 2 mM KH<sub>2</sub>PO<sub>4</sub> and 8 mM Na<sub>2</sub>HPO<sub>4</sub>.

PBS-T and PB-T consisted of PBS and PB, respectively, containing 0.05 % of the surfactant Tween-20.

Borate buffer solution (BB) was prepared with 100 mM boric acid and adjusted to pH 9.2 with 5M NaOH.

#### 5.3.1.2 Apparatus and electrodes

The electrochemical transducers were homemade Screen-Printed Carbon Electrodes (SPCEs) and all electrochemical measurements were performed using an Autolab 20 (EcoChemie) device.

The readings of the electrochemical assays were performed by Differential Pulse Voltammetry (DPV), scanning the potential between -0.3 V and +0.3 V, with pulse amplitude of 0.05 V, step potential of 0.001 V and a pulse time of 0.1 s. After drop casting of each sample on the sensor, an equilibration time of 30 s and a preconditioning stage of 60 s at -0.2 V were applied prior to run DPV.

#### 5.3.1.3 Methods

##### 5.3.1.3.1 Preparation of the conjugated BNPs /anti-p24 antibody

The conjugation of BNPs with anti-p24 antibody was performed according to the following procedure: 1 mL of BNPs suspension ( $4.15 \cdot 10^{-11}$  M) was centrifuged at 8000 rcf and resuspended in 1 mL of 15 µg/mL of anti-p24, in PBS, and incubated at 25 °C overnight under shaking at 650 rpm. Then, a centrifugation at 8000 rcf was performed for 10 minutes, followed by reconstitution of BNPs/anti-p24 in milliQ water.

### 5.3.1.3.2 Preparation of the immunocomplex

The preparation of MBs-based immunocomplex was performed following a method previously optimized at Nanobioelectronics & Biosensors group, with some modifications. 7.5  $\mu\text{L}$  of MBs were washed three times with BB solution, then they were resuspended in 450  $\mu\text{L}$  of a solution of p24 antigen at 10  $\mu\text{g}/\text{mL}$ , incubated for 1 hour at 37  $^{\circ}\text{C}$ , under gentle mixing in a TS-100 ThermoShaker. The formed MBs/p24 were separated from the reaction solution and washed three times with BB solution. Then, they were resuspended in the blocking solution, consisting of BSA at 20  $\text{mg}/\text{mL}$  in PB-T, to block any unfunctionalized site on MBs surface, for 1h at 25  $^{\circ}\text{C}$ , under shaking. After washings with PB-T and PB, the MBs/p24 were incubated with 450  $\mu\text{L}$  of BNPs/anti-p24 at different concentrations, for 1h at 25  $^{\circ}\text{C}$ , under shaking. Then the immunocomplex was washed with PB-T and PB, ready to be resuspended in PBS for electrochemical measurements.

### 5.3.1.3.3 Electrochemical evaluation of conjugated BNPs/anti-p24 antibody

BNPs/Anti-p24 conjugates were diluted in PBS buffer at different concentrations and electrochemically studied, through DPV voltammetry. On the basis of the obtained results, the interaction with the corresponding antigen was evaluated.

## 5.3.2 Results and discussion

BNPs/anti-p24 conjugates, were analysed on homemade SPCEs at different concentrations, corresponding to different dilution factors (1:2, 1:5, 1:10, 1:100 and 1:1000), with respect to the starting stock solution. A dynamic trend was observed, as reported in Figure 56. Therefore, the immunoreaction between p24 adsorbed on MBs and the corresponding BNPs/anti-p24 was studied.

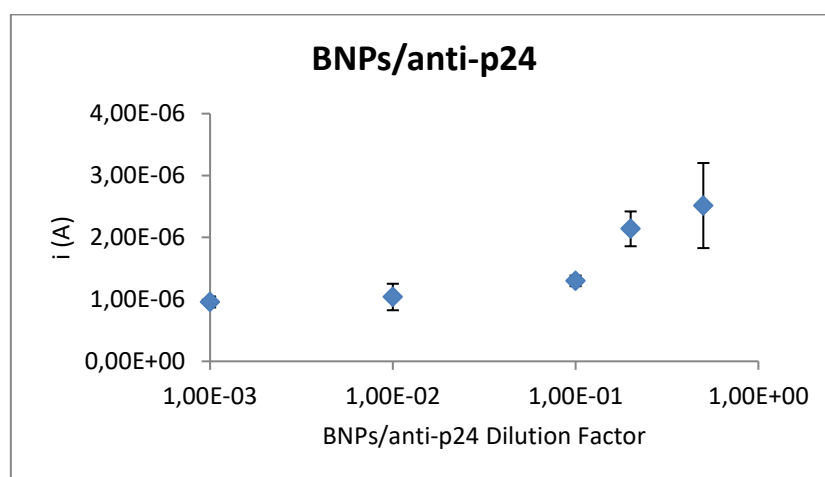
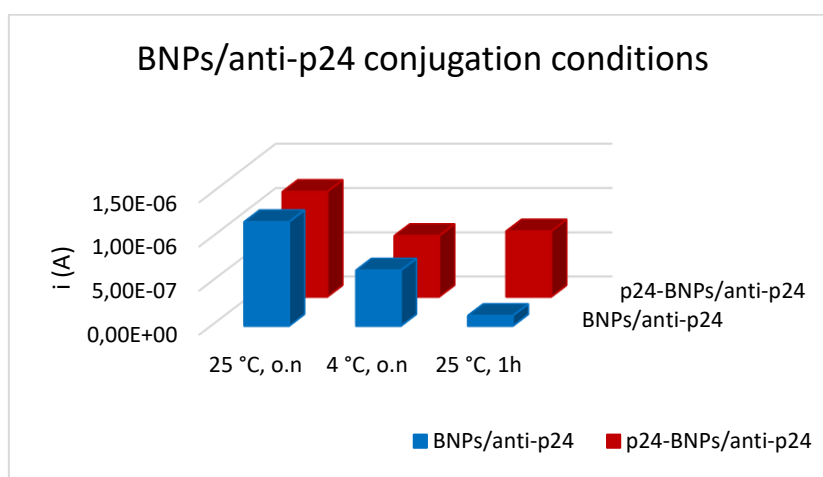


Figure 56 Electrochemical evaluation of BNPs-conjugated with anti-p24 antibody at different dilution factors (1:2, 1:5, 1:10, 1:100 and 1:1000).

Preliminary evaluation of the immunoreactivity did not evidence the effectiveness of the anti-p24-interaction, showing blank signals (unfunctionalized MBs) comparable to positive experiments

performed on p24-functionalized MBs. It was supposed that the reactivity of anti-p24 could be compromised during the conjugation process, carried out at 25 °C for a quite long time, i.e. overnight. To confirm this hypothesis, two alternative conjugation conditions were evaluated: BNPs were reacted at 25 °C for 1h or at 4 °C, overnight. The silver oxidation current reported in Figure 57 show that the conjugation carried out at 4°C overnight does not result in a distinction between blank and positive signals, probably due to a not optimal interaction between BNPs and antibodies at this temperature. Better results were obtained performing the conjugation at 25 °C for 1h, leading to two distinct signals, indicating a good antigen/antibody interaction, and showing that 1 h is enough to ensure particles linkage, avoiding possible alterations of the quaternary structure of the antibody.



**Figure 57 Evaluation of different conjugation condition in terms of time and temperature of BNPs/anti-p24 incubation.**

### 5.3.3 Conclusions

In this preliminary study, BNPs were conjugated with anti-p24 antibodies in perspective of development of a magnetoimmunosensor for sensitive diagnosis of HIV infection, through detection of its capsid protein p24. BNPs/antibodies were electrochemically evaluated and, after dynamic response during the analysis, p24-BNPs/antibody interaction was studied. On the basis of these very preliminary results, it was necessary to evaluate different conditions for the conjugation step, in order to obtain the best yield and to avoid the alteration of the immunoreactivity of the antibody. The conjugation carried out for 1h at 25°C seems to be the best starting condition for the prosecution of the research project shared with the Nanobioelectronics & Biosensors Group of the Catalan Institute of Nanoscience and Nanotechnology, aimed to realization of a magnetoimmunosensor for high sensitive detection of p24 capsid protein.

## 6. BIOSENSORS FOR FOOD SAFETY APPLICATION

As previously introduced, amperometric immunosensors are widely exploited in several fields of applications, in particular not only for medicine and clinical diagnostic, but also for food quality control and environmental monitoring, thanks to their ease of use, low costs and very good analytical performances. In the present section, it is described the development of a competitive immunosensor for the detection of celiotoxic prolamins for safety assessment of declared gluten-free products.

### 6.1 CELIAC DISEASE AND GLUTEN-FREE FOODS

Celiac disease (CD) is one of the most common food-induced disease in humans caused by intolerance to gluten storage proteins of wheat and other common cereals (rye, oats and barley) in genetically susceptible individuals. It is an immune mediated enteropathy causing inflammation in the small intestine and triggered by ingestion of gluten-containing foods. Commonly, CD appears in early childhood with symptoms like chronic diarrhoea and failure to thrive. However, symptoms can also appear in late stage of life, including diarrhoea, fatigue and weight loss due to the malabsorption and anaemia.

The only treatment for CD is a strict and permanent gluten-free diet, avoiding all gluten-containing foods produced from wheat, rye, barley and certain variety of oats.

The market offers a great variety of gluten-free products, which can be consumed by CD patients. However, it has to be taken into account that some products declared as gluten-free could be contaminated during the entire production chain, from raw materials to transport and storage [118]. In this context, the availability of analytical strategies for the detection and quantification of gluten in food is essential not only for the assessment of food safety of declared gluten-free foods, but also to monitor the industry practice quality along the production chain.

The actual European legislation (Commission Regulation No. 41/2009) [119], according to recommendations of the Codex Alimentarius Standard 118-1979 revisited in 2008, established a maximum gluten level of 20 mg/kg of gluten for gluten-free products, whereas “very low gluten” foods are allowed to contain gluten levels up to 100 mg/kg [120].

Gluten is defined “as a protein fraction from wheat, rye, barley, oats or their crossbred varieties and derivatives, to which some persons are intolerant and that is insoluble in water and 0.5 mol/L NaCl” [121]. This protein fraction comprises hundreds of different components and corresponds to the storage proteins exclusively present in the starchy endosperm of the grains. Following the classical definition of Osborne, cereal storage proteins soluble in aqueous alcohols without reduction of disulphide bonds are designated as “prolamins” (gliadins for wheat) and the insoluble proteins as “glutelins” [122]. Although Shewry and coworkers used the term “prolamins” for all storage proteins (including glutelins) [123], in the following described work it is used the classical definition of prolamins, according to Osborne.

The prolamins/gluten conversion factor is usually set to 2 [124], but such a conventional value is not fully reliable, since gluten composition can vary according to its botanical origin (e.g., cereal species, varieties), agricultural conditions in which the plants are produced (e.g., climate, soil, fertilization),

and food processing procedures (e.g., heating, enzymatic degradation, mechanical and chemical processing).

## 6.2 ANALYTICAL METHODS FOR GLUTEN DETECTION

Reliable analytical methods for gluten detection and quantification in foods require good sensitivity, specificity, reproducibility, robustness and the availability of certified reference material, which is currently missing. Furthermore, they should be applicable not only to raw materials but also to processed food. In fact, as for prolamins, the traditional extraction protocol involving aqueous alcohol, usually 40-70% (v/v) ethanol, is effective only on raw materials, but not for processed foods since gluten solubility and properties are modified by thermal, chemical, mechanical or enzymatic processes.

For these reasons, in the last years many efforts have been made for the development of extraction solutions, composed by denaturing and reducing agents, able to improve gluten recovery from processed foods respect to that reachable by the use of only aqueous alcohol. The extraction Cocktail Solution (CS), developed and patented by D.E. Mendez [125], was endorsed by the Association of Official Agricultural Chemists (AOAC) of the U.S. Department of Agriculture. CS was proved suitable for food and raw materials, containing mercaptoethanol (ME) and guanidine as denaturing and disaggregating agents, respectively. However, CS resulted not compatible with competitive ELISA assay, as discussed by Mena and coworkers [126]. For this reason, another extracting solution, called UPEX® (Universal Prolamin and glutelin Extractant Solution), was developed [126] consisting on combination of reducing Tris (2-carboxyethyl)-phosphine (TCEP) and anionic surfactant N-lauroylsarcosine (patent WO 2011/07039 A2), with the advantage to be compatible with all gluten analysis procedures.

After the choice of an appropriate and exhaustive procedure of gluten extraction, different methods are available for gluten detection and quantification, among them the most commonly used are ELISA-based.

The Mendez group developed a sandwich ELISA based on a monoclonal antibody (R5) directed against epitopes occurring in CD-toxic sequences of prolamins [125]. R5 ELISA proved capable of recognizing prolamins from wheat, rye, and barley to the same degree. The R5-based sandwich ELISA kit is commercialized by R-Biopharm under the trade name of RIDASCREEN® and has been also endorsed by AOAC as official analytical method for quality assessment of gluten-free food. In 2012, a competitive ELISA using R5 monoclonal antibody was developed [127].

Furthermore, an ELISA competitive assay involving the monoclonal antibody G12 was developed by Amaya-González and co-workers in 2011 [128]. In this study the immunodominant peptide 33-mer from alpha2-gliadin was proposed as standard for calibration of the assay, exploiting amperometric flow-injection analysis as detection system.

Amperometric immunosensors, that can be considered as ELISA assay transposition to sensing devices, combine the high specificity and selectivity of ELISA with a fast and low cost analysis and the possibility of miniaturization for *in situ* analysis, exploiting disposable screen-printed electrodes as sensing substrates [129, 130].

Until now, there are a limited number of publications showing electrochemical immunosensors, being used for the determination of gluten: among them Nassef et al. [131] developed a sandwich immunosensor based on the combination of a capture antibody, anchored to the electrodic surface

through dithiol compounds, and a reading antibody directed against the immunodominant CD epitope  $\alpha 56-75$ , with a reliable and sensitive detection of gliadin in a short time, with minimal operator manipulation. Furthermore, Laube et al. [132] reported a competitive immunosensor for the determination of gliadin in natural or pre-treated food samples, extracted with aqueous ethanol.

In this context, the aim of the present project was the development of an amperometric immunosensor for determination of celiotoxic prolamins, based on gliadin immobilization, with a particular attention on sample treatments methods. It has to be pointed out that until now competitive immunosensors have not yet been successfully applied to analysis of processed food, for which CS or UPEX solutions are necessary for prolamins exhaustive extraction, whereas in this work aqueous ethanol and CS were used and proved effective in gliadin extraction.

### **6.3 Published Paper: Competitive immunosensor based on gliadin immobilization on disposable carbon-nanogold screen-printed electrodes for rapid determination of celiotoxic prolamins: compatibility assessment of the immunodevice with different sample treatment approaches**

#### **Abstract**

The first competitive disposable amperometric immunosensor based on gliadin-functionalized carbon/nanogold screen-printed electrodes was developed for rapid determination of celiotoxic prolamins. To date, no competitive spectrophotometric or electrochemical immunoassays have yet been successfully applied to gluten detection in processed food samples, which require the use of complex prolamins extraction solutions containing additives with denaturing, reducing and disaggregating functions. Thus, in this work great effort was put into the optimization and performance evaluation of the immunosensor in terms of suitability as a screening tool for analysis of cereal-based food samples. For this purpose aqueous ethanol or complex extracting mixtures, as the patented Cocktail Solution®, were proved effective in the extraction of gliadin. Good sensitivity was achieved after optimization of the immunocompetitive assay, giving limit of detection and limit of quantitation of 8 and 22 ng/ml of gliadin, respectively, for ethanol extracts. The immunosensor was proved to be suitable also for samples extracted with Cocktail Solution® after a proper dilution. Analysis of real samples of different flours proved the suitability of the immunosensing device as a powerful tool for safety assessment of raw materials used for the formulation of dietary products for celiac disease patients. Findings evidence as the immunosensor combines good analytical performances with very simplified set-up protocol and suitability for rapid screening analysis performed with inexpensive and portable instrumentation [112].

### 6.3.1 Experimental

#### 6.3.1.1 Reagents and solutions

Polyclonal anti-gliadin (wheat) fractionated antiserum from rabbit (Ab anti-Gli), Alkaline Phosphatase conjugated Anti-Rabbit IgG (Ab-AP), Gliadin from wheat (G3375 product number), sodium chloride, potassium chloride, Tris(2-carboxyethyl)phosphine hydrochloride, ethanol (EtOH), Trizma® base, Tween-20, N-laurylsarcosine sodium salt,  $\alpha$ -casein from bovine milk, were purchased from Sigma–Aldrich (Milan, Italy).

Sodium phosphate monobasic, Sodium phosphate bibasic and magnesium chloride were purchased from Carlo Erba (Milan, Italy). Hydroquinone Diphosphate (HQDP) was purchased from Metrohm Italiana (Origgio-VA, Italy). RIDASCREEN® Gliadin ELISA kit and patented Cocktail extracting Solution (CS) were purchased from R-Biopharm AG (Darmstadt, Germany).

Rice, corn, barley, rye, buckwheat, oats, mile, chestnut, chickpeas, quinoa and potato flours as well as durum wheat pasta, breadcrumb, crackers and biscuits were purchased from local supermarkets.

Deionized water was obtained from an in-house Milli-Q water purification system Alpha Q-Water (Millipore, Billerica, MA, USA).

Buffer solutions: Phosphate Buffered Saline (PBS 10 x and 1 x), PBS-T, TRIS, TRIS-T and “Reading buffer” (RB) were prepared according the usual procedure, previous described in Chapter 4.

#### 6.3.1.2 Apparatus and electrodes

Gold nanoparticles screen-printed electrodes (GNP- SPCEs), furthermore, the readings of the electrochemical assays were performed by Differential Pulse Voltammetry (DPV), scanning the potential between -0.5 V and +0.3 V, with a pulse amplitude of 0.05, step potential of 0.005 V and a pulse time of 0.1 s.

All electrochemical measurements were performed with a  $\mu$ Autolab III electrochemical workstation (EcoChemie, Utrecht, NL) equipped with GPES 4.0 version customized software.

#### 6.3.1.3 Samples preparation and immunosensors development

Fortified samples, used as standards for immunosensor development and validation, were obtained by adding powder gliadin to rice flour, used as blank matrix, and homogenizing the mixture before extraction.

The quantification of prolamin content in the extracts was performed by RIDASCREEN® Gliadin ELISA kit and using the NanoDrop ND-1000 spectrophotometer (NanoDrop technologies, Wilmington, Germany), as reported in a previous work of Manfredi et al. [133].

Samples were extracted using both aqueous ethanol and CS, according to the following procedures: an amount of 200 mg of sample were suspended in 2 mL of 60% (v/v) ethanol and incubated for 1 hour at room temperature under shaking. Then, after centrifugation at 5800 rpm for 10 minutes at room temperature, the supernatant was removed and pellet was further treated through a procedure described in the above mentioned work [133]. Obtained supernatants were recollected in a tube, ready to be used. CS extraction was performed according to the procedure of Valdes et al. [125], also suggested by RIDASCREEN® ELISA Kit.

After samples preparation, GNP-SPCEs were functionalized with 30  $\mu\text{L}$  of 0.5 mg/L gliadin solution, obtained diluting the ethanolic extract of gliadin in RIDASCREEN® diluent. Incubation was performed in drop casting at +4°C, overnight. After washing with PBS-T, to remove unreacted gliadin, a blocking treatment with 30  $\mu\text{L}$  of 20 mg/mL of  $\alpha$ -casein solution in PBS-T on each electrode at room temperature for 1 hour, was performed, followed by careful washing with PBS-T and PBS buffer.

The prepared gliadin-modified GNP-SPCEs were used to develop the competitive electrochemical immunoassay. Thus, 30  $\mu\text{L}$  of standard solutions and/or fortified sample extracts were mixed with 3  $\mu\text{L}$  of Ab anti-Gli in PBS (1 x), corresponding to Ab anti-Gli stock solution dilution of 1:250, were incubated for 1 hour at room temperature. As principle of immunocompetitive assay, gliadin in sample inhibits antibody binding to the immobilized gliadin, thus, increasing analyte concentration will reduce the amount of Ab anti-Gli bound to the modified immunosensor surface. Then, sensors were carefully washed with PBS-T and TRIS to remove non-specifically bound material. Finally, in order to detect the Ab anti-Gli immobilized on the electrode surface, 30  $\mu\text{L}$  of reading antibody enzyme-conjugated, Ab-AP, diluted in TRIS buffer by a proper factor from the original stock solution, were incubated on each immunosensor, at room temperature for 1 hour with.

Before DPV measurements, immunosensors was careful washed with TRIS-T and RB to remove unreacted enzyme. Figure 58 shows the immunosensors setup.

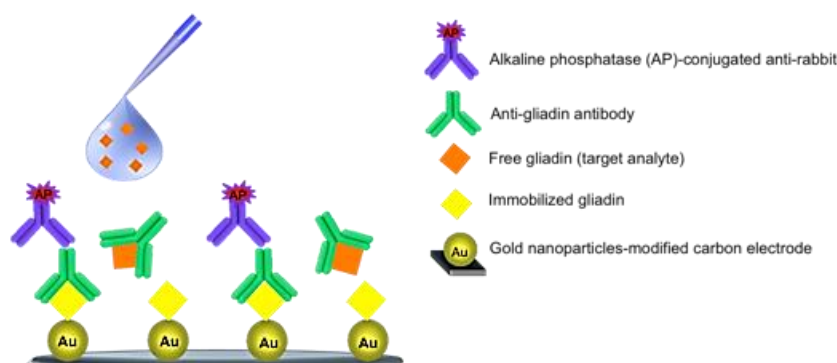


Figure 58 Immunosensors setup.

HQDP was used as enzyme substrate of Alkaline Phosphatase, in order to obtain, as enzymatic product, the electroactive specie Hydroquinone, which was oxidized to Quinone (Q) during the DPV scan, giving the gliadin-related analytical signal. Thus, 1 mg/mL solution of HQDP dissolved in RB was deposited on the immunosensors surface, then, before to run DPV measurements, in order to allow completeness of enzymatic reaction and HQ pre-concentration, an equilibration time of 90 s and a preconditioning stage of 30 s at -0.5 V were applied.

Optimization of immobilized gliadin and Ab anti-Gli in competition concentrations was performed by two-factor and 3-levels experimental design. Then, obtained data were processed by 2-way Analysis of Variance (ANOVA) with interactions, using the Statgraphics Centurion XV statistical software.

Then, developed immunosensor was validated by using fortified rice flour, according to the Eurachem guidelines [134]. The absence of gluten in rice flour, used as blank matrix, was previously verified



by RIDASCREEN® Gliadin ELISA. The detection (LOD) and quantitation (LOQ) limits were assessed as the concentration of analyte giving a signal that is  $2ts_b$  and  $10s_b$  above the mean blank signal, respectively, where  $s_b$  is the standard deviation of the blank signal obtained from ten independent blank measurements and  $t$  is the constant of the t-Student distribution (one-tailed) at 95 % confidence level. At least three replicate measurements (independent immunoassays carried out with different gliadin-modified GNP-SPCEs on the same extract) were carried out for all standards and samples. Trueness was calculated in terms of percent recovery as a ratio of the concentration determined in fortified rice flour, compared to the true concentration of the pure authentic standard at two concentration levels (i.e. LOQ and intermediate calibration level).

### 6.3.2 Results and discussion

The experimental design was performed with the aim to reach the optimal conditions of 50 % signal inhibition for a gliadin concentration of 50 ng/mL, corresponding to 10 mg/kg gliadin in the raw standard material, extracted with aqueous ethanol. Thus, different concentrations of gliadin on GNP-SPCEs surface were explored over the 0.5-50 mg/L range, as well as Ab anti-Gli concentrations, diluting Ab in the 1:1000 to 1:10 range (commercial stock solution at 6.5 mg/mL). ANOVA results show that both factors (Gli and Ab anti-Gli) and their interaction have a significant effect ( $p$ -value  $<0.05$ ) on the immunosensor response, as reported in Figure 59.

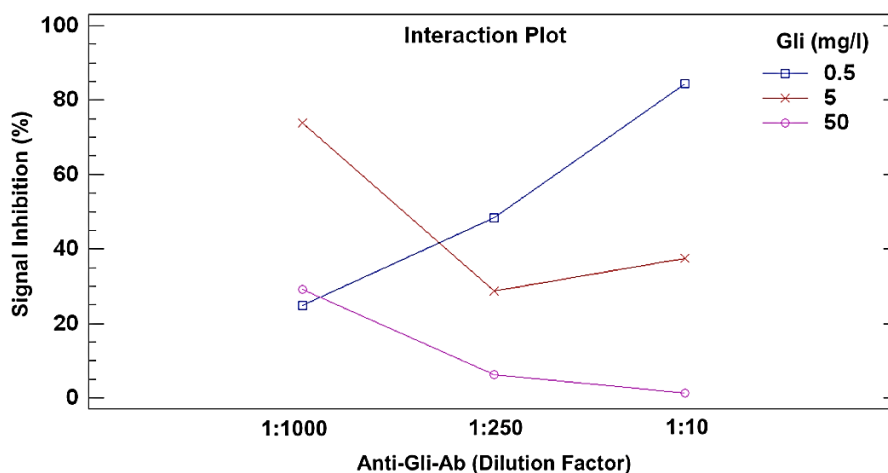


Figure 59 Interaction plot from 2-ways ANOVA with interaction, carried out on the dataset from the experimental design.

The interaction plot shows that the expected 50 % signal inhibition corresponds to 0.5 mg/L of gliadin on GNP-SPCEs and Ab anti-Gli diluted of 1:250. Thus, working at these optimal conditions DPV scans were recorded over the 0.25-250 ng/mL gliadin sample concentration range, as reported in Figure 60.

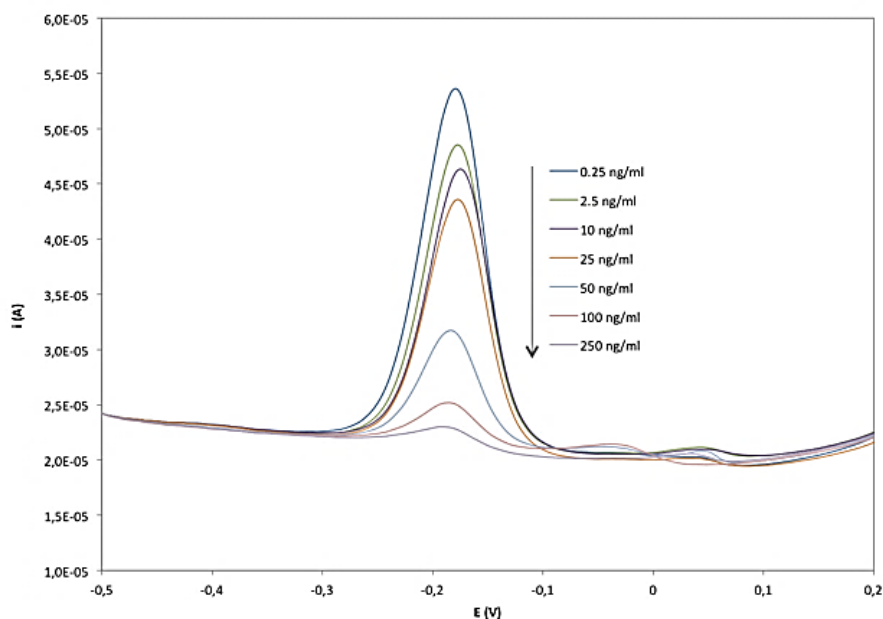


Figure 60 DPV scans related to different gliadin standard solutions over the 0.25-250 ng/ml concentration range.

Response curves were obtained normalizing the current values observed for each concentration ( $S$ ) as a function of the signal from zero level ( $S_0$ ) obtained without gliadin in competition. The normalized signals, expressed as percentage values ( $S/S_0 \times 100$ ), were plotted versus the logarithm of of the gliadin concentration. The inhibition curve (Figure 61) was obtained interpolating the dataset with the four-parameter logistic function, as conventional for competitive immunoassays, as reported in Section 4.2.4.2.1. Data fitting was performed using the software product Microcalc OriginPro 8.5.

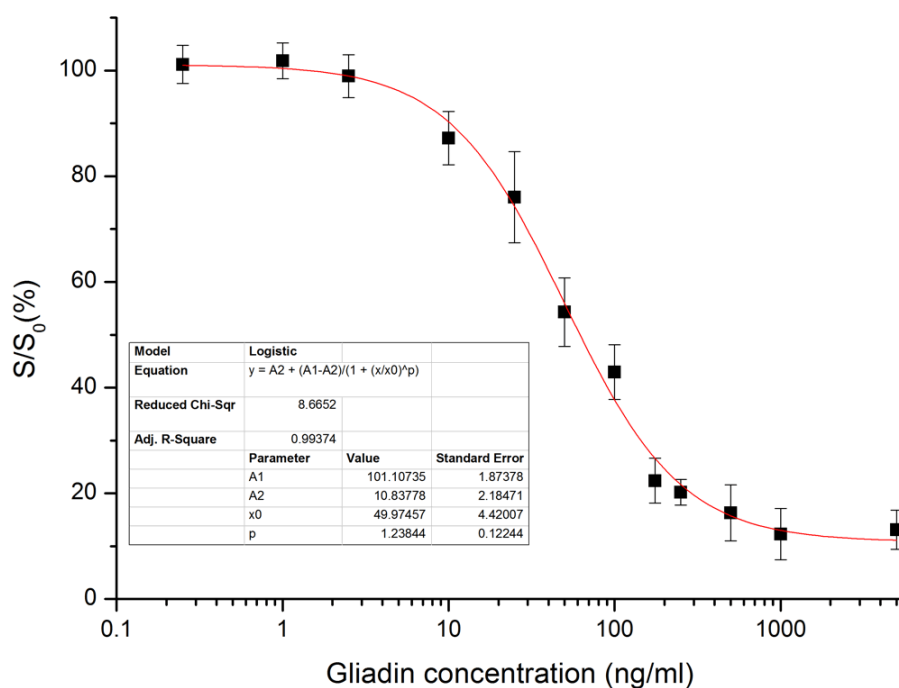


Figure 61 Inhibition curve related to dataset of matrix-free gliadin standard solution. *Inset table*: fitted curve parameters.

Developed immunosensor showed good analytical performance in terms of sensitivity, precision and trueness. LOD and LOQ values of 8 and 22 ng/mL, respectively, were calculated and compared with other methodological approaches, as reported in Table 4.

**Table 4 Comparison of analytical immunosensor performance respect to other methodological approaches.**

Analytical Approach	LOD (ng/mL)	LOQ (ng/mL)	Reference
Competitive amperometric immunosensor	8	22	Present study
Sandwich ELISA	1.5	N.D. <sup>a</sup>	[9]
Competitive ELISA	0.36	1.22	[18]
Competitive ELISA-Amperometric FIA	1.0 <sup>b</sup>	N.D. <sup>a</sup>	[19]
Amperometric immunosensor	5.5	N.D. <sup>a</sup>	[24]
Amperometric magneto-immunosensor	5.1	N.D. <sup>a</sup>	[25]
Magneto-ELISA	5.7	N.D. <sup>a</sup>	[25]

<sup>a</sup> Not Declared, <sup>b</sup> not referred to gliadin, but to immunodominant 33-mer peptide

As for precision, relative standard deviation (RSD) always lower than 10% (n = 3) were observed over the explored concentration range. Trueness was assessed analysing standard solutions not included in the calibration dataset, giving recovery rates ranging from 89 to 104 %. As for shelf life of the developed immunosensors, we verified as the blocking treatment with casein, as well as preventing the occurrence of non-specific responses, also guarantees the maintenance of the reactivity of the gliadin-modified GNP-SPCEs electrodic substrate. Focused experiments carried out over one month (at least) did not show significant changes in the responses, under dark storage at 4°C.

### 6.3.2.1 Evaluation of matrix effect on immunosensor response

Evaluation of matrix effect did not show significant nonspecific response, in terms of modification of the binding properties of the polyclonal anti-gliadin antibody. Cross-reactivity was evaluated in terms of signal inhibition rates, performed with prolamins, zeins, hordeins, secalin and avenins, extracted with aqueous ethanol from corn, barley, rye, buckwheat and oats flours, are in accordance with the cross-reactivity data declared for the Ab anti-Gli, indicating that immunosensor is not affected by nonspecific signal inhibition. The cross-reactivity rates (reported in Table 5) were calculated using the response to rice flour as zero-reference.

**Table 5 Cross-reactivity rates of investigated cereals prolamins.**

Cereal	Related Prolamins	Cross-response rate (%)
Barley	Hordeins	75 ± 3
Rye	Secalins	95 ± 1
Corn	Zeins	No Inhibition
Buckwheat	-	No Inhibition
Oats	Avenins	No Inhibition

### 6.3.2.2 Extracting solutions and compatibility with developed immunosensor

The immunosensing determination of gliadin at trace levels depends also on the efficiency of the sample treatment. Concerning prolamins extraction, among available extracting solutions, the aqueous ethanol has been demonstrated suitable only for raw materials, whereas processed food requires the use of more complex extraction solutions containing reducing and/or denaturing agents. Thus, in perspective of the immunosensor application for safety assessment of both raw materials and processed foods specifically formulated for CD patients, in this work its compatibility with complex extraction solutions for treatment of processed food samples were studied.

Preliminary studies evidenced that UPEX® solution is not compatible with the developed competitive electrochemical immunoassay: in particular, a strong interference in terms of signal inhibition occurred, also in the absence of gliadin standard (false positive), when the extracting solution contained the sodium salt of N-laurylsarcosine, whereas other components did not affect the response. On the basis of these findings, showing that such a surfactant strongly interferes with the immunocompetition, the study was focused on the compatibility of CS with the developed immunodevice. Although the RIDASCREEN® Gliadin competitive kit is declared not compatible with the use of CS, and this fact was also confirmed by the findings of Laube et al [132], dealing with a competitive magnetoimmunosensor developed on tosyl-activated magnetic beads and only tested for analysis of milk and beer spiked with gliadin and extracted with aqueous ethanol, it was decided to evaluate CS compatibility with the present developed immunodevice.

To do this, rice flour solutions (blank) obtained extracting with CS were diluted according different ratios, i.e. 1:12.5 or 1:62.5, as suggested in the protocol of the RIDASCREEN® Sandwich-type ELISA kit for gluten free or low-gluten samples, respectively. Then, diluted extracts were spiked with different amounts of standard gliadin, in order to evaluate the response range in terms of signal inhibition associated with gliadin concentration.

Results of these experiments evidenced that the 12.5-fold diluted extracts are not compatible with the competitive immunosensor, since no signal inhibition was observed upon spiking with gliadin over the 0.1-10000 ng/mL concentration range. Conversely, 62.5-fold diluted extracts resulted to be suitable for analysis with the immunosensor, showing a dynamic response over the same concentration range. The inhibition curve is reported in Figure 62.

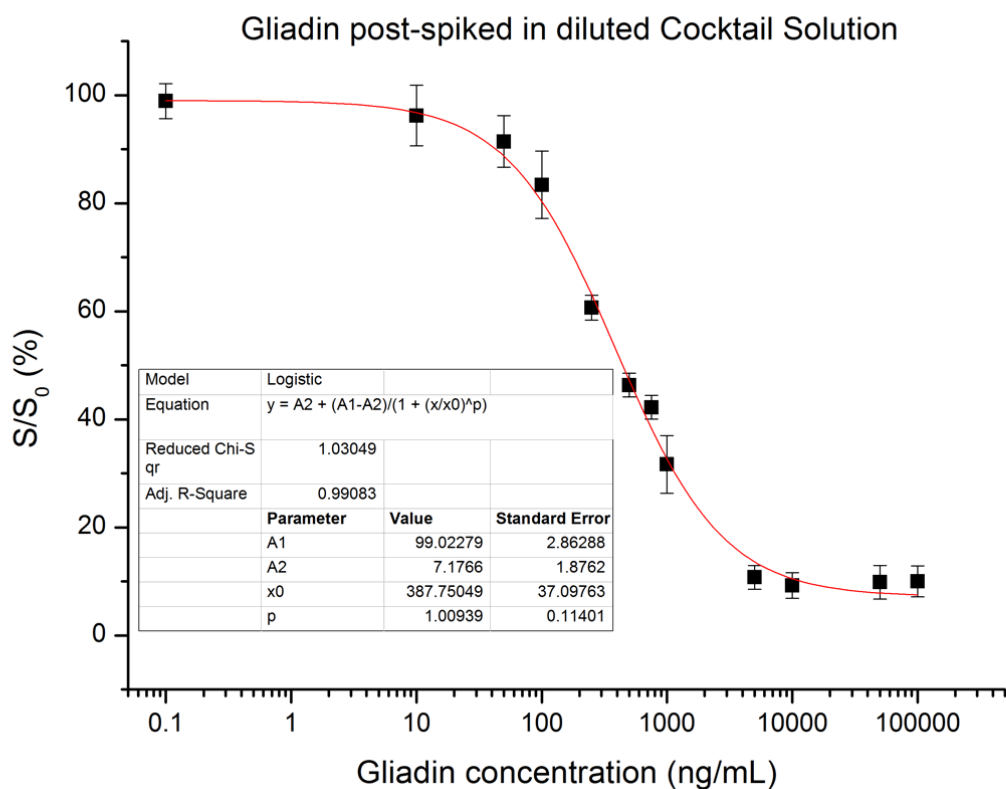


**Figure 62** Inhibition curve related to the dataset from analysis of 62.5-fold diluted CS, post-spiked with different amounts of gliadin. *Inset table:* fitted curve parameters.

Under these conditions, LOD and LOQ values of 30 and 93 ng/mL, respectively, were calculated. High precision was also observed, RSD values being always lower than 5%. On the basis of the obtained results, different samples of rice flour spiked with solid gliadin standard were prepared and extracted with CS, according to RIDASCREEN® assay protocol. Then, extracts were diluted 1:62.5 and analyzed with the immunosensor. The relative inhibition curve is reported in Figure 63, where the gliadin concentration is referred to the original spiked amount of gliadin in rice flour (mg/kg).

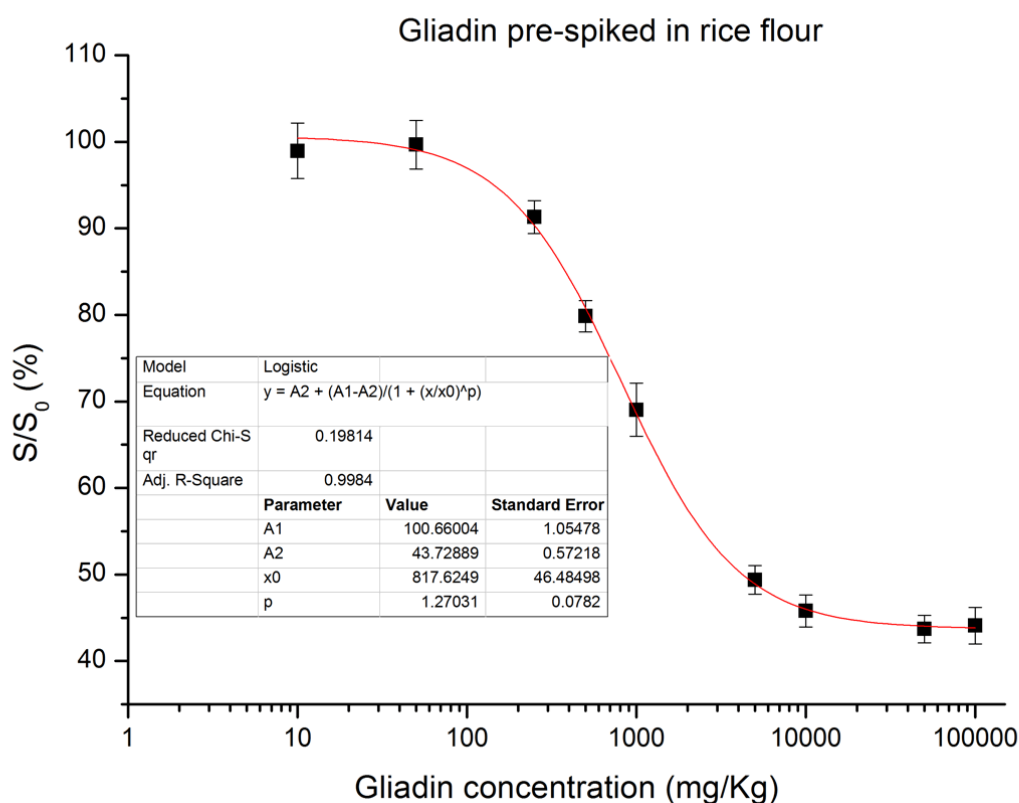


**Figure 63** Inhibition curve relate to the dataset from analysis of blank matrix (rice flour) samples spiked with different amounts of gliadin and extracted with CS. *Inset table*: fitted curve parameters.

In this case, LOD and LOQ values of 162 and 498 mg/kg, respectively, were obtained. An excellent precision, with RSD values (three measurements with independent sensors on the same extract) always lower than 3%, was also observed.

It is important to underline that LOD and LOQ values referred to the original raw material (rice flour spiked with gliadin) are not depending on the intrinsic performance of the sensing device, that would be suitable for safety assessment of gluten free products, but they depend on the high dilution factor of the extracted solutions, that was necessary to limit the interference of CS components on the immunocompetition process. Furthermore, the inhibition cut-off value ( $S_{\min} = 43.7\%$ ) is explainable in terms of reaching the gluten solubility limit for spiked concentrations higher than 10000 mg/kg.

### 6.3.2.3 Developed immunosensor application for analysis of real sample

Considering the findings about the extent of the interference of the CS to be used for the extraction of processed food samples the developed immunosensor was used to analyze different flours, declares as gluten-free, but labelled with the warning of possible contamination from gluten at trace levels. Specifically there were evaluated flours from chickpeas, quinoa, mile, chestnut and potato, after extraction with aqueous ethanol, by using both developed immunosensor and RIDASCREEN® kit (Sandwich-type ELISA), as reference method.

For all samples the gluten content was found less than LODs with both methods. For trueness assessment, samples of biscuits, crackers, breadcrumb and durum wheat pasta were extracted with CS, according to the experimental procedure reported in the commercial RIDASCREEN® kit. Being commercial kit not suitable for analysis of gluten-containing foods, extracted samples were diluted 100.000 fold, by using “sample diluent” included in the kit, before performing the assay.

A good agreement between the results from ELISA kit and the responses of developed immunosensor was found, as reported in Table 6.

**Table 6** Gliadin content found with ELISA RIDASCREEN® kit and with developed immunosensor in processed food samples, containing gluten. Means and standard deviations calculated from three replicated assay.

Food	Gliadin Concentration (mg/kg)		Recovery Rate (%)
	ELISA commercial Kit	Developed Immunosensor	
Breadcrumb	81983 ± 7962	67191 ± 3810	82
Durum Wheat Pasta	27070 ± 2626	22616 ± 2001	83
Biscuit	66430 ± 7710	56698 ± 4689	85
Crackers	60058 ± 6617	53633 ± 5120	89

### 6.3.3 Conclusions

In this study the first competitive disposable immunosensor based on screen-printed electrodes for rapid screening of gliadin in gluten-free food products was developed. It combines good analytical performance with very simple set-up protocol as well as inexpensive and portable instrumentation. Another aspect challenged for the first time was a systematic study aimed at investigating the compatibility of the competitive immunosensor with sample treatment protocols applicable to processed foods and involving the use of complex extracting solution as the patented CS. On the basis of the obtained results, it can be stated that the developed immunosensor can be used as promising tool for safety assessment of raw materials, used for the formulation of dietary products for CD patients. The devised method was characterized by inherent sensitivity, simplicity, speed, and cost benefits coupled to high selectivity.



## REFERENCES

- [1] Pure and Applied Chemistry, 63 (1991):1247-1250.
- [2] Cammann, K., *Bio-sensors based on ion-selective electrodes*. Analytical Chemistry (1977): 1-9.
- [3] Turner, A.P.F, Karube, I., Wilson, G.S., *Biosensors: fundamentals and applications* (1987).
- [4] Alberts, B., Johnson, A., Lewis, J., Raff, M., Roberts, K., Walter, P., *The adaptive immune system*. Chapter 24, Molecular Biology of the Cell, 4th edition (2002).
- [5] Abbas, A. K., Lichtman, A. H., Pillai, S., *Antibodies and antigens*. In: Abbas, A. K., Lichtman, A. H., Pillai, S., eds. Cellular and Molecular Immunology. 8th ed. Philadelphia, PA: Elsevier Saunders; (2015):chap 5.
- [6] Woof, J. M., Burton, D. R., *Human antibody–Fc receptor interactions illuminated by crystal structures*. Nature Reviews Immunology 4 (2004): 89-99.
- [7] Lippa, P. B., Sokoll, L. J., Chan, D. W. *Immunosensors—principles and applications to clinical chemistry*. Clinica Chimica Acta 314 (2001): 1-26.
- [8] Lequin, R. M., *Enzyme immunoassay (EIA)/enzyme-linked immunosorbent assay (ELISA)*. Clinical Chemistry 51 (2005): 2415-2418.
- [9] Voller, A., Bartlett, A., Bidwell, D. E., *Enzyme immunoassays with special reference to ELISA techniques*. Journal of Clinical Pathology 31 (1978): 507-520.
- [10] Gründler, P., *Chemical sensors: an introduction for scientists and engineers*. Springer Science & Business Media (2007).
- [11] Li, X., Tian, J., Garnier, G., & Shen, W., *Fabrication of paper-based microfluidic sensors by printing*. Colloids and Surfaces B: Biointerfaces 76 (2010): 564-570.
- [12] Protti, P., *Introduzione alle moderne tecniche di Analisi Voltammetriche e Polarografiche*, AMEL srl – Manuale di Voltammetria, IV Edizione (2001).
- [13] Bakker, E., Telting-Diaz, M., *Electrochemical sensors*. Analytical Chemistry 74 (2002): 2781-2800.
- [14] Li, M., Li, Y. T., Li, D. W., Long, Y. T., *Recent developments and applications of screen-printed electrodes in environmental assays—a review*. Analytica Chimica Acta 734 (2012): 31-44.
- [15] Cagnini, A., Palchetti, I., Lionti, I., Mascini, M., Turner, A. P., *Disposable ruthenized screen-printed biosensors for pesticides monitoring*. Sensors and Actuators B: Chemical 24 (1995): 85-89.
- [16] Wang, J., Pedrero, M., Sakslund, H., Hammerich, O., Pingarron, J., *Electrochemical activation of screen-printed carbon strips*. Analyst 121 (1996): 345-350.
- [17] Hart, J. P., Wring, S. A., *Recent developments in the design and application of screen-printed electrochemical sensors for biomedical, environmental and industrial analyses*. TrAC Trends in Analytical Chemistry 16 (1997): 89-103.
- [18] Ricci, F., Adornetto, G., Palleschi, G., *A review of experimental aspects of electrochemical immunosensors*. Electrochimica Acta 84 (2012): 74-83.
- [19] Scouten, W. H., Luong, J. H., Brown, R. S., *Enzyme or protein immobilization techniques for applications in biosensor design*. Trends in biotechnology 13 (1995): 178-185.
- [20] Sharma, S. K., Sehgal, N., Kumar, A., *Biomolecules for development of biosensors and their applications*. Current Applied Physics 3 (2003): 307-316.
- [21] Merkoçi, A. (ed.), *Biosensing using nanomaterials*. John Wiley & Sons (2009).
- [22] Gleiter, H., *Nanostructured materials: basic concepts and microstructure*. Acta Materialia 48 (2000): 1-29.

- [23]Graham, A. P., Duesberg, G. S., Hoenlein, W., Kreupl, F., Liebau, M., Martin, R., Rajasekharan, A.P., Pamler, W., Seidel, R., Steinhoegl, W., Unger, E., *How do carbon nanotubes fit into the semiconductor roadmap?* Applied Physics A 80 (2005): 1141-1151.
- [24]Guo, S., Wang, E., *Synthesis and electrochemical applications of gold nanoparticles.* Analytica Chimica Acta 598 (2007): 181-192.
- [25]Jung, Y., Jeong, J. Y., Chung, B. H., *Recent advances in immobilization methods of antibodies on solid supports.* Analyst 133 (2008): 697-701.
- [26]Sam, S., Touahir, L., Salvador Andresa, J., Allongue, P., Chazalviel, J. N., Gouget-Laemmel, A. C., Henry de Villeneuve, C. Moraillon, A., Ozanam, F., Gabouze, N., Djebbar, S. *Semiquantitative study of the EDC/NHS activation of acid terminal groups at modified porous silicon surfaces.* Langmuir 26 (2009): 809-814.
- [27]Kausaite-Minkstimiene, A., Ramanaviciene, A., Kirlyte, J., Ramanavicius, A., *Comparative study of random and oriented antibody immobilization techniques on the binding capacity of immunosensor.* Analytical Chemistry 82 (2010): 6401-6408.
- [28]Tlili, A., Abdelghani, A., Hleli, S., & Maaref, M. A., *Electrical Characterization of a Thiol SAM on Gold as a First Step for the Fabrication of Immunosensors based on a Quartz Crystal Microbalance.* Sensors 4 (2004): 105-114.
- [29]Luo, X., Morrin, A., Killard, A. J., Smyth, M. R., *Application of nanoparticles in electrochemical sensors and biosensors.* Electroanalysis 18 (2006): 319-326.
- [30]Daniel, M. C., Astruc, D., *Gold nanoparticles: assembly, supramolecular chemistry, quantum-size-related properties, and applications toward biology, catalysis, and nanotechnology.* Chemical Reviews 104 (2004): 293-346.
- [31]Kurita, K., Yoshino, H., Nishimura, S. I., Ishii, S., Mori, T., Nishiyama, Y., *Mercapto-chitins: a new type of supports for effective immobilization of acid phosphatase.* Carbohydrate Polymers 32 (1997): 171-175.
- [32]Monteiro, O. A., Airoidi, C., *Some studies of crosslinking chitosan–glutaraldehyde interaction in a homogeneous system.* International Journal of Biological Macromolecules 26 (1999): 119-128.
- [33]Liu, Y., Li, Y., Liu, S., Li, J., Yao, S., *Monitoring the self-assembly of chitosan/glutaraldehyde/cysteamine/Au-colloid and the binding of human serum albumin with hesperidin.* Biomaterials 25 (2004): 5725-5733.
- [34]Huang, M., Khor, E., Lim, L.Y., *Uptake and cytotoxicity of chitosan molecules and nanoparticles: effects of molecular weight and degree of deacetylation.* Pharmaceutical Research 21 (2004): 344-353.
- [35]Khan, T. A., Peh, K. K., Ch'ng, H. S., *Reporting degree of deacetylation values of chitosan: the influence of analytical methods.* Journal of Pharmacy and Pharmaceutical Sciences 5 (2002): 205-212.
- [36]Migneault, I., Dartiguenave, C., Bertrand, M. J., Waldron, K. C., *Glutaraldehyde: behavior in aqueous solution, reaction with proteins, and application to enzyme crosslinking.* Biotechniques 37 (2004): 790-806.
- [37]Kawahara, J. I., Ohmori, T., Ohkubo, T., Hattori, S., Kawamura, M., *The structure of glutaraldehyde in aqueous solution determined by ultraviolet absorption and light scattering.* Analytical Biochemistry 201 (1992): 94-98.

- [38]Kawahara, J. I., Ishikawa, K., Uchimaru, T., Takaya, H., *Chemical cross-linking by glutaraldehyde between amino groups: its mechanism and effects*. In G.Swift, C.E. Carraher Jr., and C.N. Bowman (Eds.), *Polymer Modification*. Plenum Press, New York. (1997):119-131.
- [39] Emini, E. A. *The human immunodeficiency virus: biology, immunology, and therapy*. Princeton University Press, (2002).
- [40]Montagnier, L., *A history of HIV discovery*. *Science* 298.5599 (2002): 1727-1728.
- [41]Levy, J. A., *HIV pathogenesis and long-term survival*. *Aids* 7.11 (1993): 1401-1410.
- [42]Kheiri, F., Sabzi, R. E., Jannatdoust, E., Shojaeefar, E., Sedghi, H., *A novel amperometric immunosensor based on acetone-extracted propolis for the detection of the HIV-1 p24 antigen*. *Biosensors and Bioelectronics* 26.11 (2011): 4457-4463.
- [43]Goldsby, R.A., Kindt, T. J., Osborne, B. A., *Immunology*, 4th edition. W H Freeman & Co., January (2000).
- [44]Lozano, R., Naghavi, M., Foreman, K., Lim, S., Shibuya, K., Aboyans, V., Abraham, J., Adair, T., Aggarwal, R., Ahn, S. Y., AlMazroa, M. A., Alvarado, M., Anderson, H. R., Anderson, L. M., Andrews, K. G., Atkinson, C., Baddour, L. M., Barker-Collo, S., Bartels, D. H., *Global and regional mortality from 235 causes of death for 20 age groups in 1990 and 2010: a systematic analysis for the Global Burden of Disease Study 2010*. *The Lancet*, 380 (2013), 2095-2128.
- [45]Lee, S., Kim, Y. S., Jo, M., Jin, M., Lee, D. K., & Kim, S., *Chip-based detection of hepatitis C virus using RNA aptamers that specifically bind to HCV core antigen*. *Biochemical and Biophysical Research Communications* 358 (2007): 47-52.
- [46]McAdam-Marx, C., McGarry, L. J., Hane, C. A., Biskupiak, J., Deniz, B., Brixner, D. I., *All-Cause and Incremental Per Patient Per Year Cost Associated with Chronic Hepatitis C Virus and Associated Liver Complications in the United States: A Managed Care Perspective*. *Journal of Managed care and Specialty Pharmacy*17 (2011): 531-546.
- [47]Messina, J. P., Humphreys, I., Flaxman, A., Brown, A., Cooke, G. S., Pybus, O. G., Barnes, E. *Global distribution and prevalence of hepatitis C virus genotypes*. *Hepatology* 61 (2015): 77-87.
- [48]Gower, E., Estes, C., Blach, S., Razavi-Shearer, K., Razavi, H., *Global epidemiology and genotype distribution of the hepatitis C virus infection*. *Journal of Hepatology* 61 (2014): S45-S57.
- [49]Rosen, H. R., *Chronic hepatitis C infection*. *New England Journal of Medicine* 364 (2011): 2429-2438.
- [50]*Updated U.S. Public Health Service guidelines for the management of occupational exposures to HBV, HCV, and HIV and recommendations for postexposure prophylaxis*. U.S. Public Health Service. *Morbidity and Mortality Weekly Report (MMWR) Recommendations and Reports*, 50 (2001):1–52.
- [51]Thomas, D. L., Zenilman, J. M., Alter, H. J., Shih, J. W., Galai, N., Carella, A. V., Quinn, T. C., *Sexual transmission of hepatitis C virus among patients attending sexually transmitted diseases clinics in Baltimore—an analysis of 309 sex partnerships*. *Journal of Infectious Diseases* 171 (1995): 768-775.
- [52]Zanetti, A. R., Paccagnini, S., Principi, N., Pizzocolo, G., Caccamo, M. L., Amico, E. D., Cambiè, G., Vecchi, L., *Mother-to-infant transmission of hepatitis C virus*. *The Lancet* 345 (1995): 289-291.
- [53]Gibb, D. M., Goodall, R. L., Dunn, D. T., Healy, M., Neave, P., Cafferkey, M., Butler, K., *Mother-to-child transmission of hepatitis C virus: evidence for preventable peripartum transmission*. *The Lancet* 356 (2000): 904-907.
- [54]*Coinfezione Hiv/Hcv*. LILA (Lega Italiana per la Lotta all'AIDS). May (2016). <http://www.lila.it/it/vivere-con-hiv>

- [55]Mauss, S., Valenti, W., DePamphilis, J., Duff, F., Cupelli, L., Passe, S., Solsky, J., Torriani, F., Dieterich, D., Larrey, D., *Risk factors for hepatic decompensation in patients with HIV/HCV coinfection and liver cirrhosis during interferon-based therapy.* AIDS 18 (2004): (Suppl) F21–F25.
- [56]Sulkowski, M. S., Thomas, D. L., *Hepatitis C in the HIV-infected person.* Annals of Internal Medicine 138 (2003): 197-207.
- [57]Nasta, P., Cattelan, A. M., Maida, I., Gatti, F., Chiari, E., Puoti, M., Carosi, G., *Antiretroviral therapy in HIV/HCV Co-infection Italian consensus workshop.* (2013).
- [58]Pineda, J. A., Romero-Gómez, M., Díaz-García, F., Girón-González, J. A., Montero, J. L., Torre-Cisneros, J., Andrade, R.J., González-Serrano, M., Aguilar, J., Aguilar-Guisado, M., Navarro, J.M., Salmerón, J., Caballero-Granado, F.J., García-García J.A., *HIV coinfection shortens the survival of patients with hepatitis C virus-related decompensated cirrhosis.* Hepatology 41 (2005): 779-789.
- [59]Graham, C. S., Baden, L. R., Yu, E., Mrus, J. M., Carnie, J., Heeren, T., Koziel, M. J., *Influence of human immunodeficiency virus infection on the course of hepatitis C virus infection: a meta-analysis.* Clinical Infectious Diseases 33 (2001): 562-569.
- [60]Ragni, M. V., Belle, S. H., *Impact of human immunodeficiency virus infection on progression to end-stage liver disease in individuals with hemophilia and hepatitis C virus infection.* Journal of Infectious Diseases 183 (2001): 1112-1115.
- [61]Martín-Carbonero, L., Soriano, V., Valencia, E., García-Samaniego, J., López, M., González-Lahoz, J., *Hepatocellular carcinoma in HIV-infected patients with chronic hepatitis C.* The American Journal of Gastroenterology 96 (2001): 179-183.
- [62]Darby, S. C., Ewart, D. W., Giangrande, P. L., Spooner, R. J., Rizza, C. R., Dusheiko, G. M., Lee, C. A., Ludlam, C. A., Preston, F. E., *Mortality from liver cancer and liver disease in haemophilic men and boys in UK given blood products contaminated with hepatitis C.* The Lancet 350 (1997): 1425-1431.
- [63]Eyster, M. E., Diamondstone, L. S., Lien, J. M., Ehmann, W. C., Quan, S., Goedert, J. J., *Natural history of hepatitis C virus infection in multitransfused hemophiliacs: effect of coinfection with human immunodeficiency virus.* JAIDS Journal of Acquired Immune Deficiency Syndromes 6 (1993): 602-610.
- [64]Rockstroh, J. K., Mocroft, A., Soriano, V., Tural, C., Losso, M. H., Horban, A., Kirk, O., Phillips, A., Ledergerber, B., Lundgren, J., *Influence of hepatitis C virus infection on HIV-1 disease progression and response to highly active antiretroviral therapy.* Journal of Infectious Diseases 192 (2005): 992-1002.
- [65]Dorrucchi, M., Pezzotti, P., Phillips, A. N., Lepri, A. C., Rezza, G., *Coinfection of Hepatitis C Virus with Human Immunodeficiency Virus and Progression to AIDS.* Journal of Infectious Diseases, 172 (1995):1503–1508.
- [66]Piroth, L., Duong, M., Quantin, C., Abrahamowicz, M., Michardiere, R., Aho, L. S., Grappin, M., Buisson, M., Waldner, A., Portier, H., Chavanet, P., *Does hepatitis C virus co-infection accelerate clinical and immunological evolution of HIV-infected patients?* AIDS, 12 (1998):381–388.
- [67]Greub, G., Ledergerber, B., Battegay, M., Grob, P., Perrin, L., Furrer, H., Burgisser, P., Erb, P., Boggian, K., Piffaretti, J-C., Hirschel, B., Janin, P., Francioli, P., Flepp, M., Telenti, A., *Clinical progression, survival, and immune recovery during antiretroviral therapy in patients with HIV-1 and hepatitis C virus coinfection.* The Swiss HIV Cohort Study.” Lancet, 356 (2000):1800–1805.

- [68] Soriano, V., Martin, J. C., González-Lahoz, J., *HIV-1 progression in hepatitis C-infected drug users*. *Lancet*, 357 (2001):1361–1362.
- [69] Sulkowski, M. S., Moore, R. D., Mehta, S. H., Chaisson, R. E., Thomas, D. L., *Hepatitis C and progression of HIV disease*. *JAMA*, 288 (2002):199–206.
- [70] Tedaldi, E. M., Baker, R. K., Moorman, A. C., Alzola, C. F., Furhrer, J., McCabe, R. E., Wood, K. C., Holmberg, S. D., *Influence of coinfection with hepatitis C virus on morbidity and mortality due to human immunodeficiency virus infection in the era of highly active antiretroviral therapy*. *Clinical Infectious Diseases* 36 (2003): 363-367.
- [71] McMichael, A.J., “HIV vaccines.” *Annual Review of Immunology* 24 (2006):227–255.
- [72] Garber, D. A., Silvestri, G., Feinberg, M. B., *Prospects for an AIDS vaccine: three big questions, no easy answers*. *Lancet Infectious Diseases*, 4 (2004): 397–413.
- [73] Zheng, L., Jia, L., Li, B., Situ, B., Liu, Q., Wang, Q., Gan, N., *A sandwich HIV p24 amperometric immunosensor based on a direct gold electroplating-modified electrode*. *Molecules* 17 (2012): 5988-6000.
- [74] Johnson, C., Baggaley, R., Forsythe, S., Van Rooyen, H., Ford, N., Mavedzenge, S. N., Corbett, E., Natarajan, P., Taegtmeier, M., *Realizing the potential for HIV self-testing*. *AIDS and Behavior* 18 (2014): 391-395.
- [75] Ling, A. E., Robbins, K. E., Brown, T. M., Dunmire, V., Thoe, S. Y. S., Wong, S. Y., Leo, Y. S., Teo, D., Gallarda, J., Phelps, B., Chamberland, M.E., Busch, .MP., Folks, T.M., Kalish, M.L., *Failure of routine HIV-1 tests in a case involving transmission with preseroconversion blood components during the infectious window period*. *JAMA* 284 (2000): 210-214.
- [76] de Almeida Pondé, R. A., *Genomic detection of human immunodeficiency virus (HIV) by nucleic acid amplification test in a frequent platelet donor during the pre-seroconversion period*. *Archives of Virology* 156 (2011): 2085-2090.
- [77] Constantine, N. T., van der Groen, G., Belsey, E. M., Tamashiro, H., *Sensitivity of HIV-antibody assays determined by seroconversion panels*. *Aids* 8 (1994): 1715-1720.
- [78] Fiebig, E. W., Wright, D. J., Rawal, B. D., Garrett, P. E., Schumacher, R. T., Peddada, L., Heldebrant, C., Smith, R., Conrad, A., Kleinman, S. H., Busch, M. P., *Dynamics of HIV viremia and antibody seroconversion in plasma donors: implications for diagnosis and staging of primary HIV infection*. *Aids* 17 (2003): 1871-1879.
- [79] Daskalakis, D., *HIV diagnostic testing: evolving technology and testing strategies*. *Topics in antiviral medicine* 19 (2010): 18-22.
- [80] Owen, S. M., *Testing for acute HIV infection: implications for treatment as prevention*. *Current Opinion in HIV and AIDS* 7.2 (2012): 125-130.
- [81] Dax, E.M., Farrugia, A., Vyas, G.N., (Eds.), *Evolving approaches to estimate risks of transfusion-transmitted viral infections: incidence-window period model after ten years*. Vyas (Eds.), *Advances in Transfusion Safety – vol. IV, Developments in Biologicals (Basel)*, vol. 127, S. Karger Publishers, Inc., Farmington, CT, (2007): 87–112.
- [82] Westreich, D. J., Hudgens, M. G., Fiscus, S. A., Pilcher, C. D., *Optimizing screening for acute human immunodeficiency virus infection with pooled nucleic acid amplification tests*. *Journal of Clinical Microbiology* 46, (2008):1785-1792.
- [83] Teeparuksapun, K.; Hedstrom, M.; Wong, E. Y.; Tang, S.; Hewlett, I. K.; Mattiasson, B., *Ultrasensitive Detection of HIV-1 p24 Antigen Using Nanofunctionalized Surfaces in a Capacitive Immunosensor*. *Analytical Chemistry*, 82 (2010):8406– 8411.

- [84] Böni, J., Opravil, M., Tomasik, Z., Rothen, M., Bisset, L., Grob, P. J., Lüthy, R., Schüpbach, J., *Simple monitoring of antiretroviral therapy with a signal-amplification-boosted HIV-1 p24 antigen assay with heat-denatured plasma*. *AIDS*, 11 (1997): F47-F52.
- [85] Patel, P., Mackellar, D., Simmons, P., Uniyal, A., Gallagher, K., Bennett, B., Sullivan, T. J., Kowalski, A., Parker, M. M., LaLota, M., Kerndt, P., Sullivan, P. S., *Detecting acute human immunodeficiency virus infection using 3 different screening immunoassays and nucleic acid amplification testing for human immunodeficiency virus RNA, 2006-2008*. *Archives of Internal Medicine* 170 (2010): 66-74.
- [86] Strader, D. B., Wright, T., Thomas, D. L., Seeff, L. B., *Diagnosis, management, and treatment of hepatitis C*. *Hepatology* 39 (2004): 1147-1171.
- [87] Morota, K., Fujinami, R., Kinukawa, H., Machida, T., Ohno, K., Saegusa, H., Takeda, K., *A new sensitive and automated chemiluminescent microparticle immunoassay for quantitative determination of hepatitis C virus core antigen*. *Journal of Virological Methods* 157 (2009): 8-14.
- [88] Hofmann, W. P., Dries, V., Herrmann, E., Gärtner, B., Zeuzem, S., Sarrazin, C., *Comparison of transcription mediated amplification (TMA) and reverse transcription polymerase chain reaction (RT-PCR) for detection of hepatitis C virus RNA in liver tissue*. *Journal of Clinical Virology* 32 (2005): 289-293.
- [89] Lee, S., Kim, Y. S., Jo, M., Jin, M., Lee, D. K., Kim, S., *Chip-based detection of hepatitis C virus using RNA aptamers that specifically bind to HCV core antigen*. *Biochemical and Biophysical Research Communications* 358 (2007): 47-52.
- [90] Laperche, S., Le Marrec, N., Girault, A., Bouchardeau, F., Servant-Delmas, A., Maniez-Montreuil, M., Gallian, P., Levayer, T., Morel, P., Simon, N., *Simultaneous detection of hepatitis C virus (HCV) core antigen and anti-HCV antibodies improves the early detection of HCV infection*. *Journal of Clinical Microbiology*, 43 (2005):3877–3883.
- [91] Widell, A., Molnegren, V., Pieksma, F., Calmann, M., Peterson, J., Lee, S. R., *Detection of hepatitis C core antigen in serum or plasma as a marker of hepatitis C viremia in the serological window-phase*. *Transfusion Medicine*, 12, (2002):107–113.
- [92] Leary, T. P., Gutierrez, R. A., Muerhoff, A. S., Birkenmeyer, L. G., Desai, S. M., Dawson, G. J., *A chemiluminescent, magnetic particle-based immunoassay for the detection of hepatitis C virus core antigen in human serum or plasma*. *Journal of Medical Virology* 78 (2006): 1436-1440.
- [93] Bouvier-Alias, M., Patel, K., Dahari, H., Beaucourt, S., Larderie, P., Blatt, L. C., Hezode, G., Picchio, D., Dhumeaux, A. U., Neumann, J., G. McHutchison, J-M., Pawlotsky, G., *Clinical utility of total HCV core antigen quantification: a new indirect marker of HCV replication*. *Hepatology* 36 (2002): 211-218.
- [94] Gaudy, C., Thevenas, C., Tichet, J., Mariotte, N., Goudeau, A., Dubois, F., *Usefulness of the hepatitis C virus core antigen assay for screening of a population undergoing routine medical checkup*. *Journal of Clinical Microbiology* 43 (2005): 1722-1726.
- [95] Zanetti, A. R., Romanò, L., Brunetto, M., Colombo, M., Bellati, G., Tackney, C., *Total HCV core antigen assay: a new marker of hepatitis C viremia for monitoring the progress of therapy*. *Journal of Medical Virology* 70 (2003): 27-30.26.
- [96] Tanaka, N., Moriya, K., Kiyosawa, K., Koike, K., Aoyama, T., *Hepatitis C virus core protein induces spontaneous and persistent activation of peroxisome proliferator-activated receptor  $\alpha$  in transgenic mice: Implications for HCV-associated hepatocarcinogenesis*. *International Journal of Cancer* 122 (2008): 124-131.

- [97]Krishnadas, D. K., Li, W., Kumar, R., Tyrrell, D. L., Agrawal, B., *HCV-core and NS3 antigens play disparate role in inducing regulatory or effector T cells in vivo: Implications for viral persistence or clearance*. Vaccine 28 (2010): 2104-2114.
- [98]Moscato, G. A., Giannelli, G., Grandi, B., Pieri, D., Marsi, O., Guarducci, I., Batini, I., Altomare E., Antonaci, S., Capria, A., Pellegrini, G., Sacco, R., *Quantitative determination of hepatitis C core antigen in therapy monitoring for chronic hepatitis C*. Intervirology 54.2 (2010): 61-65.
- [99]Lochhead, M. J., Todorof, K., Delaney, M., Ives, J. T., Greef, C., Moll, K. Rowley, K., Vogell, K., Myatt, C., Zhang, X-Q., Logan, C., Benson, Constance, S. R., Schooley, R. T., *Rapid multiplexed immunoassay for simultaneous serodiagnosis of HIV-1 and coinfections*. Journal of clinical microbiology 49.10 (2011): 3584-3590.
- [100]Zhao, C., and Xinyu, L., *A portable, paper-based multiplexing immunosensor for detection of HIV and HCV markers in serum*. 2015 Transducers-2015 18th International Conference on Solid-State Sensors, Actuators and Microsystems (TRANSDUCERS). IEEE, 2015.
- [101]Chang, L., Song, L., Fournier, D. R., Kan, C. W., Patel, P. P., Ferrell, E. P., Pink, B. A., Minnehan, K. A., Hanlon, D. W., Duffy, D. C., Wilson, D. H., *Simple diffusion-constrained immunoassay for p24 protein with the sensitivity of nucleic acid amplification for detecting acute HIV infection*. Journal of Virological Methods 188 (2013): 153-160.
- [102]Zhou, L., Huang, J., Yu, B., Liu, Y., You, T., *A Novel Electrochemiluminescence Immunosensor for the Analysis of HIV-1 p24 Antigen Based on P-RGO@ Au@ Ru-SiO<sub>2</sub> Composite*. Applied Materials & Interfaces 7 (2015): 24438-24445.
- [103]Zhang, Y., Yang, H., Yu, J., Wei, H., *Rapid and sensitive detection of HIV-1 p24 antigen by immunomagnetic separation coupled with catalytic fluorescent immunoassay*. Analytical and Bioanalytical Chemistry 408 (2016): 6115-6121.
- [104]Ma, C., Xie, G., Zhang, W., Liang, M., Liu, B., Xiang, H., *Label-free sandwich type of immunosensor for hepatitis C virus core antigen based on the use of gold nanoparticles on a nanostructured metal oxide surface*. Microchimica Acta 178 (2012): 331-340.
- [105]Ma, C., Liang, M., Wang, L., Xiang, H., Jiang, Y., Li, Y., Xie, G., *MultisHRP-DNA-coated CMWNTs as signal labels for an ultrasensitive hepatitis C virus core antigen electrochemical immunosensor*. Biosensors and Bioelectronics 47 (2013): 467-474.
- [106]Giannetto, M., Elviri, L., Careri, M., Mangia, A., Mori, G., *A voltammetric immunosensor based on nanobiocomposite materials for the determination of alpha-fetoprotein in serum*. Biosensors and Bioelectronics 26.5 (2011): 2232-2236.
- [107]Giannetto, M., Mori, L., Mori, G., Careri, M., Mangia, A., *New amperometric immunosensor with response enhanced by PAMAM-dendrimers linked via self assembled monolayers for determination of alpha-fetoprotein in human serum*. Sensors and Actuators B: Chemical 159 (2011): 185-192.
- [108]Lai, G., Yan, F., Wu, J., Leng, C., Ju, H., *Ultrasensitive multiplexed immunoassay with electrochemical stripping analysis of silver nanoparticles catalytically deposited by gold nanoparticles and enzymatic reaction*. Analytical chemistry 83 (2011): 2726-2732.
- [109]Lai, G., Wang, L., Wu, J., Ju, H., Yan, F., *Electrochemical stripping analysis of nanogold label-induced silver deposition for ultrasensitive multiplexed detection of tumor markers*. Analytica Chimica Acta 721 (2012): 1-6.

- [110]Manfredi, A., Mattarozzi, M., Giannetto, M., Careri, M., *Piezoelectric immunosensor based on antibody recognition of immobilized open-tissue transglutaminase: An innovative perspective on diagnostic devices for celiac disease*. Sensors and Actuators B: Chemical 201 (2014): 300-307.
- [111]March, C., Manclús, J. J., Jiménez, Y., Arnau, A., Montoya, A., *A piezoelectric immunosensor for the determination of pesticide residues and metabolites in fruit juices*. Talanta 78.3 (2009): 827-833.
- [112]Manfredi, A., Giannetto, M., Mattarozzi, M., Costantini, M., Mucchino, C., Careri, M., *Competitive immunosensor based on gliadin immobilization on disposable carbon-nanogold screen-printed electrodes for rapid determination of celiotoxic prolamins*. Analytical and Bioanalytical Chemistry 408 (2016): 1-10.
- [113]Fanjul-Bolado, P., Hernández-Santos, D., González-García, M. B., Costa-García, A., *Alkaline phosphatase-catalyzed silver deposition for electrochemical detection*. Analytical Chemistry 79 (2007): 5272-5277.
- [114]Neves, M. M., González-García, M. B., Delerue-Matos, C., Costa-García, A., *Multiplexed electrochemical immunosensor for detection of celiac disease serological markers*. Sensors and Actuators B: Chemical 187 (2013): 33-39.
- [115]Luo, X., Morrin, A., Killard, A. J., Smyth, M. R., *Application of nanoparticles in electrochemical sensors and biosensors*. Electroanalysis 18 (2006): 319-326.
- [116]De la Escosura-Muñiz, A., Ambrosi, A., Merkoçi, A., *Electrochemical analysis with nanoparticle-based biosystems*. Trends in Analytical Chemistry 27 (2008): 568-584.
- [117]De la Escosura-Muñiz, A., Maltez-da Costa, M., Merkoçi, A., *Controlling the electrochemical deposition of silver onto gold nanoparticles: Reducing interferences and increasing the sensitivity of magnetoimmuno assays*. Biosensors and Bioelectronics 24 (2009): 2475-2482.
- [118]Foschia, M., Horstmann, S., Arendt, E. K., Zannini, E., *Nutritional therapy—Facing the gap between coeliac disease and gluten-free food*. International Journal of Food Microbiology 239 (2016): 113-124.
- [119]Codex Alimentarius Commission, Joint Food and Agriculture Organization of the United Nations/World Health Organization Food Standards Program (2008) *Food Speciality Dietary Use for Persons Intolerant Gluten*, CODEX STAN 118-1979. Revised 2008.
- [120]Commission Regulation (EC) No 41/2009 of 20 January 2009, *Concerning the composition and labelling of foodstuffs suitable for people intolerant to gluten*, Official Journal of the European Union L16 (2009): 3-5.
- [121]ALINORM 08/31/26, Appendix III, Codex Alimentarius Commission, Rome: WHO, 2008.
- [122]Osborne TB., *The vegetable proteins*, second ed., Longmans, London, 1924.
- [123]Shewry, P. R., Miflin, B. J., Kasarda, D. D., *The structural and evolutionary relationships of the prolamin storage proteins of barley, rye and wheat*. Philosophical Transactions of the Royal Society of London B: Biological Sciences 304 (1984): 297-308.
- [124]Diaz-Amigo, C., Popping, B., *Accuracy of ELISA detection methods for gluten and reference materials: a realistic assessment*. Journal of Agricultural and Food Chemistry 61 (2013):5681–5688.
- [125]Valdés, I., García, E., Llorente, M., Méndez, E., *Innovative approach to low-level gluten determination in foods using a novel sandwich enzyme-linked immunosorbent assay protocol*. European Journal of Gastroenterology & Hepatology 15 (2003): 465-hyhen.



- [126]Mena, M. C., Lombardía, M., Hernando, A., Méndez, E., Albar, J. P., *Comprehensive analysis of gluten in processed foods using a new extraction method and a competitive ELISA based on the R5 antibody*. Talanta 91 (2012): 33-40.
- [127]Haas-Lauterbach, S., Immer, U., Richter, M., Oehler, E., *Gluten fragment detection with a competitive ELISA*. Journal of AOAC International 95 (2012): 377-381.
- [128]Amaya-González, S., de-los-Santos-Álvarez, N., Lobo-Castañón, M. J., Miranda-Ordieres, A. J., Tuñón-Blanco, P., *Amperometric quantification of gluten in food samples using an ELISA competitive assay and flow injection analysis*. Electroanalysis 23 (2011): 108-114.
- [129]Couto, R. A. S., Lima, J. L. F. C., Quinaz, M. B., *Recent developments, characteristics and potential applications of screen-printed electrodes in pharmaceutical and biological analysis*. Talanta 146 (2016): 801-814.
- [130]Renedo, O. D., Alonso-Lomillo, M. A., Martínez, M. A., *Recent developments in the field of screen-printed electrodes and their related applications*. Talanta 73 (2007): 202-219.
- [131]Nassef, H. M., Bermudo Redondo, M. C., Ciclitira, P. J., Ellis, H. J., Fragoso, A., O'Sullivan, C. K., *Electrochemical immunosensor for detection of celiac disease toxic gliadin in foodstuff*. Analytical Chemistry 80 (2008): 9265-9271.
- [132]Laube, T., Kergaravat, S. V., Fabiano, S. N., Hernández, S. R., Alegret, S., Pividori, M. I., *Magneto immunosensor for gliadin detection in gluten-free foodstuff: towards food safety for celiac patients*. Biosensors and Bioelectronics 27 (2011): 46-52.
- [133]Manfredi, A., Mattarozzi, M., Giannetto, M., Careri, M., *Multiplex liquid chromatography-tandem mass spectrometry for the detection of wheat, oat, barley and rye prolamins towards the assessment of gluten-free product safety*. Analytica Chimica Acta 895 (2015): 62-70.
- [134]*Eurachem Guide The Fitness for Purpose of Analytical Methods: a Laboratory Guide to Method Validation and Related Topics*, first English ed., LCG, Teddington Ltd (1998) 1.0 <http://www.eurachem.org/>